

**A MÖSSBAUER INVESTIGATION
OF IRON AND IRON ALLOY
FISCHER-TROPSCH CATALYSTS**

J.W. NIEMANTSVERDIET

DISSERTATIE DRUKKERIJ
wibro
HELMOND
TELEFOON 04920-23981

A MÖSSBAUER INVESTIGATION OF IRON AND IRON ALLOY FISCHER-TROPSCH CATALYSTS



PROEFSCHRIFT

Ter verkrijging van de graad van doctor in de technische wetenschappen aan de Technische Hogeschool Delft, op gezag van de Rector Magnificus Prof. Ir. B. Th. Veltman, voor een commissie aangewezen door het college van dekanen te verdedigen op donderdag 14 april 1983 te 16.00 uur.

door

JOHANNES WILLEM NIEMANTSVERDRIET

Doctorandus in de natuurkunde
geboren te Amsterdam

BIBLIOTHEEK TU Delft
P 1729 4390



817220

C



VERVALLEN

C10081
72205

P1729
4390

Dit proefschrift is goedgekeurd

door de promotor: PROF. DR. J. J. VAN LOEF

en de copromotor: PROF. DR. V. PONEC

aan mijn ouders

aan Marianne

PREFACE

The oil crisis of 1973 and the growing awareness that oil resources are not inexhaustible, as expressed in the report of the Club of Rome "Limits to growth", have raised a considerable interest in the use of coal as an energy source and a feedstock for the chemical industry. Coal constitutes about 76% of the proven fossil fuel reserves, oil only about 14%.

Although the direct application of coal as an energy carrier, for example by burning it for electricity generation, will undoubtedly remain important, it is realized also that coal has a number of disadvantages in comparison to liquid or gaseous energy carriers. Coal is a solid and therefore difficult in handling, transport and storage. It contains contaminations like ash forming compounds and sulphur, which may cause severe environmental problems. From the chemical point of view coal has a low, unfavorable H/C ratio, and it cannot be cracked directly to products as low olefins, which are desirable feedstocks for the chemical industries. Moreover, the vast worldwide refining capacity built in the last decades cannot easily be rebuilt to process coal.

Many of these problems are circumvented if coal is converted into liquid or gaseous products, which can be used as fuels or as feedstocks. Basically there are two ways to convert coal into liquids or gases. In the first place, coal can be dissolved in an organic solvent to increase the H/C ratio and secondly, coal can be gasified with oxygen and steam to form synthesis gas, a mixture of mainly two gases: CO and H₂. Synthesis gas can also be produced from other carbon sources, for example by steam reforming of natural gas, or by partial oxidation of heavy petroleum fractions (synthesis gas from the bottom of the barrel). As figure 1 illustrates, a large number of products can be derived from synthesis gas by means of catalytic processes. One of these processes is the Fischer-Tropsch synthesis, the production of hydrocarbons from CO and H₂ with iron or cobalt catalysts. The characterization of iron and iron alloy Fischer-Tropsch catalysts forms the subject of investigation in this thesis.

The conversion of synthesis gas into hydrogen, methane or methanol can be

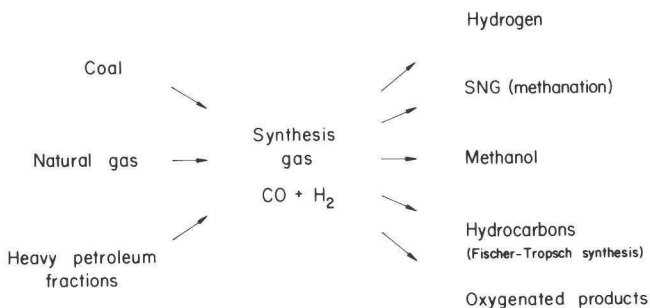


Fig. 1 Production and use of synthesis gas

performed with high selectivity, almost 100%. Such is not the case in the Fischer-Tropsch synthesis. Here a broad range of products is formed, which varies from the simplest hydrocarbon, CH_4 , to the longer molecules which are present in gasoline, diesel oil or even waxes. As will be described in chapter one of this thesis, lack of selectivity is one of the major drawbacks of the Fischer-Tropsch process. Modification of the catalyst by addition of promoters, like potassium or manganese oxide, or by alloying with other metals may be a means to improve the selectivity of the synthesis towards desirable products, such as low olefins or oxygenated hydrocarbons.

At present, production of H_2 , SNG (substitute natural gas) and methanol occurs on a commercial scale. Fischer-Tropsch synthesis is only used in South Africa, where inexpensive coal is available and a strong desire exists to become independent of foreign oil suppliers. The conversion of synthesis gas into oxygenated hydrocarbons as acetic acid or ethanol, with catalysts which are usually based on rhodium, may be a promising possibility for the future.

This thesis deals with the characterization of iron and iron alloy Fischer-Tropsch catalysts by means of Mössbauer spectroscopy. In the first two chapters we will review the Fischer-Tropsch synthesis and Mössbauer spectroscopy. The carburization of unsupported and unpromoted iron catalysts during Fischer-Tropsch synthesis is the subject of study in the chapters three, four and five, whereas the implications of the carburization process for the catalytic behavior of iron catalysts will be discussed in chapter six. In the

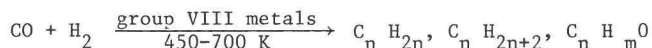
next chapter we describe the characterization of manganese promoted iron catalysts, which are believed to be selective for the production of low olefins as ethylene and propylene. Chapter eight deals with the characterization of an iron alloy catalyst, FeRh/SiO₂. This so called supported bimetallic cluster catalyst shows a high selectivity for the synthesis of oxygenated hydrocarbons from CO and H₂. A final discussion in chapter nine concludes this thesis.

CONTENTS

	Preface	iv
1	Hydrogenation of Carbon Monoxide	1
2	Theory of Mössbauer Spectroscopy	12
3	Behavior of Metallic Iron Catalysts during Fischer-Tropsch Synthesis Studied with Mössbauer Spectroscopy, X-ray Diffraction, Carbon Content Determination, and Reaction Kinetic Measurements	37
4	Carburization of α -Fe as a Function of H_2/CO Ratio	45
5	A Mössbauer Study of Surface Effects on Iron Fischer-Tropsch Catalysts	56
6	On the Time-Dependent Behavior of Iron Catalysts in Fischer-Tropsch Synthesis	64
7	Fe-MnO Fischer-Tropsch Catalysts for the Production of Light Olefins	68
8	A Mössbauer Study of Bimetallic FeRh/SiO ₂ Catalysts	89
9	Concluding Remarks	118
	Samenvatting (Summary in Dutch)	126
	Dankwoord / Acknowledgements	130

Introduction.

The Fischer-Tropsch process is the synthesis of a mixture of hydrocarbons and their derivatives from the gases CO and H₂ over Fe, Co or Ru catalysts. These hydrocarbons can be unsaturated (olefins, general formula C_nH_{2n}, n > 1), saturated (paraffins, C_nH_{2n+2}, n ≥ 1) and eventually oxygenated (general formula C_nH_mO, n, m ≥ 1). Closely related to Fischer-Tropsch synthesis are methanation (the formation of CH₄ from CO and H₂ over Ni catalysts) and, perhaps a little further away from the Fischer-Tropsch synthesis than methanation, methanol (CH₃OH) synthesis. In this chapter we will not confine ourselves to Fischer-Tropsch synthesis only, but, more generally consider CO hydrogenation over group VIII metals:



An overwhelming quantity of literature exists on the subject. This chapter is mainly based on a few recent reviews by Bell¹, Biloen and Sachtler², Ponec³, and Somorjai⁴.

History.

The history of the catalytic hydrogenation of CO⁵ goes back to 1902, when Sabatier and Senderens⁶ discovered the reaction of CO and H₂ to CH₄ with a Ni catalyst. Eleven years later reactions of CO and H₂ to higher hydrocarbons and oxygenated products over supported Co and Os were disclosed in patents by the Badische Anilin und Soda Fabrik⁷. In 1923 Fischer and Tropsch⁸ reported similar reactions at high pressures, with alkali promoted iron catalysts. Further research in Germany led in 1936 to the first commercial Fischer-Tropsch plant, which worked with a Co-based catalyst. Nine other plants followed and during the second world war Germany produced a part of its own gasoline, diesel oil, lubricants and waxes via Fischer-Tropsch synthesis. At the end of the war some of the plants had been des-

troyed, the others closed shortly thereafter.

The German Fischer-Tropsch research was continued in the USA during the years after the second world war. Apparently, there were two reasons for this. First, the low price of CH_4 from newly explored sources in the USA made production of synthesis gas (CO, H_2) from CH_4 and H_2O very attractive. Second, futurologists expected that the production of fuels from crude oil would not keep pace with an explosively growing car industry. The post-war Fischer-Tropsch research led to the well-known book by Storch, Golumbic and Anderson "The Fischer-Tropsch and related syntheses"⁹, which is up to today an important reference work on the subject.

In the 1950's large quantities of cheap oil became available and the interest in Fischer-Tropsch synthesis declined everywhere. Except in South Africa. Since 1955 this country has been using its large quantities of easily mineable coal in Fischer-Tropsch plants to fulfill in this way its wish to become independent of external oil suppliers.

The oil crisis of 1973 and the growing concern that oil wells may dry up somewhere in the next century has renewed the interest in coal as a feedstock for fuels and chemicals. Undoubtedly, the Fischer-Tropsch synthesis represents a "proven technology" for the conversion of coal-derived synthesis gas into many products. However, this does not imply that the process is economically attractive. One reason is the relatively high price of synthesis gas, which at present would account for 60-70% of the total price of the products. Lack of selectivity, which makes costly separations of the various products necessary, is another key problem. At present virtually all petrochemical industries and catalyst manufacturers carry out some research on the Fischer-Tropsch synthesis and the effort is mainly directed at reaching improved selectivities towards desirable products. Although some times favorable results have been reported, it is not expected that Fischer-Tropsch synthesis will be used on a commercial scale in about the next 20 years, except in emerging situations. Methane and methanol syntheses on the other hand appear to be economically viable processes and also the direct synthesis of various oxygenated products from syngas would be desirable.

Much of the academic research has focussed on the understanding of the mechanism of CO hydrogenation. This includes such aspects as the chemisorption of CO on the catalyst, the sequence of elementary reaction steps, the modelling of product distributions and the role of various promoters. In the following paragraphs we will review some of these aspects.

Group VIII metal catalysts.

All group VIII metals catalyze the reaction between CO and H₂, each metal with a different activity and its own characteristic product selectivity. Of course, these selectivities are also greatly affected by the choice of the reaction conditions, as temperature, pressure, H₂ : CO ratio in the feed gas and conversion level and, not to forget, by the presence of promoters in the catalyst. Table I gives the selectivities of the group VIII metals under certain optimum conditions, usually at high pressure. The remarkable differences in product selectivities between Pd, Ir; Pt and the other metals suggest that different reaction mechanisms are involved. We will come to this later in in this chapter.

Table I. Characteristic product selectivities of the group VIII metals in CO hydrogenation (under certain optimum process conditions).

catalyst	products
Fe	paraffins, olefins and oxygenated products
Co	paraffins in gasoline and diesel oil range
Ni	methane (~ 100%)
Ru	high molecular weight paraffins
Rh	paraffins or oxygenated products
Pd	methanol (~ 100%)
Os	liquid paraffins, olefins, oxygenated products
Ir	methanol and methane
Pt	methanol and methane

Table II. Catalytic activity of the group VIII metals in CO hydrogenation at 275°C, atmospheric pressure, H₂/CO = 3 and conversion below 5%.

catalyst	N _{CH₄} * 10 ³ a)	catalyst	N _{CH₄} * 10 ³ a)
Ru	181	Rh	13
Fe	57	Pd	12
Ni	32	Pt	2.7
Co	20	Ir	1.8

a) N_{CH₄}: number of CH₄ molecules formed per metal surface atom and per second. Data from Vannice¹¹.

At low pressure, 1 atm., methane is the predominant reaction product with all the group VIII metals. Vannice¹¹ investigated these metals (with the exception of Os), supported on alumina, in CO hydrogenation at 275°C and 1 atm total pressure. He expressed the catalytic activities as turnover numbers: the number of product molecules that is formed per metal atom at the surface and per second. This allows one to compare the intrinsic activity of one catalytic site for all the group VIII metals. Some of Vannice's results are given in table II. Large differences in activity exist, the most and the least active metal, Ru and Ir respectively, differ by a factor of about 100.

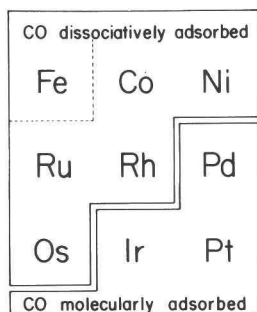


Fig. 1 CO adsorption on group VIII metals at reaction temperatures.

The first chemical step in any heterogeneous-catalytic reaction is the adsorption of the reactants on the surface of the catalyst. H₂ is readily adsorbed and dissociated on the group VIII metals¹². Also CO adsorption occurs on all these metals, but dissociation does not follow in all cases¹. At room temperature CO dissociates only on Fe. At reaction temperatures,

200 - 350 °C, CO dissociates easily on six out of nine metals, as is illustrated in figure 1. Only on Pd, Ir and Pt CO is to a great extent molecularly adsorbed at reaction temperatures. Again we note a difference between Pd, Ir, Pt and the other group VIII metals.

On all metals CO is absorbed with the axis C-O perpendicularly to the surface, the chemisorption bond is mainly that between the metal and the carbon atom. The adsorption is called linear, bridged or multiply bound when respectively one, two or more metal atoms are involved in coordinating CO (fig. 2). The chemisorption bond between CO and the metal consists of two contributions: 1) donation of electrons from the 5σ orbital of the CO molecule into the unoccupied metal orbitals and 2) backdonation of electrons from occupied metal orbitals into the unoccupied π^* orbitals of the CO molecule. The 5σ orbital is non bonding with respect to the C-O bond, therefore 5σ donation will not promote the dissociation of the CO molecule. The π^* however, is an antibonding orbital with respect to the C-O bond. Thus backdonation from the metal will weaken the C-O bond, and possibly promote dissociation of the CO molecule.¹

The exact mechanism of C-O bond breaking is not clear yet. It seems probable that some kind of bending of the perpendicularly adsorbed CO molecule must occur in order to enable the formation of a metal-oxygen bond.¹ Such a process requires the participation of an ensemble of several metal atoms. Araki and Ponec¹³ have presented clear evidence that, indeed, an ensemble of Ni atoms at the surface of the metal is involved in CO dissociation. Diluting Ni with Cu, which does not adsorb CO, led to a strong decrease in CO dissociation, much stronger than proportional to the number of Cu atoms in the surface of the NiCu alloy.

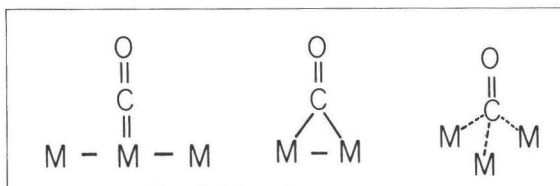


Fig. 2. Linear, bridged and multiple CO adsorption on the group VIII metal M.

Mechanism of CO hydrogenation.

At a first glance the catalytic reaction between CO and H₂ looks like a relatively simple reaction. Nevertheless, its mechanism has been the subject of controversy for many years. This is mainly due to the fact that several suggested mechanisms, which employed different intermediates, were all able to describe the experimental data adequately. During the last five years a number of crucial experiments have been carried out, that have led to an almost generally accepted reaction mechanism. For detailed reviews on this subject we refer to Bell¹ and Biloen and Sachtler.²

Vannice¹¹ analyzed his results over the group VIII metals in terms of a power rate law:

$$N_{\text{CH}_4} = A e^{-E_a/RT} P_{\text{H}_2}^X P_{\text{CO}}^Y \quad (1)$$

in which N_{CH_4} is the number of CH₄ molecules formed per site per second, A is the preexponential factor, E_a the activation energy, R the gas constant, T the absolute temperature, P the partial pressure and X and Y the order in H₂ and CO respectively. For the group VIII metals that dissociate CO at reaction temperature Vannice found activation energies in the range 21-27 kcal/mole and a slightly negative order in CO, whereas for Pd, Ir and Pt, which adsorb CO mostly molecularly, E_a was in the range 17-20 kcal/mole and Y was slightly positive. In all cases the order in H₂ was positive, between 0.7 and 1.6. Again we note the different behavior of the metals Pd, Ir and Pt, this time manifesting itself in slightly different kinetic parameters. It is clear that a good kinetic model should lead to the power rate law as standing above, with the correct values for the reaction orders X and Y.

Another observation which must be accounted for is that the distributions of hydrocarbons longer than C₂ formed upon CO hydrogenation often obey the so called Schulz-Flory distribution. This is often true even under industrial conditions.¹⁴

A Schulz-Flory product distribution implies that the hydrocarbons are formed in a polymerization process, in which the monomers are formed in

situ in the CO + H₂ reaction. If c_n is the relative concentration of hydrocarbons with n carbon molecules than

$$c_n = (\ln^2 \alpha) \alpha^n \quad (2)$$

or

$$\log c_n = 2 \log(\ln \alpha) + n \log \alpha \quad (3)$$

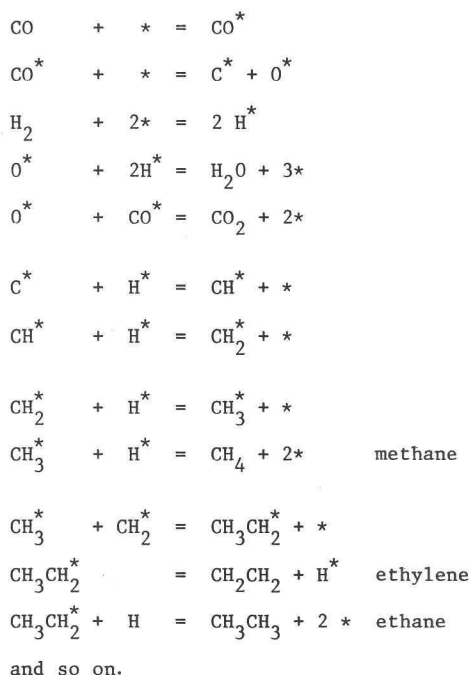
where α , the chain growth parameter, is the probability that a hydrocarbon with n molecules will continue to grow and $\ln^2 \alpha$ is a normalization constant. From equation (2) it is apparent that for any particular α between 0 and 1 a distribution of products arises, whereas the product distribution approaches 100% CH₄ (or 100% CH₃OH) in the limit for $\alpha \rightarrow 0$.

The distribution of products that are formed in the Fischer-Tropsch process has first been analyzed by Herington¹⁵ and later by Anderson⁹. In parallel to this and partly earlier Schulz described the distribution of products of any polymerization reaction by equation (2), a function which now bears his and Flory's name. Although Anderson's distribution function describes the Fischer-Tropsch product distribution as good as the Schulz-Flory distribution, the latter is used more frequently.

Unfortunately several kinetic models are equally well conceivable which are consistent with Vannice's data¹¹ and also the concept of a Schulz-Flory distribution. Vannice obtained an excellent description of his results with a model based on CHOH* intermediates and CO bond dissociation in these complexes as the rate determining step. According to Biloen and Sachtler² a model which involves C* intermediates and the reaction C* + x H* as the rate determining step also leads to an adequate description of the results. Araki and Ponc¹³, Wentrcek et al.¹⁶, Biloen et al.¹⁷ and Rabo et al.¹⁸ have clearly shown that carbon atoms at the surface of the catalyst (C*), are the key intermediates in CO hydrogenation over Ni, Co and Ru and that, at least with these catalysts oxygen containing intermediates of the type CHOH or CO play a negligible role, both in initiation and in chaingrowth. Brady and Petit¹⁹ showed that CH₂ species are possibly the insertable monomers involved in

chain growth, since the reaction between H_2 and diazomethane CH_2N_2 (which decomposes into CH_2 and N_2) led to unbranched hydrocarbons with an almost Schulz-Flory product distribution.

So at present it is believed that CO hydrogenation over Co, Ni and Ru starts with the dissociative adsorption of CO and H_2 , after which partial hydrogenation leads to CH_x species. For the sake of simplicity we will assume that $X=2$. Methane is formed by complete hydrogenation of this CH_2 species, whereas longer hydrocarbons are formed via a repeated CH_2 insertion in alkyl groups, as indicated in figure 3. The termination reaction determines whether the hydrocarbon molecule leaves the catalyst surface as alkane or alkene. This mechanism can be represented by the following sequence of elementary steps as suggested by Bell¹, in which * is an active site on the surface of the catalyst and CO^* is a chemisorbed CO molecule:



This scheme of reactions for the hydrogenation of CO is valid only at differential conditions, i.e. when CO conversions are of the order of 1%.

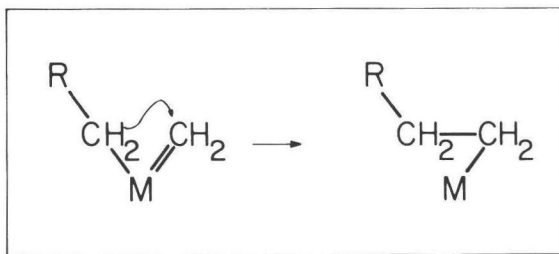


Fig. 3. Chain growth by means of CH_2 insertion in alkyl groups on the group VIII metal M ($\text{R} = \text{C}_n\text{H}_{2n+1}$, $n \geq 0$).

At higher conversions secondary reactions of the products, in particular addition of olefins to form longer hydrocarbons, formation of oxygenated products and hydrogenolytic reactions may occur. Such reactions will be ignored in this thesis. Since it deals only with low pressure Fischer-Tropsch synthesis this simplification is indeed permissible.

For CO hydrogenation over Pd, Ir and Pt a different mechanism might be operative, since CO^* does not dissociate easily under reaction conditions. According to Rabo et.al.¹⁸ the chemisorbed CO^* on Pd is less reactive to H_2 than the surface carbon C^* that is formed on Ni, Ru and Co. The same will probably be true for Ir and Pt. Although the reaction mechanism for the formation of hydrocarbons via molecularly adsorbed CO is not yet known, it is conceivable that intermediates of the CHOH^* type could be involved, whereas chain growth might occur e.g. via insertion of CO into a metal-carbon bond.

The usefulness of describing the Fischer-Tropsch synthesis in terms of a sequence of elementary steps among which one step is rate determining, has recently been questioned by Rofer-De Poorter.¹² She notes that some intermediates may be produced by more than one reaction path and that a particular intermediate may yield more than one product. She proposes to describe the Fischer-Tropsch mechanism with a network of 55 elementary reactions,

Such a rigorous approach is in principle correct. However, in order to perform calculations on such a complex network a very large set of differential equations would be required. In practice this means that unless the

conditions are such that many of the 55 reactions in the network will have an almost zero rate, analysis of experimental data is impossible, even in a qualitative sense. In this thesis we will only interpret our results qualitatively in terms of a reaction scheme that is very similar to the one proposed by Bell.¹ However, we will keep in mind that the other reaction paths mentioned by Rofer-De Poorter may also be involved.

Fischer-Tropsch synthesis over iron catalysts.

So far iron has been excluded from the discussion of the reaction mechanism of CO hydrogenation over the group VIII metals. Although CO adsorbs readily on iron and dissociates on iron even at room temperature,¹ the reaction scheme as is has been outlined above cannot be applied to the $\text{CO} + \text{H}_2$ reaction over iron. The reason for this is that iron is not stable under reaction conditions, it is converted into iron carbides. The relation between the carburization process of iron and its activity for the Fischer-Tropsch synthesis has been a matter of much controversy ever since Fischer and Tropsch postulated that iron carbides are intermediates in the synthesis.¹ The relation between carburization and catalytic activity will be the subject of the chapters 3, 5 and 6 of this thesis.

References.

1. A.T. Bell, Catal.Rev.- Sci.Eng., 23, 203(1981).
2. P. Biloen and W.M.H. Sachtler, Adv.Catal. 30, 165(1981).
3. V. Ponec, Catal.Rev.- Sci.Eng., 18, 151(1978).
4. G.A. Somorjai, Catal.Rev.- Sci.Eng., 23, 189(1981).
5. C. Masters, Adv. Organomet. Chem. 17, 61(1979).
6. P. Sabatier and J.B. Senderens, Hebd.Seances Acad. Sci. 134, 514(1902).
7. German Patents 293,787(1913), 295,202 and 295,203(1914).
8. F. Fischer and H. Tropsch, Brennst.Chem. 4, 276 (1923).
9. H.H. Storch, N. Golumbic and R.B. Anderson, "The Fischer-Tropsch and Related Syntheses", Wiley, New York, 1951.

10. D.L. King, J.A. Cusumano and R.L. Garten, Catal.Rev.-Sci.Eng. 23, 233 (1981).
11. M.A. Vannice, J.Catal. 37, 449(1975); J. Catal. 37, 462(1975).
12. C.K. Rofer-DePoorter, Chem.Rev. 81, 447(1981) and references therein.
13. M. Araki and V. Ponec, J. Catal. 44, 439 (1976).
14. G. Henrici-Olivé and S. Olivé, J. Catal. 60, 481 (1979).
15. E.F.G. Herington, Chem. and Ind. 1946, 347
16. P.R. Wentrcek, B.J. Wood and H. Wise, J.Catal. 43, 363 (1978).
17. P. Biloen, J.N. Helle, and W.M.H. Sachtler, J.Catal. 58, 95(1979).
18. J.A. Rabo, A.P. Risch and M.L. Poutsma, J.Catal. 53, 295 (1978).
19. R.C. Brady III and R. Petit, J.Am.Chem.Soc. 102, 6181(1980).

Introduction.

The Mössbauer effect can in short be described as the recoilless emission and resonant absorption of gamma rays originating from the decay of nuclear excited states. The effect has been named after its discoverer, Rudolf L. Mössbauer, who demonstrated the effect with the nuclide ^{191}Ir in 1957¹. He has been awarded the Nobel Price for Physics in 1961.

Since its discovery, Mössbauer Spectroscopy, or Nuclear Gamma Resonance spectroscopy as it is sometimes also called, has rapidly developed to become a standard tool for the investigation of solids. Applications are widespread and range from the fields of archeology and fine arts to geology, physics, chemistry, metallurgy and biology.

Mössbauer spectroscopy owes its success to a large extent to the fact that gamma rays involved in nuclear transitions are quanta of an unparalleled narrow range in energy. It is this spectral precision that enables the detection of the minute changes in the nuclear energy levels, such as resulting from a change in chemical state or in magnetic and electric surroundings of the atom to which the nucleus under investigation belongs.

In this chapter we will give a short treatment of the Mössbauer effect in iron and we will limit ourselves to those aspects that are relevant to the rest of this thesis. For a more complete treatment of the theory we refer to the books of Wertheim², of Wegener³ and of Greenwood and Gibb⁴. An excellent review of the application of Mössbauer spectroscopy to catalysis has been published by Dumesic and Topsøe⁵.

Mössbauer effect in iron.

Mössbauer spectroscopy can easily be applied to iron by means of the 14.4 keV transition in the nucleus of the isotope ^{57}Fe , which occurs naturally in iron for about 2%. ^{57}Co is used as a source, it decays according to the scheme in figure 1. With regard to the hyperfine interactions which contain the information concerning the chemical and magnetic state of the

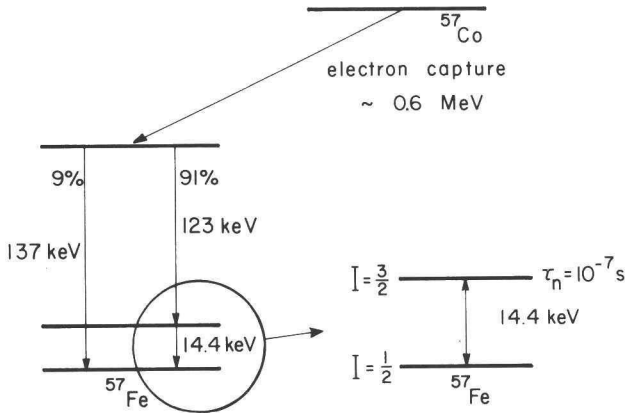


Fig. 1 The decay of ^{57}Co to ^{57}Fe . The encircled part is the commonly used Mössbauer transition in ^{57}Fe .

atom in a way that will be discussed later, it is important to note that the spins of the ^{57}Fe nucleus in the ground and the excited states are $\frac{1}{2}$ and $\frac{3}{2}$, which means that the degeneracies of these levels are two- and four-fold, respectively.

When a large number of emission events is considered, the energy distribution of the emitted radiation $I(E)$ has a Lorentzian shape, and $I(E)$ is proportional to

$$\frac{1}{(E-E_0)^2 + \left(\frac{\Gamma_n}{2}\right)^2} \quad (1)$$

So $I(E)$ has a maximum at $E=E_0$ and a full width at half maximum Γ_n , the natural linewidth. The latter is related to the lifetime τ_n of the excited level by means of Heisenberg's energy-time uncertainty relation and for the 14.4 keV excited state in ^{57}Fe it follows that $\Gamma_n = 4.6 \times 10^{-9} \text{ eV}$.

The very high resolving power of Mössbauer spectroscopy is readily apparent when we realise that the narrow linewidth Γ_n and the gamma energy E_0 result in an energy resolution in the order of 10^{-12} ! This means that it is possible and indeed useful to modulate the energy of the emitted

14.4 keV gamma rays by using the Doppler effect and giving the source a Doppler velocity of about 10^{-12} times the velocity of light, which is in the order of mm s^{-1} . A Mössbauer spectrum is simply a plot of the gamma ray intensity transmitted by the resonant absorber as a function of the Doppler velocity v of the source, which is related to the energy as

$$E(v) = E_0 \left(1 + \frac{v}{c} \right) \quad (2)$$

Due to hyperfine interactions the energy difference E'_0 between the ground state and the excited state of nuclei in the absorber may be slightly different from E_0 . The absorption spectrum can be described by the energy dependence of the cross section for resonant absorption:

$$\sigma(E) = \frac{\sigma_0 \left(\frac{\Gamma}{2} \right)^2}{(E - E'_0)^2 + \left(\frac{\Gamma}{2} \right)^2} \quad (3)$$

which with (2) can be expressed as a function of Doppler velocity v as

$$\sigma(v) = \frac{\sigma_0 \left(\frac{\Gamma}{2} \right)^2}{\left(E_0 - E'_0 + \frac{v}{c} E_0 \right)^2 + \left(\frac{\Gamma}{2} \right)^2} \quad (4)$$

In (3) and (4) Γ is the linewidth of the absorption peak and σ_0 the cross section for resonant absorption. In order to observe all hyperfine interactions in ^{57}Fe that are of interest in this thesis, we need Doppler velocities in the range of -10 to $+10 \text{ mm s}^{-1}$.

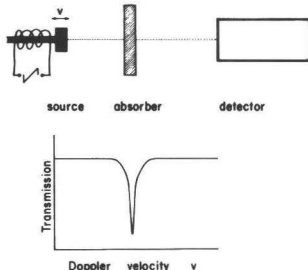


Fig. 2 Schematical picture of a Mössbauer spectrometer and a spectrum.

A schematical picture of a Mössbauer experiment in the transmission mode is given in figure 2. Before discussing the chemical and magnetic information that can be derived from a Mössbauer spectrum we will consider the conditions under which the Mössbauer effect can be observed.

Recoilfree emission and absorption

When a free ^{57}Fe nucleus decays from the excited state to the ground state, the energy difference E_0 between these states is released and it will be shared by the emitted gamma ray and the recoil of the nucleus. The recoil energy E_R can be calculated from the conservation laws for energy and momentum: $E_R = E_0/2Mc^2$, in which M is the mass of the nucleus. For ^{57}Fe $E_R = 2 \times 10^{-3}$ eV. When the emitted gamma quant, with energy $E_\gamma = E_0 - E_R$, encounters a free ^{57}Fe nucleus which is in the ground state, resonant absorption cannot take place as exchange of recoil energy occurs and because E_R is much larger than the linewidths of both the emission and the absorption peak. Instead the gamma quant should have an energy equal to $E_0 + E_R$ in order to be resonantly absorbed. This demonstrates that the Mössbauer effect cannot be observed in free atoms, like in a gas or a liquid.

However, in the solid state, where the atoms of the source and the absorber are each bound in a lattice, the recoil energy will be shared by the lattice as a whole. It depends on the characteristic energy $\hbar\omega$ of the lattice vibrations, the phonons, whether or not the Mössbauer effect can be observed. In case $E_R \geq \hbar\omega$, the recoil energy of each emission or absorption event will be dissipated by the lattice and the Mössbauer experiment fails. If on the other hand $E_R < \hbar\omega$ a totally different situation arises. According to the Correspondence Principle of Quantum Mechanics - expectation values follow the laws of Classical Mechanics - the average recoil energy per emission or absorption event, when calculated over a large number of such events, must be equal to E_R . Since $E_R < \hbar\omega$, a certain fraction of emission and absorption events takes place without exchange of recoil energy. This fraction is called

the recoilless fraction and will be denoted by f .

In a rigorous quantum mechanical calculation it can be shown that

$$f = \exp(-k_{\gamma}^2 \langle x^2 \rangle) \tag{5}$$

in which k_{γ} represents the magnitude of the gamma wave vector and $\langle x^2 \rangle$ the mean squared displacement of the atoms in the lattice, caused by the lattice vibrations. From (5) one can easily see that the recoilless fraction will be low in the case of soft vibrational modes, in which $\langle x^2 \rangle$ will be relatively large, while in case of an infinitely rigid lattice f approaches unity. The displacement $\langle x^2 \rangle$ can be calculated when a model for the lattice vibrations is adopted.

In general the Debye model is quite appropriate. According to this model f is given as a function of temperature T and of a parameter θ_D , the Debye temperature, by

$$f = \exp \left[- \frac{3}{2} \frac{E_R}{k_B \theta_D} \left(1 + 4 \frac{T^2}{\theta_D^2} \int_0^{\theta_D/T} \frac{x dx}{e^x - 1} \right) \right] \tag{6}$$

in which k_B is Boltzmann's constant. The Debye temperature θ_D characterizes

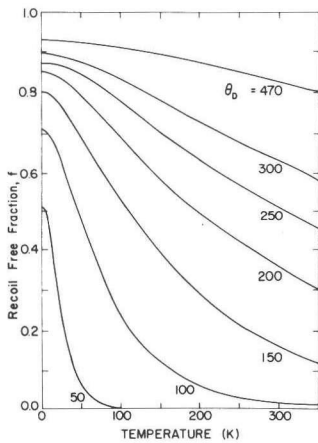


Fig. 3 The recoilless fraction f in the Debye model (θ_D is the Debye temperature in Kelvin).

the lattice vibrations, θ_D is high for a rigid lattice and low for a lattice exhibiting soft vibrational modes. As equation (6) indicates, f increases with decreasing temperature and with increasing Debye temperature, even at $T = 0$ (figure 3).

Hyperfine interactions

Although Mössbauer spectroscopy makes use of transitions between energy states of the *nucleus*, one obtains nevertheless information about the *atom* and its *surroundings* owing to the existence of hyperfine interactions. First, the positions of the nuclear levels and hence the energy at which absorption takes place, depend slightly upon the chemical state of the atom to which the nucleus belongs. Secondly, the degeneracy of the levels can partially or completely be removed by the influence of the neighbouring atoms. As a consequence the levels are split and more absorption peaks arise in the spectrum.

In this section we will briefly discuss the hyperfine interactions in ^{57}Fe and the Mössbauer parameters which characterize them. In general these parameters enable the identification of the iron compounds in the absorber.

a) The *isomer shift* (I.S.) is a measure for the electron density at the nucleus of an atom in the absorber relative to that at the atomic nucleus of the source. Usually the isomer shift of the absorber under study is expressed in terms of that of a reference compound. The existence of an isomer shift is the consequence of the Coulomb interaction between the positively charged nucleus and negatively charged s-electrons, the wave functions of which overlap with the nucleus. Since the nuclear size in the excited state differs from that in the ground state, the Coulomb interaction energies in both states are not identical. The isomer shift can be expressed by

$$\text{I.S.} = \frac{2\pi}{3} Z e^2 (|\psi_a(0)|^2 - |\psi_r(0)|^2) (R_e^2 - R_g^2) \quad (7)$$

in which Z is the atomic number of the Mössbauer atom, e the electron charge, $\psi(0)$ the wavefunction of the s electrons at the nucleus, the subscripts a and r refer to absorber and reference compound respectively, R_e and R_g are the effective radii of the nucleus in the excited state and the ground state, respectively.

The contribution of the 4 s electrons to the s -electron density $|\psi_a(0)|^2$ will be determined by the chemical state of the ^{57}Fe atom, and since in ^{57}Fe the quantity $(R_e - R_g)$ is sufficiently large the I.S. yields useful information about the valence state of the iron in the absorber.

It should be noted that the isomer shift contains a contribution from the thermal motion of the individual atoms in the absorber. The expression (2) for the Doppler velocity is in fact a series expansion, which has been truncated after the first order term. This is justified since in (2) $\frac{v}{c}$ is typically of the order of 10^{-12} and hence $\frac{v^2}{c^2}$ vanishes. An individual atom in the absorber, however, possesses a velocity \dot{x} due to lattice vibrations and \dot{x} is much larger than v . Since the lattice vibrations are very fast with respect to the time scale at which absorption events take place, we have to consider the average values of \dot{x} and \dot{x}^2 with respect to time, $\langle \dot{x} \rangle$ and $\langle \dot{x}^2 \rangle$ respectively. The former term is zero, and the second order term which has not been included in the series expansion (2) adds to the isomer shift, thereby making the latter temperature dependent:

$$\text{I.S.}(T) = \text{I.S.}(0) - E_0 \frac{\langle \dot{x}^2 \rangle}{2c^2} \quad (8)$$

The term $E_0 \frac{\langle \dot{x}^2 \rangle}{2c^2}$ is called the second order Doppler shift and like $\langle x^2 \rangle$ it can be expressed as a function of temperature and of θ_D in the Debye model.

b) *The electric quadrupole splitting.* A ^{57}Fe nucleus in its ground state possesses a spherically shaped charge distribution and hence it has no electric quadrupole moment. In the 14.4 keV excited state, on the

other hand, the charge distribution is shaped like a prolate ellipsoide and hence the excited ^{57}Fe nucleus has a positive electric quadrupole moment.

When an excited nucleus experiences the presence of an electric field gradient the nucleus reacts by orienting itself with respect to the direction of this gradient. Two orientations of the nucleus or rather of its quadrupole moment are possible and a splitting of the excited level is observed, in which the originally fourfold degeneracy is partially removed, as indicated in figure 4. The splitting between the levels, the electric quadrupole splitting ΔE_Q , is proportional to the magnitude of the electric field gradient (EFG) at the nucleus. The origin of the EFG is due to charges arising from asymmetrically distributed electrons in incompletely filled shells of the atom itself and to charges on neighbouring ions in a crystal lattice with a symmetry lower than cubic.

The relative intensities of the peaks in a quadrupole split spectrum, a doublet, depend on the angle ψ between EFG and the direction of the gamma rays. The intensities are given in table I.

We note that for a randomly oriented polycrystalline absorber the line intensities are equal, since the average values of $\cos^2\psi$ and $\sin^2\psi$ are $\frac{1}{3}$ and $\frac{2}{3}$ respectively. We further remark that if only one angle ψ_0 between EFG and the gamma rays occurs, the peak intensities are equal for $\psi_0 = 54.73^\circ$, while the largest difference in intensities is observed for $\psi_0 = 0$.

Table I Angular dependence of the peak intensities in a quadrupole doublet of ^{57}Fe .

peak	transition	relative intensity
1	$\pm \frac{1}{2} \rightarrow \pm \frac{1}{2}$	$1 + \frac{3}{2} \sin^2 \psi$
2	$\pm \frac{1}{2} \rightarrow \pm \frac{3}{2}$	$\frac{3}{2} + \frac{3}{2} \cos^2 \psi$

ψ : angle between EFG and gamma radiation

It is possible also that the recoilless fraction has an angular dependence $f = f(\psi)$ that shows up in the intensities of the peaks in a quadrupole doublet. In this rather exceptional case the expressions for the relative intensities in table I must be multiplied with $f(\psi)$, with the result that the peak intensities in a randomly oriented polycrystalline sample are no longer equal. This effect is called the Goldanskii-Karyagin⁶ effect. We would like to emphasize that whenever this effect is suspected to be present in a particular spectrum, it should be carefully verified whether the asymmetry does not arise from some preferential orientation in the absorber, or from saturation effects which will be discussed later in this chapter.

c) *Magnetic hyperfine splitting.* The magnetic hyperfine splitting or nuclear Zeeman splitting arises from the interaction between the nuclear magnetic dipole moment and the magnetic field H at the nucleus. This interaction removes the degeneracy of the nuclear levels completely, in the following way.

A nuclear state with spin I , gyromagnetic ratio g and magnetic quantum numbers $m_I = -I, -I+1, \dots, I$ splits on application of a magnetic field H in $2I+1$ equally spaced levels, while the difference in energy between two adjacent levels is $g \mu_n H$, where μ_n is the nuclear magneton. The ground state of ^{57}Fe with $I = 1/2$ and a gyromagnetic ratio g^0 splits into two levels with a spacing of $g^0 \mu_n H$ and the excited state, with $I = 3/2$ and g^* , splits into four levels with a spacing between two adjacent levels of $g^* \mu_n H$. On absorption of a gamma ray transitions between the levels are allowed when the change in magnetic quantum number is 0 or ± 1 , which means that there are six transitions, as is illustrated in figure 4 with the spectrum of metallic iron, $\alpha\text{-Fe}$. A Mössbauer spectrum consisting of six peaks is often called a sextuplet.

When in addition to a magnetic field an electric field gradient is also present, the four levels of the excited state obtain an extra shift in energy, due to the interaction of the nuclear quadrupole moment with the EFG. We will confine ourselves here to the case in

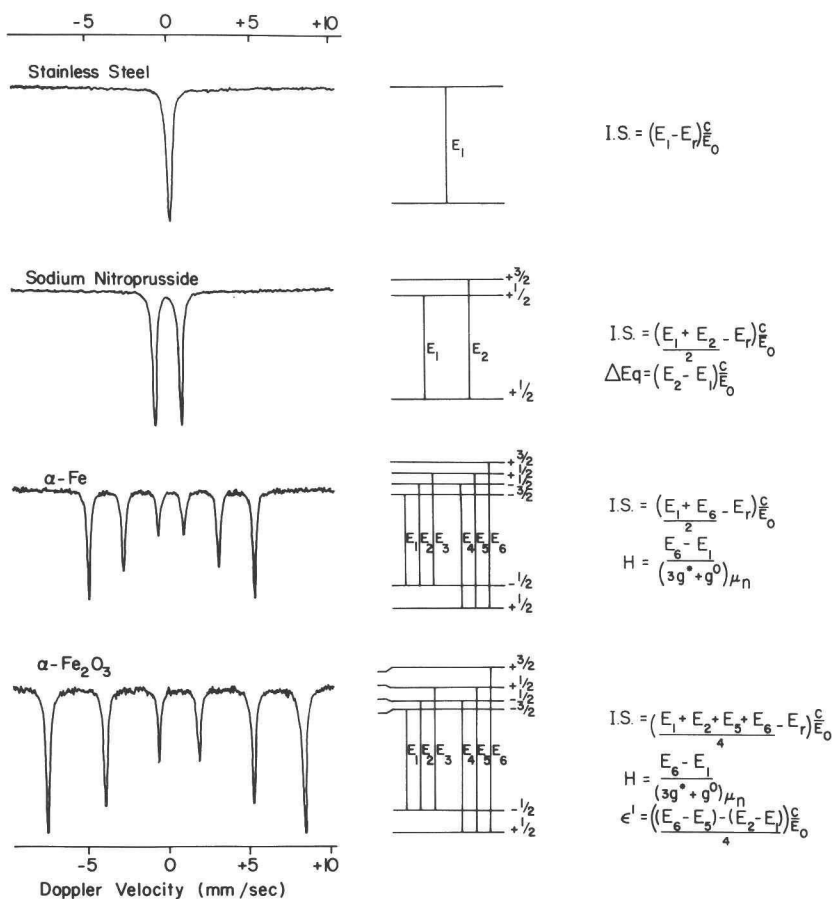


Fig. 4 Examples of Mössbauer spectra, corresponding transitions and expressions for the Mössbauer parameters for the different hyperfine interactions in the isotope ^{57}Fe .

which the quadrupole interaction can be considered as a small perturbation on the magnetic hyperfine interaction and in which the EFG is axially symmetric. Under these conditions the two levels characterized by $m_I = \pm \frac{3}{2}$ are shifted with an energy $+\epsilon'$ and the levels with $m_I = \pm \frac{1}{2}$ with an energy $-\epsilon'$, as indicated in figure 4 for the case of $\alpha\text{-Fe}_2\text{O}_3$ (note that $\alpha\text{-Fe}_2\text{O}_3$ at room temperature has a negative value of ϵ' : -0.10 mm/s). Like ΔE_Q , the quadrupole shift ϵ' is proportional to the

Table II Angular dependence of the peak intensities in a magnetically split Mössbauer spectrum of ^{57}Fe

peak	transition		relative intensity
1	$-\frac{1}{2}$	$-\frac{3}{2}$	$\frac{9}{4} (1 + \cos^2 \theta)$
6	$-\frac{1}{2}$	$+\frac{3}{2}$	
2	$-\frac{1}{2}$	$-\frac{1}{2}$	$3 \sin^2 \theta$
5	$+\frac{1}{2}$	$+\frac{1}{2}$	
3	$-\frac{1}{2}$	$+\frac{1}{2}$	$\frac{3}{4} (1 + \cos^2 \theta)$
4	$+\frac{1}{2}$	$-\frac{1}{2}$	

θ : angle between magnetic field and gamma rays.

magnitude of the EFG, but ϵ' depends also upon the angle ϕ between the EFG and the magnetic field. Under the conditions formulated above ϵ' and ΔE_Q are related by :

$$\epsilon' = \frac{1}{2} \Delta E_Q \frac{3\cos^2\phi - 1}{2} \quad (9)$$

The relative intensities of the six peaks in magnetically split Mössbauer spectra depend on the angle θ between the direction of the magnetic field and the gamma rays. They are given in table II. We note that for a randomly oriented absorber the intensities of the six peaks in the spectrum have a ratio of 3 : 2 : 1 : 1 : 2 : 3, whereas at any particular value of θ the relative intensities are 3 : x : 1 : 1 : x : 3, with $0 \leq x \leq 4$. Deviations from this ratio can be caused by saturation effects which will be discussed in the next section.

Total resonant absorption and saturation effects

Information about the recoilless fraction f and the Debye temperature of an absorber can be obtained from the total resonant absorption A , which is simply the total absorption area of the Mössbauer spectrum. For thin

absorbers with relatively few ^{57}Fe atoms, A is proportional to n , the number of ^{57}Fe atoms in the absorber and to f . This linear relationship disappears when n increases since saturation effects come into play. To which extent the total resonant absorption is saturated depends first of all on n and f , but also on the linewidth of the absorption peaks and on the nature of the spectrum: saturation will be stronger in a doublet than in a sextuplet, since in the latter the total resonant absorption is distributed among six peaks instead of two peaks in the former.

In order to account for the presence of saturation effects one usually defines an effective absorber thickness t^i for each of the N peaks, labeled i in the spectrum:

$$t^i = b^i \sigma_0 n f \quad i = 1, \dots, N \quad (10)$$

The coefficients b^i define the relative intensity of the i^{th} peak in a Mössbauer spectrum of N peaks such that $\sum_{i=1}^N b^i = 1$. So for a sextuplet belonging to a randomly oriented absorber $N = 6$ and $b^1 = b^6 = 1/4$, $b^2 = b^5 = 1/6$ and $b^3 = b^4 = 1/12$, while in a spectral doublet, belonging to a randomly oriented absorber in which a Goldanski-Karyagin effect is absent, $N = 2$ and $b^1 = b^2 = \frac{1}{2}$. In case $t^i \lesssim 1$ the total resonant absorption can be approximated by:

$$A = \frac{1}{2} \pi f_s \Gamma_n \sum_{i=1}^N t^i \left(1 - \frac{\Gamma_n}{\Gamma_a - \Gamma_s} * \frac{t^i}{4} \right) \quad (11)$$

in which f_s is the recoilless fraction of the source, Γ_a the linewidth of the peaks in the spectrum of the absorber in the limit for $t^i \rightarrow 0$ and Γ_s the linewidth of the source's emission spectrum.

Also the linewidth of the absorption peaks is influenced by saturation effects. When the observed linewidth of the i^{th} peak is written as $\Gamma_a + \Delta\Gamma^i$ and we consider the case $t^i \lesssim 1$ than $\Delta\Gamma^i$ can be expressed as a function of t^i as follows:

$$\Delta\Gamma^i = \frac{1}{4} \Gamma_n t^i \quad (12)$$

Saturation effects can easily be recognized in magnetically split Mössbauer spectra: first the intensity ratio of the first and third peaks is smaller than 3 as can be derived from (10) and (11), and secondly the linewidths of the absorption peaks increase in going from the inner peaks to the outer peaks, as expression (12) indicates.

It is quite remarkable that the subject of saturation is more or less ignored in some of the standard textbooks on Mössbauer spectroscopy, in spite of the fact that the effects can be considerable. For a thorough treatment of saturation effects we refer to an excellent paper by Mørup and Both⁷.

Mössbauer spectra of very small particles

A relatively large fraction of the atoms of an effective catalyst is at the surface and hence catalysts are often present as particles with linear dimensions between 1 and 100 nm. Particles of such small size exhibit features which are absent in the Mössbauer spectra of bulk materials.

The occurrence of superparamagnetism is one of the best-known properties of very small particles. In Mössbauer spectra it is the collapse of a magnetically split spectrum into an apparently paramagnetic doublet or singlet at a temperature well below the Curie or Neel point of the corresponding bulk material, due to fast relaxation of the magnetization vector as a whole.

At temperatures below the superparamagnetic transition temperature the hyperfine splitting H is generally lower than in bulk materials^{8,9}. This reduction in H increases with decreasing particle dimensions and increasing temperature. As a distribution in particle size is practically always present in samples of very small particles, the Mössbauer spectrum of such a sample is often a superposition of magnetically split spectra which differ in the value of H .

A third difference between very small particles and bulk materials can be found in the recoilless fraction f^{10} . In bulk materials f is determined solely by the lattice vibrations, as described earlier in this chapter. In very small particles however, f contains an additional contribution from the thermal motion of the particle itself, a solid state-like Brownian motion, and the recoilless fraction can be written as:

$$f = f_p \cdot f_l \quad (13)$$

In this expression f_p is the recoilless fraction due to particle motion and f_l represents the lattice contribution which can be expressed as (6) in the Debye model. In principle, the effect of particle motion can be distinguished from the other effects by determining the Debye temperatures θ_D from the temperature dependence of both the total resonant absorption and the isomer shift. In the absence of particle motion, $f_p = 1$, both values of θ_D should be equal. When however the particles are in motion, f_p is smaller than 1 and as a consequence the value for θ_D following from the temperature dependence of the total resonant absorption is too small, whereas the temperature dependence of the isomer shift still yields the correct Debye temperature.

Analysis of the Mössbauer spectra

In the course of our investigation we have used various computer programs to analyse the Mössbauer spectra, some of which already existed and others which had to be developed. In fact the aim of the calculations is to convert a spectrum, consisting of 400 intensities at 400 velocities into a few parameters which characterize the spectrum with respect to the hyperfine interactions, the lattice vibrations and the composition of the iron compounds.

In this section we will give a short outline of the mathematics underlying these calculations. Computer programs, however, will not be discussed. For simplicity we will exclude relaxation phenomena, since

they play no role in our investigations. Furthermore, with regard to spectra that are magnetically split we will confine ourselves to the cases in which (i) the electric quadrupole interaction can be considered as a small perturbation on the magnetic interaction, (ii) the EFG is axially symmetric, (iii) higher order quadrupole interactions are absent and (iv) the absorber is sufficiently thin so that line broadening due to saturation effects is absent.

We further remark that readers who are less interested in mathematical details can skip this section without any consequences for a good understanding of the catalytic aspects treated in the following chapters.

Mathematical description of a Mössbauer spectrum

Suppose S_v^m , $v = 1, \dots, 400$ represents an experimental Mössbauer spectrum, measured in 400 equidistant velocity channels in transmission mode, while Y_v^m , $v=1, \dots, 400$ represents the blank spectrum, the spectrum measured when no absorber is present and such that Y_v^m and S_v^m coincide for velocities at which no resonant absorption occurs. Since the distance between source and absorber is not constant, but a function of the source velocity, Y_v^m varies with v . When a spectrometer of the constant acceleration type is used Y_v^m has approximately the shape of a parabola.

Assuming that both S_v^m and Y_v^m have been measured, we define the normalized absorption spectrum

$$s_v^m = 1 - S_v^m / Y_v^m \quad . \quad v = 1, \dots, 400 \quad (14)$$

With this definition we can express the total resonant absorption A as

$$A = \sum_{v=1}^{400} s_v^m \quad (15)$$

The experimental spectrum s_v^m , $v=1, \dots, 400$ will differ from the "true" Mössbauer spectrum s_v , since the former contains statistical

fluctuations ϵ_v which are typically of the order of magnitude

$$\left((S_v^m)^{-1} + (Y_v^m)^{-1} \right)^{\frac{1}{2}} (1 - s_v^m)$$

The relation between s_v and s_v^m is given by

$$s_v^m = s_v + \epsilon_v, \quad v=1, \dots, 400 \quad (16)$$

The ratio $|\epsilon_v|/s_v^m$ depends on the length of time during which the spectra S_v^m and Y_v^m have been recorded and it approaches zero when the recording time becomes infinitely long.

Now suppose that s_v represents either a singlet, a doublet or a sextuplet. Any of the spectra encountered in this thesis can be considered to consist of a combination of these three kinds of elementary spectra. We will label the peaks in either of these elementary spectra by means of an index $i = 1, \dots, N$, in which N is the number of peaks in each elementary spectrum, hence $N = 1, 2$ or 6 . The relative intensity of the i^{th} peak will be denoted with I_i and we will define $I_1 = 1$; In case of very thin and randomly oriented absorbers the relative intensities I_i will be proportional to the parameters b^i introduced earlier. Now we can define the resonant absorption of the i^{th} peak in the spectrum as

$$A_i = \frac{I_i}{\sum_{j=1}^N I_j} A \quad (17)$$

The Mössbauer spectrum s_v is entirely determined by the Mössbauer parameters, which form together a vector \underline{x} . The number of components in \underline{x} depends upon the nature of the spectrum. The Mössbauer parameters fall into two groups: first the parameters I.S., ΔEQ , ϵ' and H , which determine the positions of the peaks with respect to the velocity channels and secondly the parameters Γ , I_i and A , which determine the width and the intensity of the peaks. For the purpose of calculations we will express

the Mössbauer parameters in terms of velocity channels, with the exception of the dimensionless intensities I_i .

The N Lorentzian shaped absorption peaks of s_v have centers which correspond with the velocity channels v_i , $i=1, \dots, N$ and we assume that all peaks have the same linewidth Γ . The velocity channel corresponding with a zero isomer shift will be denoted by v'_0 .

Using these assumptions and definitions we arrive at the following expression for an elementary Mössbauer spectrum:

$$s_v(x) = \frac{A}{\frac{1}{2} \pi \Gamma \sum_{j=1}^N I_j} \sum_{i=1}^N \frac{I_i \left(\frac{1}{2} \Gamma\right)^2}{(v-v'_i)^2 + \left(\frac{1}{2} \Gamma\right)^2} \quad (18)$$

which is equivalent to

$$s_v(x) = \frac{A}{\frac{1}{2} \pi \Gamma \sum_{j=1}^N I_j} \sum_{i=1}^N L(I_i, \Gamma, v_i) \quad (19)$$

where L represents the Lorentzian shaped peak. Expression (18), or (19), does not define the spectrum completely and we will derive additional expressions which relate the peak positions v_i to the positional Mössbauer parameters.

$N = 1$, a singlet

The Mössbauer spectrum consisting of a single line can be described by the following set of Mössbauer parameters: $x = (I.S., \Gamma, A)$. The position v_1 of the peak is simply given by

$$v_1 = v'_0 + I.S. \quad (20)$$

and the spectrum s_v is entirely determined by (18) and (20).

$N = 2$, a doublet

To describe a doublet we need the following parameters

$\underline{x} = (I.S., \Delta E_Q, \Gamma, I_2, A)$ in which $I_1 = 1$ by convention. The peak positions v_1 and v_2 are given by

$$v_i = v'_0 + I.S. + (-1)^i \frac{1}{2} \Delta E_Q \quad i = 1, 2 \quad (21)$$

Hence a Mössbauer doublet is mathematically described by expressions (18) and (21).

$N = 6$, a sextuplet

We will consider the case in which the six peaks are shifted by means of a small quadrupole interaction, as in figure 4^d. Here the set of Mössbauer parameters is $\underline{x} = (I.S., \varepsilon', H, I_2, I_3, A)$ in which we assume that $I_1 = I_6 = 1$, $I_2 = I_5$ and $I_3 = I_4$. Before deriving expressions for the peak positions v_i , $i = 1, \dots, 6$ we note that the relative distances between the peaks in a sextuplet are governed by the gyromagnetic ratio's of the ground state and the excited state in the ^{57}Fe nucleus, as can be seen from the energy level schemes in figure 4.

It is convenient to define the distances between the peaks:

$$\Delta_{ij} = v_j - v_i \quad i = 0, 1, \dots, 6 \quad (22)$$

in which v_0 is defined by:

$$v_0 = (v_1 + v_2 + v_5 + v_6)/4 \quad (23)$$

With these definitions the following relations are valid:

$$\left. \begin{aligned} \Delta_{12} + 2\varepsilon' &= \Delta_{23} = \Delta_{45} = \Delta_{56} - 2\varepsilon' = \frac{g^*}{g^o + 3g^*} \Delta_{16} \\ \Delta_{34} &= \frac{g^o - g^*}{g^o + 3g^*} \Delta_{16} \end{aligned} \right\} \quad (24)$$

which form an important criterium for judging the quality of a computer

fit to an experimental spectrum, as it will be discussed later. In order to derive an expression for the peak positions v_i we need the following relations

$$\left. \begin{aligned}
 \Delta_{10} &= \frac{1}{2} H - \epsilon' \\
 \Delta_{20} &= \frac{1}{2} \frac{g^o + g^*}{g^o + 3g^*} H + \epsilon' \\
 \Delta_{30} &= \frac{1}{2} \frac{g^o - g^*}{g^o + 3g^*} H + \epsilon' \\
 \Delta_{40} &= -\frac{1}{2} \frac{g^o + g^*}{g^o + 3g^*} H + \epsilon' \\
 \Delta_{50} &= -\frac{1}{2} \frac{g^o + g^*}{g^o + 3g^*} H + \epsilon' \\
 \Delta_{60} &= -\frac{1}{2} H - \epsilon'
 \end{aligned} \right\} \quad (25)$$

In (25) we have implicitly used that $H = \Delta_{16}$ and $\epsilon' = \frac{1}{4} (\Delta_{56} - \Delta_{12})$. In combining the expressions (22) through (25) the following simple expression for the peak positions v_i is obtained:

$$v_i = v'_o + \text{I.S.} - \Delta_{i0} \quad i=1, \dots, 6 \quad (26)$$

and hence a sextuplet is determined by (18), (25) and (26).

Fitting procedures

Fitting with single Lorentzian lines

The usual way to derive Mössbauer parameters from a spectrum s_v^m is to fit a Lorentzian line $L(I_j', \Gamma_j, v_j)$ to each of the N' peaks in the spectrum, such that the expression

$$\sum_{v=1}^{400} \left| s_v^m - \sum_{j=1}^{N'} L(I_j', \Gamma_j, v_j) \right|^2 \quad (27)$$

is a minimum with respect to the $3N$ adjustable parameters $I_j^!$, Γ_j , v_j , for $j=1, \dots, N'$. Afterwards the peaks are distributed over the elementary subspectra and for each subspectrum of N peaks the expression $\sum_{i=1}^N L(I_i, \Gamma_i, v_i)$ is written according to the right hand side of (18). Next the positional Mössbauer parameters are calculated from the peak positions v_i .

This fitting procedure, although commonly applied, has as a great disadvantage that it uses $3N'$ adjustable parameters, which is more than required to describe a spectrum. For example, under the conditions considered here a sextuplet is determined by 6 parameters only, while the Lorentzian fitting procedure uses 18 parameters. To ensure physically meaningful fits it must be carefully verified whether the positions, intensities and widths of the peaks obtained by this procedure satisfy the mathematical description in the preceding section, in particular the expressions in (24).

In order to obtain an appropriate fit to measured spectra in which peaks belonging to different elementary subspectra overlap each other completely or partially, several runs of the fitting procedure are needed, in which parameters must be constrained to values that are considered to be physically realistic. As a consequence the method is rather time-consuming, particularly when the spectrum consists of several elementary subspectra.

Fitting with elementary spectra

In order to avoid the disadvantages of the Lorentzian fitting method we developed a fitting procedure which implicitly guarantees physically realistic results. Suppose s_v^m is the measured absorption spectrum, that has contributions from N elementary spectra s_{jv} , $j=1, \dots, N$, $v=1, \dots, 400$, given by equation (18) together with the appropriate expressions for the peak positions. Each elementary spectrum s_{jv} is entirely characterized by the vector \underline{x}^j of Mössbauer parameters: $s_{jv} = s_{jv}(\underline{x}^j)$.

The measured spectrum s_v^m is fitted with a linear combination of the

N subspectra s_{jv} in a way such that the sum of squares

$$\sum_{v=1}^{400} \left| s_v^m - \sum_{j=1}^N s_{jv}(\underline{x}^j) \right|^2 \quad (28)$$

is a minimum for the best choice of the sets of Mössbauer parameters \underline{x}^j , $j=1, \dots, N$. This is done in a computer program, using a non-linear, iterative minimalization procedure supplied by a computer library of standard subroutines (we used the IMSL routine ZXSSQ).

The main advantage of this fitting procedure is that each fit that is acceptable in the mathematical sense is automatically also acceptable from the viewpoint of physics, since the fitting occurs with realistic Mössbauer spectra.

Distributions in magnetic hyperfine fields

The broadened lines of magnetically hyperfine split Mössbauer spectra of amorphous materials or small particles with a distribution in particle size, can often be analysed in terms of a superposition of subspectra which differ in the parameters H and A , but which have the same values for the remaining Mössbauer parameters I.S., ϵ' , I_2 and I_3 . The function $A(H)$ is by definition proportional to the number of ^{57}Fe atoms in the absorber which experience a magnetic hyperfine field H . Hence a distribution of hyperfine fields $p(H)$ can be defined as

$$p(H) = \frac{A(H)}{A_0}, \quad A_0 = \int_0^{\infty} A(H) dH \quad (29)$$

so that $p(H)$ is normalized to 1.

The various methods to derive $p(H)$ from a Mössbauer spectrum reported in the literature have recently been reviewed by Wivel and Mørup¹¹. Here we will briefly describe the procedure developed by these authors, which is in fact an improved and extended version of the method published by Hesse and Rübartsch¹².

Suppose the distribution $p(H)$ falls entirely within the range between H_{\min} and H_{\max} , chosen in a way such that $p(H_{\min}) = p(H_{\max}) = 0$. In this interval we define N equidistant discrete values H_i by

$$H_i = H_{\min} + \left(\frac{i-1}{N} \right) (H_{\max} - H_{\min}), \quad i = 1, \dots, N \quad (30)$$

Next we define $p_i = p(H_i)$, $A_i = A(H_i)$, the vector $\underline{y} = (I.S., \epsilon', I_2, I_3)$ and a vector \underline{x} which contains the same parameters as in the previous sections but in a different sequence: $\underline{x}^i = (I.S., \epsilon', I_2, I_3, H_i, A_i) = (\underline{y}, H_i, A_i)$. With these definitions an elementary sextuplet fulfills the relation:

$$s_v(\underline{x}^i) = p_i s_v(\underline{y}, H_i, A_i) \quad (31)$$

in which the sextuplet is given by (18), (25) and (26). Now the measured spectrum s_v^m is fitted by a linear combination of the elementary spectra $s_v(\underline{x}^i)$, and the first condition which must be fulfilled by the parameters in \underline{y} and the distribution p_i , is that the sum of squares

$$\sum_{v=1}^{400} \left[s_v^m - \sum_{i=1}^N p_i s_v(\underline{y}, H_i, A_i) \right]^2 \quad (32)$$

is a minimum. In order to avoid physically unrealistic fluctuations in the distribution, the latter is required to be smooth. This can be achieved by minimizing the sum of squared differences

$$\sum_{i=2}^{N-1} \left[(p_{i+1} - p_i) - (p_i - p_{i-1}) \right]^2 \quad (33)$$

Finally, as mentioned before, the distribution must satisfy the condition

$$p_1 = p_N = 0 \quad (34)$$

In general it is impossible to find values of p_i , $i=1, \dots, N$ which fulfill the requirements (32) to (34) simultaneously, since these relations

result in a set of $2N + 2$ linear equation in only N variables p_i . Therefore Lagrangean multipliers β and γ are introduced, which combine the expressions (32) to (34) into one:

$$\sum_{v=1}^{400} \left[s_v^m - \sum_{i=1}^N p_i s_{iv}(\underline{y}, H_i, A_0) \right]^2 + \gamma \sum_{i=2}^{N-1} (p_{i+1} - 2p_i + p_{i-1})^2 + \beta(p_1 + p_N) \quad (35)$$

Minimalization of this expression with respect to $p_i, i=1, \dots, N$ and $\underline{y} = (I.S., \epsilon', I_2, I_3)$ is carried out in a computer program, using an iteration process. In each iteration step a non-linear minimalization routine generates the 4 components of \underline{y} , after which the N components of the distribution p_i follow from a linear minimalization procedure. The iteration stops when expression (35) reaches its minimum value.

The Lagrangean multipliers β and γ must be chosen by the experimentator and they determine the weight of requirements (34) and (33) relative to the most important requirement of a good fit, (32). Typical values of γ and β are in the range 10^{-3} to 10^{-1} .

Mössbauer spectra of mixtures

The Mössbauer spectrum obtained with an absorber that consists of a mixture of different iron compounds can in principle be analyzed using both fitting methods described before. The contribution of each of the constituents is given by its total resonant absorption A . However, such procedures become progressively more difficult when the number of different iron compounds in the absorber increases to three or more. The difficulty can be circumvented in case Mössbauer spectra are available of the constituents in a single phase. Then a more direct approach can be chosen in which linear combinations of measured single phase spectra are fitted to the spectrum of a mixture.

Suppose $s_v^m, v=1, \dots, 400$ represents the spectrum of a mixture, which

contains contributions of N different iron compounds. The spectra of these compounds in a single phase, called the base spectra, have been measured and they are denoted by $b_{i,v}$, $i=1,\dots,N$, $v=1,\dots,400$ and their total resonant absorptions A_i have been calculated with equation (15). Now the spectrum s_v^m is fitted with a linear combination of the base spectra such that the sum of squares

$$\sum_{v=1}^{400} \left(s_v^m - \sum_{i=1}^N a_i b_{i,v} \right)^2 \quad (36)$$

is a minimum for the best choice of the N coefficients a_i . Expression (36) becomes a minimum when its derivative with respect to a_i is zero

$$\frac{d}{da_j} \sum_{v=1}^{400} \left(s_v^m - \sum_{i=1}^N a_i b_{i,v} \right)^2 = 0 \quad j = 1, \dots, N \quad (37)$$

On working (37) out it is equivalent with

$$\sum_{i=1}^N \sum_{v=1}^{400} a_i b_{i,v} b_{j,v} = \sum_{v=1}^{400} b_{j,v} s_v^m \quad j = 1, \dots, N \quad (38)$$

This is a set of N linear equations, from which the coefficients a_i , $i=1,\dots,N$ are calculated with a computer program using standard routines from a computer library to carry out the matrix algebra which is involved in solving (38). The relative contribution of compound i to the spectrum of the mixture is given by $a_i A_i / A$.

This rather simple method can be applied when the absorbers are sufficiently thin so that saturation effects are absent. We believe that application of this method in the analysis of complex spectra, for example those of carbided iron catalysts, yields results that are much more reliable than the results that are obtained with the fitting procedures as described in the preceding paragraphs. However, the method requires knowledge of the Mössbauer spectra of the single phase iron compounds.

References.

- 1 R.L. Mössbauer, Z. Physik 151,124(1958); Naturwissenschaften 45,538(1958); Z. Naturforsch. 14a, 211(1959).
- 2 G.K. Wertheim, "Mössbauer Effect: Principles and Applications", Academic Press, New York, 1964.
- 3 H. Wegener, "Der Mössbauereffekt und seine Anwendung in Physik und Chemie", Bibliographisches Institut, Mannheim, 1966.
- 4 N.N. Greenwood and T.C. Gibb, "Mössbauer Spectroscopy", Chapman and Hall, London, 1971.
- 5 J.A. Dumesic and H. Topsøe, Adv.Catal. 26, 121(1977).
- 6 S.V. Karyagin, Dokl.Akad.Nauk. SSSR, 148, 1102(1963).
- 7 S. Mørup and E. Both, Nucl.Instr. and Methods, 124, 445(1975).
- 8 A.M. van der Kraan, Phys.Stat.Sol. (a) 18, 215(1973); thesis University of Technology Delft (1972).
- 9 S. Mørup and H. Topsøe, Appl.Phys. 11,63(1976).
- 10 M. Hayashi, I. Tamura, Y. Fukano, S.Kanemaki and Y. Fujio, J. Phys. C: Solid St. Phys. 13, 681(1980).
- 11 C. Wivel and S. Mørup, J.Phys. E: Sci. Instrum. 14, 605(1981).
- 12 J. Hesse and A. Rübartsch, J.Phys.E: Sci.Instrum. 7, 526(1974).

Behavior of Metallic Iron Catalysts during Fischer–Tropsch Synthesis Studied with Mössbauer Spectroscopy, X-ray Diffraction, Carbon Content Determination, and Reaction Kinetic Measurements

J. W. Niemantsverdriet,* A. M. van der Kraan,

Interuniversitair Reactor Instituut, Delft, The Netherlands

W. L. van Dijk, and H. S. van der Baan

*Laboratory for Chemical Technology, Eindhoven University of Technology, The Netherlands (Received: March 31, 1980;
 In Final Form: July 9, 1980)*

The conversion of unpromoted, unsupported metallic iron catalysts into carbides during Fischer–Tropsch synthesis ($\text{CO:H}_2\text{:He} = 1:1:3$, 1 atm) was studied with Mössbauer spectroscopy, X-ray diffraction, carbon content analysis, and reaction kinetic measurements. From a comparison between experiments at different temperatures and literature data, it is concluded that both reaction conditions and the nature of the iron catalyst determine the combination of carbides that will be formed. Investigation of single-phase carbides revealed that the X-ray diffraction pattern commonly ascribed to a pseudohexagonal carbide Fe_5C actually belongs to the carbide $\epsilon\text{-Fe}_{2.2}\text{C}$. At synthesis temperatures of 513 K and lower, unknown iron–carbon species were found, referred to as Fe_xC . It is believed that Fe_xC represents poorly defined structures between $\alpha\text{-Fe}$ and a crystallographic carbide. The behavior of metallic iron catalysts during Fischer–Tropsch synthesis at 513 K was studied in more detail as a function of time. It was found that the rate of hydrocarbon formation was initially low, passed through a maximum, and decreased thereupon, while the conversion of $\alpha\text{-Fe}$ into carbides started at a high rate and decreased rapidly. These results can be understood as the consequence of either a competition between bulk carbidization and hydrocarbon synthesis or a relatively slow activation of $\alpha\text{-Fe}$ for the formation of hydrocarbons in which bulk carbidization plays no role. Deactivation is caused by the formation of an excessive amount of inactive carbon at the surface of the catalyst.

Introduction

The main conclusion presented in a 1974 study¹ on the economy of the Fischer–Tropsch process was that, for this process to become interesting, a major improvement of the selectivity to more valuable products had to be reached. In particular in Germany the interest is focused on the development of catalysts for the production of low olefins. In their patents Kölbel² and Büssemeier³ described olefin selective catalysts containing iron metal and various oxides that are difficult to reduce.

Because our aim is to make a catalyst that is highly selective for the production of olefins, we have chosen iron metal as the main component of our catalysts.

Iron-containing catalysts are not stable during Fischer–Tropsch synthesis, but are converted into carbides. This conversion has recently been investigated by means of Mössbauer spectroscopy by Raupp and Delgass⁴ and Amelse et al.,⁵ who used iron supported on silica, by Nahon et al.,⁶ who used iron on alumina, and by Maksimov et al.,⁷ who worked with a fused iron catalyst in which various promoters were present. Also thermomagnetic analysis^{8–10} and X-ray diffraction^{9,11} have been applied to study the formation of carbides in iron catalysts under various conditions of Fischer–Tropsch synthesis. More often comparison between those studies is difficult because not all investigators seem to be aware of the existence of at least four different iron carbides. Moreover some confusion exists about the X-ray diffraction spectra of hexagonal $\epsilon\text{-Fe}_{2.2}\text{C}$ and $\epsilon\text{-Fe}_2\text{C}$, which has a monoclinic structure approaching hexagonal.

In the present investigation we have used Mössbauer spectroscopy together with X-ray diffraction analysis, carbon content determination, and reaction kinetic measurements to study the conversion of an unpromoted and

unsupported metallic iron catalyst into various phases during the Fischer–Tropsch process.

Experimental Section

Catalyst Preparation. Iron(III) oxide was precipitated from a 0.25 kmol/m³ iron(III) nitrate solution ($\text{Fe}(\text{NO}_3)_3 \cdot 9\text{H}_2\text{O}$, Merck P.A.) by slowly adding ammonium hydroxide (12% by weight ammonia, Merck P.A., 2.8 mL/min) to the suspension, which was heated to 363 K. Ammonia addition was stopped when a pH of 8 was reached. The precipitate was filtered off and washed with 100 mL of distilled water. Then the catalyst was dried at 393 K for 24 h and calcined at 673 K for 1 h. We used a sieve fraction of 0.2–0.6 mm in all experiments. In some experiments a supported catalyst was used, prepared by precipitating iron(III) hydroxide on a mixture of TiO_2 and CaO to a final weight ratio of $\text{Fe}:\text{TiO}_2:\text{CaO} = 39:32:9$.

Fischer–Tropsch Reaction Process. The reactor consisted of a 6-mm i.d. quartz tube in an electrically heated oven. An Eurotherm thyristor controller and an alumel thermocouple regulated the temperature in the reactor within 2 K. The gases, hydrogen (Hoekloos, purity > 99.9%), carbon monoxide (Matheson, c.p. > 99.5%), and helium (Hoekloos, > 99.995%) were purified over a reduced copper catalyst (BASF RJ-11, BTS catalyst) at 425 K and a molecular sieve (5A, Union Carbide) at room temperature. Standard reduction of the catalyst was at 623 K in flowing hydrogen (100 cm³/min) for 16 h. Reactions were carried out with 0.5 or 3 g of catalyst under differential conditions with a maximum conversion of 5%, at 1 atm total pressure with a 1:1:3 mixture of CO, H₂, and He, respectively, at a total gas rate of 6 L/h.

The reaction rate was defined as the number of micromoles of CO converted into C₁–C₄ hydrocarbons per gram

TABLE I: Mössbauer Parameters of Single-Phase Carbides at $T = 295$ K

carbide	Fe site	this study		lit data		ref
		IS, mm/s	H_{eff} , kOe	IS, mm/s	H_{eff} , kOe	
ϵ' - Fe_3C		0.50 ± 0.03	173 ± 2	0.51 ± 0.01	173 ± 1	5
	I	0.43 ± 0.03	189 ± 2	0.46 ± 0.02	185 ± 2	
	II	0.51 ± 0.03	218 ± 2	0.49 ± 0.02	216 ± 2	
χ - Fe_3C_2		0.47 ± 0.03	110 ± 5		124 ± 4	12
	III	0.47 ± 0.03	110 ± 5		208 ± 2	
	I	0.45 ± 0.03	212 ± 2	0.44 ± 0.01	206 ± 2	
θ - Fe_3C	I					12
	II					

of catalyst and per hour. The product gas samples were analyzed by three gas chromatographs (Philips Pye)—the first one for the detection of CO_2 , H_2O , and CO , the second for the C_1 - C_3 hydrocarbons, and the last one for the hydrocarbons from C_3 up to C_8 . After a certain period of Fischer-Tropsch reaction, the reactor was cooled down to room temperature under a flow of helium. Sometimes it was inevitable that part of the residual iron oxidized, after removing the catalyst from the reactor.

Catalyst Characterization. The fresh catalysts as well as catalysts after various periods of Fischer-Tropsch synthesis were characterized by X-ray diffraction analysis, Mössbauer spectroscopy, and determination of the carbon content. X-ray diffraction patterns of the samples were taken on a Philips diffractometer Pw 210700 with Mn filtered Fe $K\alpha$ radiation. Mössbauer spectra were obtained by using a constant-acceleration spectrometer with a ^{57}Co in Rh source. Isomer shifts (IS) are reported relative to the NBS standard sodium nitroprusside (SNP or $\text{Na}_2[\text{Fe}(\text{CN})_5\text{NO}] \cdot 2\text{H}_2\text{O}$) at room temperature, while hyperfine fields (H_{eff}) are calibrated against the 515 kOe field of α - Fe_2O_3 , also at room temperature. The carbon content of a sample was determined via its weight gain with a CNH analyzer (F & M Corp.).

Analyzing Procedures of the Mössbauer Spectra. Mössbauer spectra of single compounds were analyzed with a least-squares program of Lorentzian-shaped lines. In the final fits all peaks belonging to the same sextuplet were constrained to have equal width, and also the intensities of the first and the sixth, the second and the fifth, and the third and the fourth peaks were constrained to be equal. The distances between the peaks in the same sextuplet were constrained to the well-known ratios for iron.

In the case that the investigated sample is a mixture of different compounds, we preferred to analyze the complex spectrum in a way such that the relative amounts of the compounds present were obtained. This was done in the following way. Suppose S_k ($k = 1, \dots, 400$) represents the Mössbauer spectrum of the mixture, measured in 400 velocity channels. The spectra of the $N - 3$ different compounds present in the mixture, corrected for their geometrical background parabolas, are represented by B_{ik} ($i = 1, \dots, N - 3$ and $k = 1, \dots, 400$). The spectrum S_k has its own background parabola, which can be fitted simultaneously by defining $B_{N-2,k} = k^2$, $B_{N-1,k} = k$, and $B_{N,k} = 1$ ($k = 1, \dots, 400$). Now the problem is to find coefficients a_i for which the combination $S_k^{\text{calcd}} = \sum_{i=1}^{N-3} a_i B_{ik}$ is the best fit to the measured spectrum S_k . So the expression $\sum_{k=1}^{400} (S_k^{\text{calcd}} - S_k)^2$ is a minimum for the best choice of a_i :

$$\frac{d}{da_j} \sum_{k=1}^{400} (S_k^{\text{calcd}} - S_k)^2 = 0 \quad j = 1, \dots, N$$

or

$$\sum_{i=1}^N \sum_{k=1}^{400} B_{jk} B_{ik} a_i = \sum_{k=1}^{400} S_k B_{jk} \quad j = 1, \dots, N$$

This is a set of N linear equations, from which the set of

N coefficients a_i can be found. The product of a_i and the spectral area of the normalized spectrum B_{ik} gives the relative spectral contribution of compound i to the measured spectrum S_k .

Results

Catalysts before and after Reduction. The unreduced catalysts consisted of pure α - Fe_2O_3 as we concluded from their Mössbauer spectra and X-ray diffraction patterns. An average crystallite size of ~ 30 nm was estimated from the broadening of the X-ray lines.

After reduction the X-ray experiments only showed the pattern of α -Fe, whereas Mössbauer spectra revealed the presence of a small amount of Fe_3O_4 besides α -Fe. Since we checked that the reduction conditions were adequate to convert all iron oxide into metallic iron, we believe that the small amount of Fe_3O_4 was formed after the catalyst was removed from the reactor.

Crystallographically Different Iron Carbides. First we tried to find the reaction conditions under which the catalysts are converted into single-phase carbides. The Mössbauer spectrum of a metallic iron catalyst after 1.5 h Fischer-Tropsch synthesis at 723 K is shown in Figure 1a. During the initial period of ~ 15 min the reaction process could not be limited to differential conversions. This resulted in the formation of graphitic carbon. The Mössbauer spectrum (Figure 1a) shows that some contamination of iron oxides is present, which is probably formed after the sample was removed from the reactor. The Mössbauer parameters of this sample, given in Table I, agree within experimental error with the data of Le Caer et al.¹² for θ - Fe_3C . X-ray diffraction data are given in Table II, and these data agree with the data of Lipson and Petch¹³ for θ - Fe_3C . This sample had a carbon content of 7.7% by weight, which is higher than the value of 6.69% calculated for θ - Fe_3C . Because the Mössbauer spectrum in Figure 1a indicates a single phase except for the small oxide contamination, we conclude that some carbon layers were formed upon the surface of the catalyst during the reaction process.

A metallic iron catalyst after 24 h of Fischer-Tropsch reaction at 513 K was flushed in helium at 623 K for 1 h. The data belonging to the X-ray diffraction pattern of this sample (Table II) agree with the data for χ - Fe_3C_2 as published by Senateur.¹⁴ We measured the Mössbauer spectrum of this sample at three temperatures (Figure 1b-d). The parameters of the room-temperature spectrum (Table I) agree within experimental error with the parameters of χ - Fe_3C_2 reported by Le Caer et al.¹²

In the least-squares fit of Lorentzian line shapes, we found broader lines for the Fe(II) site than for the Fe(I) site.

The Mössbauer spectrum at 4.2 K (Figure 1d) showed two broad lines on positions that are characteristic for an oxide. These lines are not visible in the spectra at 77 and 295 K. Repeating the Mössbauer experiments revealed that the spectra did not change for several months. So we must conclude that this oxide was formed either imme-

TABLE II: X-ray Diffraction Data of Single-Phase Carbides for Angles 2θ between 50 and 60°

$\theta\text{-Fe}_3\text{C}$				$\chi\text{-Fe}_5\text{C}_2$				$\epsilon'\text{-Fe}_{2.2}\text{C}$, this study		"Fe ₂ C", ^a Barton and Gale ¹¹	
this study		Lipson and Petch ¹³		this study		Senateur ¹⁴					
2θ	I, %	2θ	I, %	2θ	I, %	2θ	I, %	2θ	I, %	2θ	I, %
50.7	20	50.76	25	50.1	25	50.08	20	52.8	25	52.73	21
51.8	20	52.24	25	52.0	50	52.06	45				
54.8	60	55.02	60			52.46	30	54.7	100	54.24	100
										54.85	
55.9	60	56.10	70	54.5	25	54.46	25				
57.0	55	57.39	60	55.4	80	55.46	70				
57.5	100	57.62	100	56.4	100	56.38	100				
58.7	55	58.90	55	57.5	30	57.54	30				
				58.3	20	57.58	40				

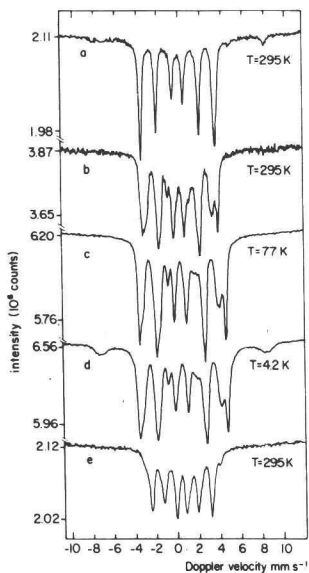
^a See text.

Figure 1. Mössbauer spectra of different iron carbides recorded at the indicated temperatures: (a) $\theta\text{-Fe}_3\text{C}$; (b-d) $\chi\text{-Fe}_5\text{C}_2$; (e) $\epsilon'\text{-Fe}_{2.2}\text{C}$ and some $\chi\text{-Fe}_5\text{C}_2$.

diately after the sample was removed from the reactor or during the Fischer-Tropsch reaction. In situ experiments will be done to clarify this point.

The Mössbauer spectrum of a Fe/TiO₂/CaO catalyst after 48-h Fischer-Tropsch reaction at 513 K is shown in Figure 1e. This spectrum contains a small contribution of $\chi\text{-Fe}_5\text{C}_2$, for which the small peak at the high positive velocity side is characteristic. From this spectrum we subtracted a contribution of the Mössbauer spectrum of $\chi\text{-Fe}_5\text{C}_2$ such that the characteristic small peak disappeared. The remaining spectrum was analyzed by means of the Lorentzian line-fitting procedure; it contains a sextuplet and a doublet. The Mössbauer parameters for the sextuplet, given in Table I, agree with the parameters published by Amelse et al.⁵ for $\epsilon'\text{-Fe}_{2.2}\text{C}$. The Mössbauer spectrum of this sample recorded at 77 K contained no doublet after the correction for $\chi\text{-Fe}_5\text{C}_2$ while the intensity of the $\epsilon'\text{-Fe}_{2.2}\text{C}$ sextuplet was stronger than in the room-temperature spectrum. So we conclude that the doublet belongs to $\epsilon'\text{-Fe}_{2.2}\text{C}$ in a superparamagnetic state. The contribution of $\epsilon'\text{-Fe}_{2.2}\text{C}$ to the total spectrum of Figure 1e is 83%. The X-ray diffraction pattern of this sample

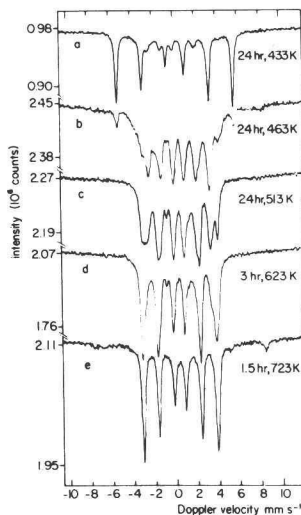


Figure 2. Mössbauer spectra of metallic iron catalysts after different periods of Fischer-Tropsch synthesis at various temperatures. Spectra were recorded at room temperature.

is shown in Figure 3c; line positions and intensities are given in Table II. Interpretation of these data is less straightforward than the interpretation of the Mössbauer spectrum. The X-ray diffraction pattern measured by us is similar to the one published by Barton and Gale¹¹ for a carbide $\epsilon\text{-Fe}_2\text{C}$ with an almost hexagonal lattice. However the Mössbauer spectrum clearly shows $\epsilon'\text{-Fe}_{2.2}\text{C}$ as the major phase in this sample and also excludes $\epsilon\text{-Fe}_2\text{C}$ as a possible constituent. In all other experiments in which Mössbauer spectroscopy revealed the presence of a considerable quantity of $\epsilon'\text{-Fe}_{2.2}\text{C}$, we measured an X-ray diffraction pattern similar to that found by Barton and Gale.¹¹ So we have concluded that the X-ray diffraction pattern published by Barton and Gale should not be attributed to almost hexagonal $\epsilon\text{-Fe}_2\text{C}$ but to hexagonal $\epsilon'\text{-Fe}_{2.2}\text{C}$. Up to now we did not succeed in preparing a single phase of the carbide $\epsilon\text{-Fe}_2\text{C}$.

Formation of Carbides at Different Temperatures. Mössbauer spectra of pure iron catalysts that were subjected to Fischer-Tropsch synthesis at various temperatures and times are shown in Figure 2. Spectra taken at temperatures higher than or equal to 513 K could be analyzed into spectral contributions of the constituents as outlined before. The spectra of Figure 1 were used as the single-phase spectra B_{ik} . The spectral contributions ob-

TABLE III: Spectral Composition of the Mössbauer Spectra of Metallic Iron Catalysts at $T = 295$ K after Fischer-Tropsch Synthesis at Various Temperatures

synthesis temp, K	synthesis time, h	spectral contribution, %				
		α -Fe	Fe_xC	ϵ' - $\text{Fe}_{2.2}\text{C}$	χ - Fe_5C_2	θ - Fe_3C
433	24	87	a	a		
463	24	13	a	a	36	
513	24			35	65	
623	3			12	47	41
723	1.5					100

^a The carbide concerned is clearly visible in the Mössbauer spectrum, although the spectral contribution could not be calculated (see text).

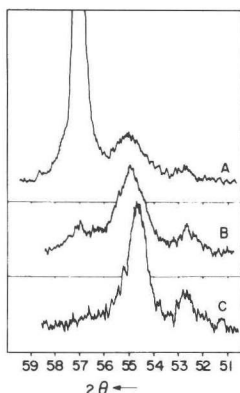


Figure 3. Relevant part of the X-ray diffraction patterns of (A) a metallic iron catalyst after 24 h of Fischer-Tropsch synthesis at 433 K, (B) the same at 463 K, and (C) a $\text{Fe}/\text{TiO}_2/\text{CaO}$ catalyst after 48 h of Fischer-Tropsch synthesis at 513 K.

tained are summarized in Table III. We have not applied this method to catalysts carburized at temperatures lower than 513 K because these samples contained a carbide phase that we could not prepare in a single phase.

After 24 h of Fischer-Tropsch synthesis at 433 K (Figure 2a), only a small part of the catalyst is converted into a carbide. The Mössbauer spectrum of this sample shows the spectrum of α -Fe and of a carbide in which a distribution of H_{eff} even up to 275 kOe occurs. Because the contribution of this carbide to the spectrum is too small to analyze properly, we confined ourselves to the calculation of the spectral contributions of α -Fe and the total amount of carbide. Because the carbide with the distribution in hyperfine fields does not seem to be the same as the ϵ - Fe_2C as reported by Maksimov,⁷ we shall refer to this carbide as Fe_xC . The X-ray diffraction pattern of this sample (Figure 3a) showed α -Fe as the major phase being present. Also some weak broad lines were visible, which we could understand as a combination of the patterns published by Hofer et al.⁹ for ϵ - Fe_2C and by Barton and Gale¹¹ for ϵ' - $\text{Fe}_{2.2}\text{C}$.

The Mössbauer spectrum of a sample after 24-h synthesis at 463 K showed besides α -Fe, χ - Fe_5C_2 , and ϵ' - $\text{Fe}_{2.2}\text{C}$ also the presence of the carbides with hyperfine fields up to 275 kOe, which we attributed to Fe_xC . Under the assumption that the Mössbauer spectrum of Fe_xC has no peaks at the position of the sixth peak of the sextuplet belonging to the Fe(II) site in χ - Fe_5C_2 , the relative contributions of χ - Fe_5C_2 and α -Fe were calculated (Table III).

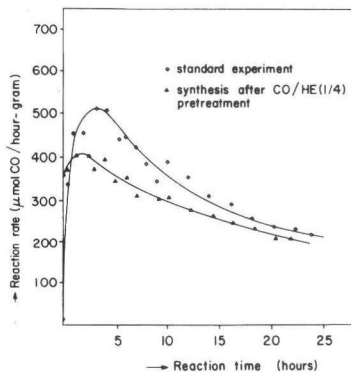


Figure 4. Reaction rates during Fischer-Tropsch synthesis over a metallic iron catalyst at 513 K.

According to the X-ray diffraction pattern of this sample (Figure 3b), ϵ' - $\text{Fe}_{2.2}\text{C}$ is the major constituent, together with χ - Fe_5C_2 and α -Fe.

The X-ray diffraction pattern of the catalyst after synthesis at 513 K for 24 h showed the presence of χ - Fe_5C_2 and ϵ' - $\text{Fe}_{2.2}\text{C}$, while the sample after 3-h synthesis at 625 K showed χ - Fe_5C_2 and θ - Fe_3C . The X-ray diffraction pattern of a catalyst after 1.5 h of synthesis at 723 K resembles the data of θ - Fe_3C .¹³

Time-Dependent Experiments at 513 K. The reaction rate of Fischer-Tropsch synthesis over a metallic iron catalyst, obtained by reducing 3 g of the precipitate, was determined as a function of time at 513 K and is given in Figure 4. The reaction rate started at zero and reached a maximum value after 3.5 h followed by a rather strong deactivation to a level of 40% of the maximum after 24 h.

After the reduced catalyst was treated with a gas mixture of 20% CO in He at 513 K for 2.5 h, the reaction rate started at a value near the maximum activity, which was achieved after 2 h. Although the value of this maximum was lower than in the case of an initially pure iron catalyst, the reaction rates tended to become equal at increasing times (Figure 4). The same result was obtained after pretreating the reduced catalyst with a gas mixture of 20% ethylene in helium.

The reaction rate of a $\text{Fe}/\text{TiO}_2/\text{CaO}$ catalyst showed a time-dependent behavior similar to that of the metallic iron catalyst.

The time-dependent behavior of a metallic iron catalyst during Fischer-Tropsch synthesis at 513 K was studied as follows. A sample obtained by reducing 0.5 g of the precipitate was subjected to synthesis for 0.5 h. After the sample was removed from the reactor, a new sample was introduced and subjected to the reaction process for a longer time and so on. We measured reaction rates and product distributions as a function of time for each experiment. No significant differences between the various experiments were found for corresponding time intervals. We concluded from this that the reaction process was sufficiently reproducible to justify the procedure used for studying the time-dependent behavior of the catalyst.

Mössbauer spectra of the catalyst samples subjected for various periods of time to the Fischer-Tropsch reaction at 513 K are shown in Figure 5. The spectra were analyzed as discussed in the Experimental Section, and the results are given in Table IV. The Mössbauer spectra of samples subjected to synthesis for 2.5 h or less indicated the

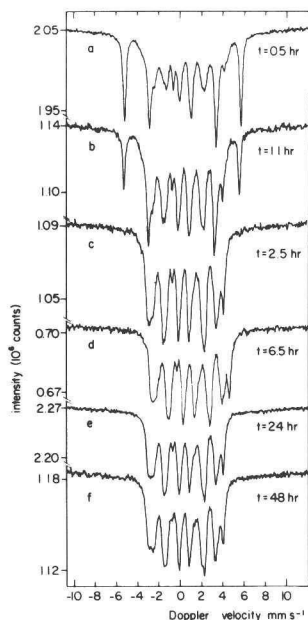


Figure 5. Mössbauer spectra of metallic iron catalyst after different periods of Fischer-Tropsch synthesis at 513 K. Spectra were recorded at room temperature.

TABLE IV: Spectral Composition of the Mössbauer Spectra of Metallic Iron Catalysts at $T = 295$ K after Different Periods of Fischer-Tropsch Synthesis at $T = 513$ K

synthesis time, h	α -Fe, %	Fe_3C , %	ϵ' - $Fe_{2.2}C$, %	χ - Fe_5C_2 , %
0.5	57	14-22	0-8	21
1.1	31	8-23	5-20	41
2.5	0	4-9	25-30	66
6.5	0	0	28	72
24	0	0	35	65
48	0	0	38	62

presence of Fe_3C . As the Mössbauer spectrum of the single phase could not be obtained, the spectral contributions of some carbides could only be calculated between certain limits (Table IV). The spectral contribution of χ - Fe_5C_2 has been calculated under the assumption that the Mössbauer spectrum of Fe_3C has no peaks at the position of the sixth peak of the Fe(II) site in χ - Fe_5C_2 . For comparison, we have plotted the catalytic reaction rate together with the relative spectral contributions to the Mössbauer spectra of α -Fe and the different carbides as a function of time in Figure 6. The results given in this figure will be discussed in the following section.

The X-ray diffraction pattern of the sample after 0.5-h reaction time predominantly showed α -Fe and furthermore broad lines at diffraction angles 2θ of 55.2 and 52.7°, respectively. We interpret these lines as being due to a combination of the diffraction lines of ϵ - Fe_3C ⁹ and ϵ' - $Fe_{2.2}C$.¹¹ After 2.5-h synthesis the α -Fe peak had nearly disappeared and the remaining pattern consisted of broad lines, attributed to contributions of ϵ' - $Fe_{2.2}C$ and χ - Fe_5C_2 . The X-ray diffraction patterns of samples after longer reaction times consisted of less broad lines. They could be identified as a combination of χ - Fe_5C_2 and ϵ' - $Fe_{2.2}C$.

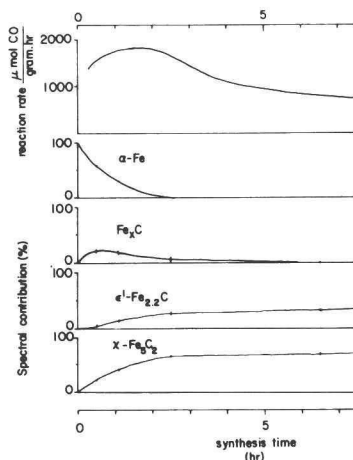


Figure 6. Reaction rates (upper curve) and relative contributions of α -Fe and the various carbides to the Mössbauer spectra during Fischer-Tropsch synthesis over a metallic iron catalyst at 513 K.

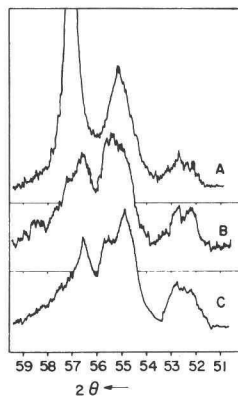


Figure 7. Relevant part of the X-ray diffraction patterns of a metallic iron catalyst after Fischer-Tropsch synthesis at 513 K for (A) 1.1, (B) 6.0, and (C) 48 h.

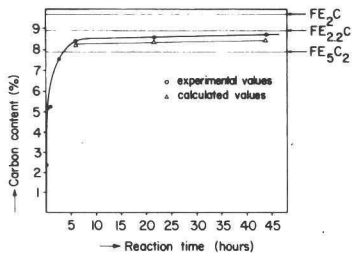


Figure 8. Weight percentage carbon in metallic iron catalyst during Fischer-Tropsch synthesis at 513 K: (O) experimental values; (Δ) values calculated from the spectral composition of the Mössbauer spectra.

Some of the X-ray diffraction patterns are shown in Figure 7.

The carbon weight content of the samples is plotted as a function of time in Figure 8. The value of 8.7% after

48 h of synthesis lies between the theoretical values for ϵ' -Fe_{2.2}C and χ -Fe₃C₂. When we assume that the carbides ϵ' -Fe_{2.2}C and χ -Fe₃C₂ have the same recoilless Mössbauer fractions, the carbon content due to the present carbide phases could be calculated for this sample from the analysis of the Mössbauer spectrum. The result is a carbon content of 8.3%, so that apparently an amount of carbon was present on the surface, corresponding to ~0.4% of the sample's total weight. For the samples after 6.5- and 24-h synthesis, the measured carbon content was also higher than the value calculated from the Mössbauer spectra.

Discussion

In our experiments four different iron carbides appeared. These carbides are the well-known θ -Fe₃C, χ -Fe₃C₂, and ϵ' -Fe_{2.2}C, and one that has not been reported before, which we have called Fe_xC. The identification of θ -Fe₃C and χ -Fe₃C₂ by means of X-ray diffraction as well as Mössbauer spectroscopy was possible in a straightforward manner. The identification of ϵ' -Fe_{2.2}C has been performed by means of the Mössbauer spectrum published by Amelse et al.⁵

Maksimov et al.⁷ are the only authors who published a Mössbauer spectrum of ϵ -Fe₂C. They analyzed their spectrum as a combination of three different sextuplets with a maximum hyperfine field of 237 kOe at the Fe(II) site. We think it is doubtful that their rather detailed analysis is correct, because the contribution of the carbide phase to the spectrum is only small. Moreover the velocity resolution of their spectrum seems to be rather poor. The Mössbauer spectrum of our sample prepared at $T = 433$ K for 24 h (Figure 3a) resembles the spectrum measured by Maksimov et al.,⁷ but our spectrum could not be characterized by three Lorentz sextuplets, because of the distribution of hyperfine fields up to 275 kOe at the Fe site with the highest hyperfine splitting. We assigned this Mössbauer spectrum to a carbide Fe_xC.

It is noteworthy that this carbide Fe_xC appeared only together with α -Fe or shortly after the moment that α -Fe had disappeared, as can be seen in Figure 6. No Fe_xC was found at a synthesis temperature higher than 513 K. The X-ray diffraction patterns of samples in which Fe_xC was present showed apart from the narrow α -Fe reflection only broad lines, and their intensity was weaker than one would expect from the analysis of the Mössbauer spectra. From these results we suggest that Fe_xC represents poorly defined structures intermediate between α -Fe and a known carbide structure. The question remains whether any relation exists between Fe_xC and the ϵ -carbide of Maksimov et al.⁷ For instance, Fe_xC might be a precursor of ϵ -carbide. More work will be done to clarify this.

In the Mössbauer spectrum of the χ -Fe₃C₂ sample measured at 4.2 K, we found a contribution characteristic for α -Fe₂O₃ though the broad lines indicate a distribution in hyperfine fields (Figure 3d). This contribution was not visible in the Mössbauer spectra measured at 77 and 295 K, respectively. Apparently the fraction of the sample in which this oxide contribution is present has a recoilless fraction which decreases rapidly with increasing temperature. It is conceivable, therefore, that it might be an oxide layer at the surface of the catalyst. However further experiments are necessary to clarify this point. The question whether this oxide layer has been formed during the Fischer-Tropsch synthesis or after removing the sample from the reactor can only be answered when Mössbauer experiments under reaction conditions are performed.

In the temperature-dependent experiments we found that Fe_xC was formed during Fischer-Tropsch synthesis at 433 and 463 K. Moreover Fe_xC was formed in an early

stage in the time-dependent experiments at 513 K. The carbides ϵ' -Fe_{2.2}C and χ -Fe₃C₂ appeared in catalysts that had been subjected to synthesis at temperatures from 463 K up to 623 K. Cementite, θ -Fe₃C, was formed at 623 and 723 K, and at the latter temperature it was the only carbide phase present. The temperature-dependent formation of carbides in metallic iron does not fit in the scheme for promoted iron catalysts as published by Sancier et al.¹⁰ As far as we are aware, no literature is available on the formation of carbides in unsupported and unpromoted metallic iron. Only Le Caer et al.¹² and Bernas et al.¹⁵ state that iron only forms single-phase χ -Fe₃C₂ at 673 K and single-phase θ -Fe₃C at 823 K in a gas mixture of 7H₂ plus 3CO. As we found that θ -Fe₃C was already formed at 623 K, the former observation is not consistent with our results.

Our sample of iron supported on a mixture of TiO₂ and CaO formed almost exclusively ϵ' -Fe_{2.2}C at 513 K, which agrees with the results of Amelse et al.⁵ for iron supported on SiO₂.

For a Fe/SiO₂ catalyst after 6 h of Fischer-Tropsch reaction, Raupp and Delgass⁴ found a Mössbauer spectrum which they analyzed with the three subpeaks of χ -Fe₃C₂, however, with an intensity ratio which differs strongly from the expected ratio 2:2:1. They ascribe this deviation to surface effects or to the presence of unknown intermediate structures. From temperature-dependent Mössbauer experiments it followed that the sample did not show a magnetic splitting above 505 K. Raupp and Delgass conclude from this result that the sample contains only χ -Fe₃C₂, which has a Curie point of 525 K. However this conclusion is not necessarily correct, because a carbide with a Curie point higher than 505 K may be present in a superparamagnetic state with a transition temperature lower than 505 K. The Mössbauer spectrum of their sample looks almost identical with the Mössbauer spectra that we have measured with samples after 6-h Fischer-Tropsch reaction or longer. These spectra could straightforwardly be analyzed as combinations of χ -Fe₃C₂ and ϵ' -Fe_{2.2}C. Thus we suggest that the Mössbauer spectrum that Raupp and Delgass⁴ measured with a Fe/SiO₂ catalyst after 6 h of Fischer-Tropsch reaction at 525 K does not represent some deformed χ -Fe₃C₂, but a combination of χ -Fe₃C₂ and ϵ' -Fe_{2.2}C, the latter phase being present in small particles with a superparamagnetic transition temperature below 505 K.

For a Fe/SiO₂ catalyst with an average diameter of 7.5 nm which has been exposed to Fischer-Tropsch synthesis at 525 K for 6 h, Raupp and Delgass⁴ find a Mössbauer spectrum which is a combination of mainly ϵ' -Fe_{2.2}C and some ϵ -Fe₂C. Temperature-dependent Mössbauer experiments confirm the presence of ϵ' -Fe_{2.2}C and some ϵ -Fe₂C. The X-ray diffraction pattern shows three reflections which the authors ascribe to ϵ -Fe₂C, which contradicts the Mössbauer experiments. Unfortunately they do not present the diffraction parameters, and we suspect that Raupp and Delgass have measured the same pattern as Barton and Gale.¹¹ As we discussed before, this pattern has to be ascribed to ϵ' -Fe_{2.2}C instead of ϵ -Fe₂C.

Nahon et al.⁶ have recently studied the formation of carbides in Fe/Al₂O₃ catalysts at 523 K. The Mössbauer spectrum of the catalyst after 19 h of Fischer-Tropsch reaction at 523 K has been ascribed by the authors to the carbide ϵ -Fe₂C. However this ascription is not right. From the observed effective hyperfine field of 184 kOe at $T = 4.2$ K, it follows that the carbide formed is ϵ' -Fe_{2.2}C.

Some authors⁴ consider ϵ' -Fe_{2.2}C as a less stable carbide. However in our experiments ϵ' -Fe_{2.2}C was formed at temperatures as high as 623 K, while Amelse et al.⁵ reported the thermal stability of ϵ' -Fe_{2.2}C on SiO₂ up to 673 K. So

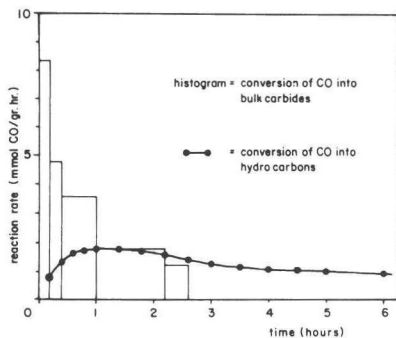


Figure 9. Conversion rate of CO into bulk carbides and into hydrocarbons during Fischer-Tropsch synthesis over metallic iron catalysts at 513 K.

we conclude that ϵ' -Fe_{2.2}C is a stable carbide, at least as stable as χ -Fe₅C₂.

In short, from the comparison of our results with those of various authors, we conclude that, apart from the temperature at which the reaction takes place, the nature of the catalyst (e.g., promoted or supported) is crucial for the process which determines which type of carbide will be formed.

Analysis of the Mössbauer spectra of catalysts after various periods of Fischer-Tropsch reaction indicates that as soon as a mixture of carbon monoxide and hydrogen is passed over the catalyst metallic iron is rapidly converted into the carbides Fe₂C, ϵ' -Fe_{2.2}C, and χ -Fe₅C₂. Apparently carbon atoms deposited at the surface by dissociative adsorption of CO can migrate into the catalyst at a high rate. In an early stage of the synthesis the catalyst will contain regions with α -Fe and regions where the carbides ϵ' -Fe_{2.2}C and χ -Fe₅C₂ are formed. Probably Fe₂C will be found in the boundary between those regions. When more and more metallic iron is converted into carbides, the diffusion rate of carbon atoms into the catalyst will slow down with the result that progressively more carbon atoms remain on the surface, forming there spots of graphite. A similar mechanism has recently been proposed by Raupp and Delgass,¹⁶ based on simultaneous kinetic and single velocity Mössbauer experiments. They noticed that during an experiment there is a linear relation between the amount of bulk carbides formed and the rate of hydrocarbon formation, and they suggest a causal relation between the two phenomena.

Another explanation is that the bulk carbide formation and the Fischer-Tropsch synthesis are in competition in such a way that a high rate of carbide formation entails a low rate of hydrocarbon formation. This presupposes that these two reactions have a common precursor (e.g., some type of surface carbon) that is formed in an overall rate-determining step. This model is supported by Figure 9, where we have plotted the conversion of CO into bulk carbides together with the conversion of CO into hydrocarbons, both as a function of time. These results suggest that iron atoms at the surface of the catalyst form the sites that are active in Fischer-Tropsch synthesis, although it is very well possible that these sites need some form of activation during the first minutes of the process. The increase of the initial activity by pretreating the catalyst with CO or C₂H₄ can be fully understood with this model. Depending on the duration of the pretreatment, a certain amount of carbon has diffused into the iron lattice. When the pretreated catalyst is then subjected to the Fischer-

Tropsch synthesis, the diffusion rate of carbon into the bulk of the catalyst is lower and the activity for the formation of hydrocarbons starts at a level well above zero.

However, since evidence that the formation of surface carbon is the rate-determining step for the reaction between carbon monoxide and hydrogen on iron catalysts is not available, we cannot exclude the possibility that hydrogenation of carbon monoxide and bulk carbide formation are two more or less autonomous processes, each with its own rate-determining step. Here a relatively slow activation of the iron surface would be the reason of the low activity for the formation of hydrocarbons during the early stage of the reaction process.

In both explanations (competition or autonomous processes) the activation for hydrocarbon synthesis can be understood by assuming that one or more carbon atoms are required to form together with iron an active ensemble where other carbon atoms are hydrogenated. This would be similar to the results of Araki and Ponec,¹⁷ who found that after ¹³C was laid down on a nickel film the rate of ¹²CH₄ formation was initially some six times greater than on a clean nickel film.

Since the measured carbon content of catalysts after Fischer-Tropsch synthesis for 6.5 h or longer is significantly higher than the carbon content of the bulk as calculated from the Mössbauer spectra, we conclude that the deactivation of the CO hydrogenation is caused by the formation of inactive carbon at the surface of the catalyst.

Conclusions

(1) The X-ray diffraction pattern which Barton and Gale¹¹ ascribed to a pseudohexagonal carbide Fe₂C should be attributed to the hexagonal carbide ϵ' -Fe_{2.2}C.

(2) During the Fischer-Tropsch synthesis at moderate temperatures (≤ 513 K), a carbide Fe₂C appears which has not been reported before. The presence of a hyperfine field distribution in the Mössbauer spectra and the weak and broad diffraction lines in the X-ray patterns indicate that Fe₂C represents poorly defined structures intermediate between α -Fe and a real carbide structure.

(3) The nature of an iron catalyst, i.e., whether or not it is promoted or supported, plays an important role in the process determining which carbide, or combination of carbides, will be formed at a given set of reaction conditions.

(4) The initially low activity of metallic iron in the Fischer-Tropsch process can be understood as the consequence of either a competition between bulk carbidization and hydrocarbon synthesis in which activation of the catalyst surface occurs relatively fast or a slow activation of the catalyst surface only. In the latter explanation bulk carbidization and hydrocarbon synthesis would be two autonomous processes.

(5) The deactivation of the catalyst is caused by the formation of spots of inactive carbon, which progressively block more active sites.

References and Notes

- (1) Frohning, C. D.; Cornils, B. *Hydrocarbon Process.* **1974**, *53*, 143.
- (2) Kölbl, H.; Tillmetz, K. D. *Ger. Offen.* 2 507 647, 1976.
- (3) Büssemeier, B.; Frohning, C. D.; Horn, G.; Kluy, W. *Ger. Offen.* 2 536 488, 1976.
- (4) Raupp, G. B.; Delgass, W. N. *J. Catal.* **1979**, *58*, 348.
- (5) Amelse, J. A.; Butt, J. B.; Schwartz, L. H. *J. Phys. Chem.* **1978**, *82*, 558.
- (6) Nahon, N.; Perrichon, V.; Turlier, P.; Bussiere, P. *J. Physique (Orsay, Fr.)* **1980**, *41*, C1-339.
- (7) Maksimov, Y. V.; Suzdalev, I. P.; Arents, R. A.; Loktev, S. M., *Kinet. Katal.* **1974**, *15*, 1293.
- (8) Loktev, S. M.; Makarenkova, L. I.; Silivskii, E. V.; Entin, S. D., *Kinet. Katal.* **1972**, *13*, 1042.
- (9) Hofer, L. J. E.; Cohn, E. M.; Peebles, W. C. *J. Am. Chem. Soc.* **1949**, *71*, 189.

- (10) Sancier, K. M.; Isakson, W. E.; Wise, H. presented at the Symposium on Advances in Fischer-Tropsch Chemistry, Anaheim Meeting, March 12-17, 1978.
- (11) Barton, G. H.; Gale, B. *Acta Crystallogr.* **1964**, *17*, 1460.
- (12) Le Caer, G.; Dubois, J. M.; Senateur, J. P. *J. Solid State Chem.* **1976**, *19*, 19.
- (13) Lipson, H.; Petch, N. J. *J. Iron Steel Inst., London* **1940**, *142*, 95.
- (14) Senateur, J. P. *Ann. Chim. (Paris)* **1967**, *2*, 103.
- (15) Bernas, H.; Campbell, I. A.; Fruchart, R. *J. Phys. Chem. Solids* **1967**, *28*, 17.
- (16) Raupp, G. B.; Delgass, W. N. *J. Catal.* **1979**, *58*, 361.
- (17) Araki, M.; Ponec, V. *J. Catal.* **1976**, *44*, 439.

Reprinted with permission of the American Chemical Society.

Introduction.

In chapter three we reported on the carburization of metallic iron, which was studied as a function of temperature and of synthesis time at 513 K. We limited ourselves, however, to the case in which the synthesis gas contained equal amounts of H_2 and CO, since this is believed to be the optimum composition for the production of unsaturated hydrocarbons¹.

Recently Unmuth et al² and van Dijk³ found that the rate of carburization depends on the synthesis gas composition. This has been established by following the increase in weight of the catalyst during the Fischer-Tropsch reaction.

In this chapter we describe an investigation in which in situ Mössbauer spectroscopy is used to study the influence of the H_2/CO ratio on the carburization rate of unsupported and unpromoted, metallic iron catalysts and on the composition of the catalyst with respect to the different iron carbides. Experiments have been carried out at two different temperatures and in two different laboratories. Carburization experiments at 515 K were done at Purdue University, West Lafayette, Indiana, U.S.A., whereas those at 575 K were done at the Interuniversitair Reactor Instituut, Delft, the Netherlands.

Experimental.

Carburization experiments at 515 K.

The chemical reactor and the gas handling system at Purdue University have been described by Delgass et al.⁴ The catalyst precursor consisted of 50 mg α - Fe_2O_3 (BASF, diameter 50 nm) and 250 mg silica (Cab-O-Sil, EH5) pressed into a wafer of 15 mm diameter. Reduction of the catalyst took place in H_2 (6 l/hr) at 400 K for 0.5 hour and at 675 K for 4 hour. The catalyst was cooled down to the reaction temperature of 515 K in flowing H_2 . After this reduction procedure the catalyst had a specific surface area of $10.9 \text{ m}^2/\text{g}$, as was determined with the BET method. Carburization was carried

out in a mixture of H_2 , CO and He at a total flow rate of 9 l/hr and with a fixed CO content of 10% by volume. We note that in the initial period of carburization the H_2/CO ratio in the reactor is higher than in the feed gas, due to residual H_2 from the reduction. After carburization during a chosen period of time of 0,5, 2 or 4 hour respectively the catalyst was cooled down to room temperature under the flow of reactants. All gases were UHP grade from Matheson, with the H_2 and CO gas being further purified by passage through an Engelhard Deoxo catalyst to remove oxygen and a bed of 5A and 13X molecular sieves to remove water. Mössbauer spectra were taken ex situ with the spectrometer to be described below.

Carburization experiments at 575 K.

The reactor used in these in situ Mössbauer experiments (figure 1) consists of an outer container made of brass (1) which is cooled with water on the outside (2) in order to permit the use of mylar windows (3). Aluminium foils (4) of 18 μm thick are used as a radiation shield. The heating block (5) is made of copper and it can be heated by means of thermocoax wires (6). The catalyst (7), pressed into a self supporting pellet, is mounted in the copper heating block (5) by means of a copper screw ring (8). The temperature is measured and regulated with a chromel-alumel thermocouple (9). The

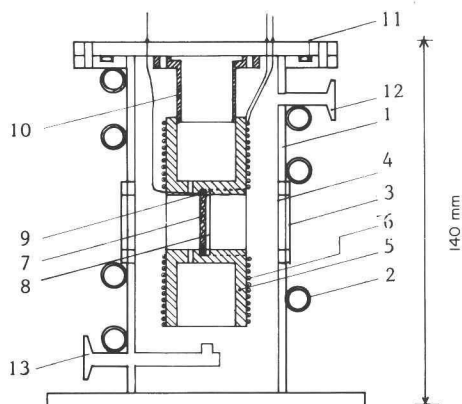


Fig. 1 Mössbauer in situ reactor. A detailed description is given in the text.

heating block and the lid of the outer container are connected by means of a stainless steel tube (10), which has been made very thin in order to minimize heat losses to the cooled part of the reactor.

The catalyst precursor consisted of 60 mg $\alpha\text{-Fe}_2\text{O}_3$ (BASF, diameter 50 nm) and 200 mg silica (Aerosil, 300 V) pressed into a wafer of 22 mm in diameter. Reduction of the catalyst was carried out as follows. After mounting the catalyst pellet in the reactor, the latter was evacuated to a pressure of 4×10^{-1} Torr and subsequently filled with argon. After heating to 77 K in Ar, reduction took place in 100% H_2 at a flow rate of 4 l/hr, during 1 hour. Before starting the carburization process the reactor was cooled to 575 K, evacuated to a pressure of 4×10^{-1} Torr and filled with Ar. Carburization occurred at 575 K during 2.5 hours in either a mixture of CO, H_2 and Ar with a constant total flowrate of 12.9 l/hr and a fixed CO content of 13 vol %, or in a mixture of CO and H_2 with a constant CO flow rate of 7.2 l/hr. The gases H_2 (Hoekloos, purity > 99.9%), CO (Hoekloos, purity > 99.5%) and Ar (purity > 99.997%) were purified separately over a reduced copper catalyst (BASF, R3-11) and a molecular sieve (Union Carbide, 5A) at room temperature. Oxygen contaminations in the purified gases were found to be lower than 5 ppm, by using an electrolytic Hersch cell.

Mössbauer spectra of samples in both series experiments were taken with a constant acceleration spectrometer, using a ^{57}Co in Rh source. Hyperfine fields were calibrated against the 515 kOe field of $\alpha\text{-Fe}_2\text{O}_3$ at room temperature, while isomer shifts are reported with respect to the NBS standard sodium nitro prusside (SNP). The following abbreviations will be used throughout this chapter. I.S.: isomer shift, H: magnetic hyperfine field, and Γ : experimental linewidth.

To determine the Mössbauer parameters of the reduced catalyst we used the method in which a calculated sextuplet is fitted to the experimental spectrum by variation of the Mössbauer parameters, as described in chapter two. The spectra of the partly carburized catalysts were analyzed, as far

as possible, by fitting them with a linear combination of base spectra of known composition. In those cases where this method could not be applied, we confined ourselves to the determination of the spectral area belonging to the first and sixth peak of the α -Fe subspectrum and the area of the total spectrum, using the method which was described in chapter two.

Results.

The Mössbauer spectra (not shown) of the catalysts which were reduced following the two different procedures as described in the experimental section, both yielded the following parameters at room temperature: I.S. = 0.27 ± 0.01 mm/s, $H = 333 \pm 2$ kOe, $\Gamma = 0.28 \pm 0.04$ mm/s. These parameters agree with those of bulk α -Fe.

In order to investigate whether the catalyst is affected by exposing it to air, the spectrum was also recorded *ex situ* at room temperature, and no difference was found in the spectrum. However, when the spectrum was recorded at 4.2 K, contributions of an iron oxide corresponding to about 12-15 % of the spectrum were observed. As it will be discussed in chapter five this oxide is mostly in the vicinity of the surface of the catalyst. Anticipating the results which will be presented in chapter five we already mention here that the spectrum of a similarly reduced catalyst recorded *in situ* at 4.2 K did not show the presence of any oxides at all. This means that a fully reduced α -Fe catalyst becomes oxidized at several layers of and near the surface, on exposing it to air at room temperature. However, the reduced catalyst that remained in the reactor and that will be used in the carburization experiments consists of 100% α -Fe.

Carburization experiments at 515 K.

Mössbauer spectra of the catalyst obtained after three different periods of carburization in mixtures of CO, H₂ and He of three different compositions are shown in figure 2. The spectra have been analyzed by fitting them with linear combinations of base spectra, the results are given in table I and figure 3. For the base spectra we used Mössbauer spectra of the

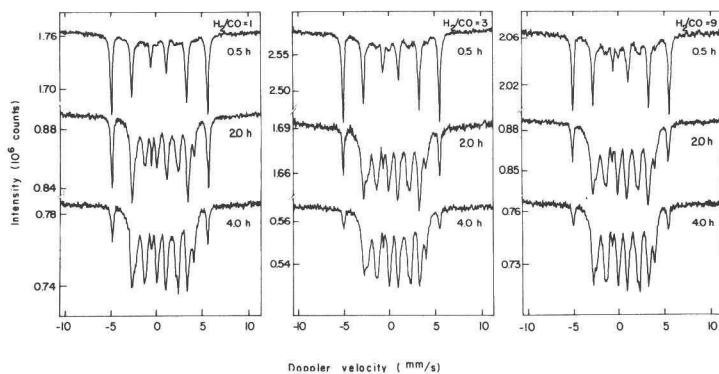


Fig. 2 Mössbauer spectra at room temperature of a metallic iron catalyst after different periods of carburization at 515 K in CO and H₂ mixtures of different compositions.

Table I Spectral composition of the Mössbauer spectra (fig. 2) of a metallic iron catalyst after carburization at 515 K.

H ₂ /CO	time (hr)	α-Fe	Fe _x C	ε'-Fe _{2.2} C	χ-Fe ₅ C ₂
				%	
1	0.5	85	a	a	a
	2.0	45	6	8	41
	4.0	21	4	21	54
3	0.5	76	6	7	11
	2.0	33	7	19	41
	4.0	16	4	30	50
9	0.5	75	9	0	16
	2.0	29	7	22	42
	4.0	16	4	24	56

Absolute uncertainty: 2 - 3 %; a) total carbide contribution: 15 %.

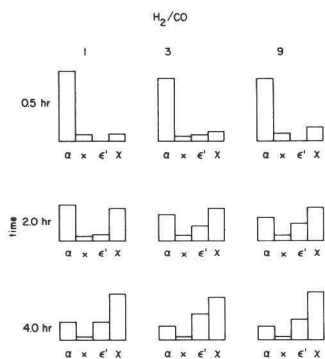


Fig. 3 Composition of the Mössbauer spectra in fig. 2, as given in table I. Abbreviations: α: α-Fe, x: Fe_xC, ε': ε'-Fe_{2.2}C, χ: χ-Fe₅C₂.

same carburized samples which have been used in chapter three.

Since we do not have a spectrum of Fe_xC as a single phase and moreover, because the spectrum of the carbide $\epsilon\text{-Fe}_{2.2}\text{C}$ has peaks in the velocity range where Fe_xC shows considerable absorption, it is not possible to separate the contributions of these phases to the Mössbauer spectra completely when they are both present. Therefore the contributions of the Fe_xC and $\epsilon\text{-Fe}_{2.2}\text{C}$ phases as mentioned in table I are less well-defined than the contributions of the other phases.

The results indicate that carburization at 515 K proceeds slower in synthesis gas with a composition in which $\text{H}_2/\text{CO} = 1$ than in synthesis gas with $\text{H}_2/\text{CO} = 3$ or $\text{H}_2/\text{CO} = 9$. The rates of carburization for the latter two compositions appear to be identical. A correlation between the compositions of the synthesis gas and the kind of iron carbide in the interior of the catalyst has not been found. In all cases the carbide $\chi\text{-Fe}_5\text{C}_2$ appears as the dominant carbide phase.

Carburization experiments at 575 K.

A different procedure was chosen for the experiments at 575 K. Here we studied the extent of carburization after a fixed period of 2.5 hours as a function of the H_2/CO ratio in the synthesis gas.

Figure 4 shows in situ Mössbauer spectra of the $\alpha\text{-Fe}$ catalyst after 2.5 hours of carburization at 575 K in a $\text{CO} + \text{H}_2 + \text{Ar}$ mixture with a constant flow of CO (1.7 l/hr) and a variable flow of H_2 . Sufficient Ar was added to keep the total gas flow constant. Also the spectra were analyzed by fitting them with linear combinations of base spectra, and the results of this analysis are given in table II.

It is seen that carburization proceeds only slowly in CO alone and that the rate of carburization increases strongly when H_2 is added to CO . As the most spectacular increase in the carburization rate occurs between $\text{H}_2/\text{CO} = 0$ and $\text{H}_2/\text{CO} = 1$, another series of experiments was carried out with H_2/CO ratios in this range. However, in order to adjust these very low H_2/CO ratios in a reproducible way it was necessary to increase the CO flow to

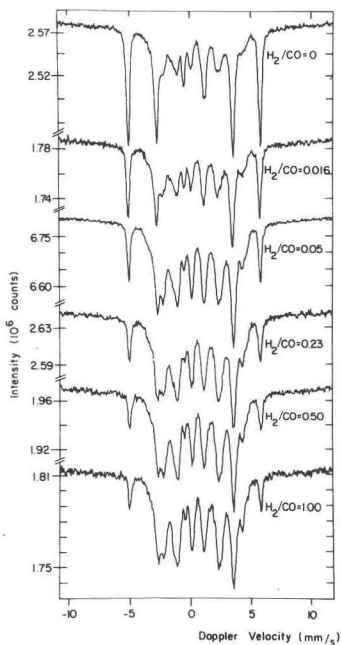
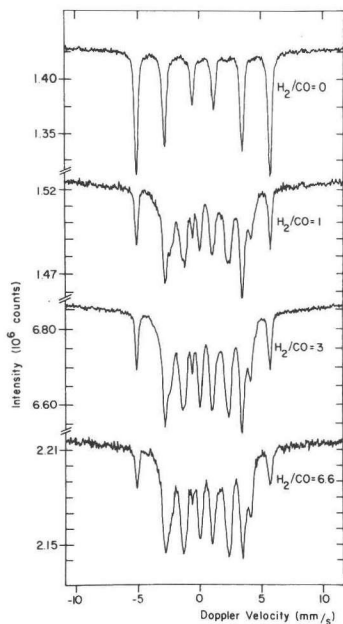


Fig. 4 (left) Mössbauer spectra at room temperature of a metallic iron catalyst after carburization at 575 K for 2.5 hour, in CO and H₂ mixtures of different compositions (CO flowrate: 1.7 l/h):

Fig. 5 (right) the same (CO flowrate: 7.2 l/h).

a constant rate of 7.2 l/hr. Mössbauer spectra of the α -Fe catalyst after carburization at 575 K in these CO rich mixtures during 2.5 hour are shown in figure 5. These spectra contain relatively large contributions of the poorly defined carbide Fe_xC. As already explained earlier, a detailed Mössbauer spectrum of this phase is not available and, therefore, the method in which linear combinations of base spectra are fitted to the experimental spectra could not be applied to the spectra in figure 5. Fortunately, the iron carbides show no absorption in the velocity range of the first and sixth peak of α -Fe. So we could calculate the spectral contribution of α -Fe, by determining the areas of the total spectrum and of the two α -Fe outer peaks assuming that the line intensities of the α -Fe subspectrum are equal to those of the reduced catalyst. The results of this calculation are shown in table III. Figure 6 shows the contribution of α -Fe to the Möss-

Table II Spectral composition of the Mössbauer spectra (fig. 4) of a metallic iron catalyst after carburization at 575 K for 2.5 hour.

H_2/CO	$\alpha-Fe$	Fe_xC	$\epsilon'-Fe_{2.2}C$	$\chi-Fe_5C_2$
0	93	a	a	a
1	34	6-11	10-15	45
3	23	3-6	20-23	51
6.6.	18	3-5	24-26	53

Absolute uncertainty: 2%; a) total carbide contribution: 7%.

bauer spectra of the partially carburized catalysts as a function of the CO/H_2 ratio. From this figure it is clear that for a given amount of CO the carburization rate increases with increasing CO/H_2 ratio. But the carburization rate also increases substantially with increasing partial pressure of CO.

In chapter three we found that one of the catalyst after 24 hours of Fischer-Tropsch synthesis and exposure to air showed contributions of an iron oxide in the Mössbauer spectrum at liquid helium temperature, which contribution could not be observed in the spectra at room temperature. It is interesting to see if such oxides have also been formed in the present samples. As the in situ reactor does not allow the recording of Mössbauer spectra at temperatures below room temperature, we had to measure the

Table III Contribution of metallic iron to the Mössbauer spectra (fig. 5) of a catalyst after carburization at 575 K for 2.5 hour.

H_2/CO	$\alpha-Fe(\%)$	H_2/CO	$\alpha-Fe(\%)$
0	52 ± 3	0.23	22
0.016	37	0.50	17
0.05	24	1.00	12

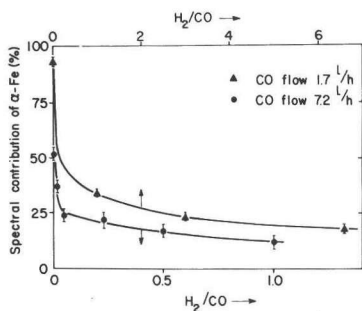


Fig. 6 Spectral contribution of α -Fe to the Mössbauer spectra of metallic iron catalysts after carburization at 575 K for 2.5 hour, as a function of the H_2/CO ratio in the synthesis gas.

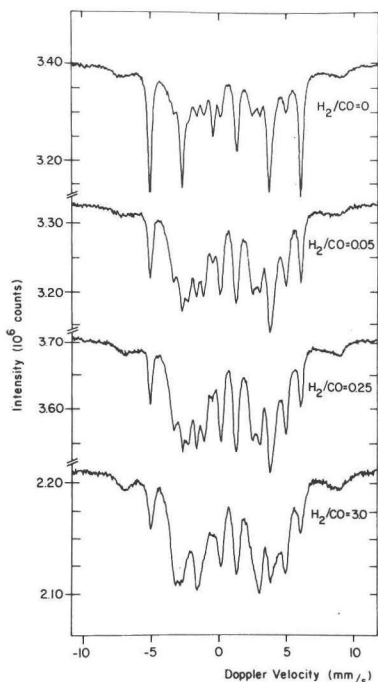


Fig. 7 Ex situ Mössbauer spectra at 4.2 K of metallic iron catalysts after carburization at 575 K.

helium spectra ex situ. The spectra are shown in figure 7 where it can be seen that oxide contributions appear indeed in the four partly carburized catalysts. The oxides account for about 8 - 12 % of the spectral areas.

Discussion

The main results of this work are:

- The rate of carburization increases with increasing hydrogen content of the synthesis gas, at fixed CO content.
- The rate of carburization increases with increasing CO pressure at constant H_2/CO ratio.

These conclusions have also been reached by van Dijk¹. He studied the weight increase of an unsupported iron catalyst at 513 K in three series of experiments: in CO as a function of CO partial pressure and in $CO+H_2$ mixtures as a function of H_2/CO ratio with fixed partial pressures of either CO or H_2 . Van Dijk observed a large increase in the weight gain of the catalyst when the gas composition varied in the H_2/CO range between 0 and 1. This is the same range in which we found the largest increase in the carburization rate. Furthermore, van Dijk found a positive order in CO for the weight increase, both in $CO+H_2$ and in CO only, consistent with our results in figure 6.

It should be noted that the two methods, Mössbauer spectroscopy and determination of the increase in weight of the catalyst, yield results that refer to different aspects of the catalysts behaviour. The weight gain of the catalyst is mainly determined by the rate at which carbon atoms are deposited at the surface, irrespective of whether these carbon atoms stay at the surface or diffuse into the bulk of the catalyst. Mössbauer spectroscopy on the contrary, detects the number of iron atoms belonging to a bulk carbide. The latter is a measure for the amount of carbon atoms that have diffused into the interior of the catalyst. As we have seen already in chapter three the difference between the total carbon content and the amount of carbon in bulk carbides can be considerable.

Unmuth et.al.² studied the increase in weight of iron supported on silica during carburization in CO and in CO + 3 H₂ at 528 K. They also found that the increase in weight proceeded considerably faster in the presence of H₂. The authors attribute this to a fast removal of oxygen atoms, originating from the dissociation of adsorbed CO at the surface, by means of a reaction with hydrogen to form water, leaving behind empty sites on the surface where new CO molecules can be adsorbed and dissociated. We will postpone a discussion on the carburization of iron to chapter five when additional information about the role of oxygen on the surface of the catalyst will be available.

With regard to the composition of the partially carburized catalysts we note that under the conditions of our investigations four iron containing phases were present: α -Fe, Fe_xC, ϵ' -Fe_{2,2}C and χ -Fe₅C₂. In all cases χ -Fe₅C₂ was the dominant carbide phase. Substantial contributions of the carbide θ -Fe₃C were not observed. These results are consistent with those of the temperature dependent carburization experiments described in chapter three.

After carburization at 515 K during 4 hour the catalysts still contained a significant amount of metallic iron, whereas in the experiments of chapter three 2.5 hour of carburization in a CO : H₂ = 1:1 mixture was sufficient to convert all metallic iron into carbides. We attribute this

difference to two factors. First, the particle size of the catalyst precursor $\alpha\text{-Fe}_2\text{O}_3$ used in this work was 50 nm, whereas that of the unreduced catalyst in chapter three was considerably smaller, 30 nm. Since the reduction of the latter catalyst has been carried out at a lower temperature than that of the former, we feel confident that the reduced catalyst that was used in chapter three was significantly smaller. Small particles carburize faster than larger ones, as was shown by Raupp and Delgass⁴. Second, a slightly higher partial pressure of CO has been used in the experiments of chapter three. One of the conclusions of the present investigation is that the carburization process has a positive order in CO.

The liquid helium spectra of figure 7 indicated that the surface of the catalysts is partially oxidized. These oxides were absent in the spectra measured both in and ex situ at room temperature. Since the catalysts have been exposed to air, it is not clear whether or not the iron oxides originate from the Fischer-Tropsch reaction. Only in the case of the reduced catalyst we can be sure that the surface became oxidized outside the reactor. This is in accordance with the observation of Geus⁵, that a metallic iron foil oxidizes to a depth of about 7 atomic layers on exposing it to air at room temperature.

Here we can only speculate on the origin of the oxides on the partially carburized catalysts. We conclude once more that in situ Mössbauer spectra of the catalyst at 4.2 K are a prerequisite in order to be able to answer the question whether or not surface oxides can be formed under Fischer-Tropsch conditions. This will be the subject of chapter five.

References

- 1 R.J. Madon, W.F. Taylor, J.Catal. 69, 32 (1981).
- 2 E.E. Unmuth, L.H. Schwartz, J.B. Butt, J.Catal. 63, 404 (1980).
- 3 W.L. van Dijk, thesis, Eindhoven, 1981.
- 4 G.B. Raupp, W.N. Delgass, J.Catal. 58, 337 (1979).
- 5 J.W. Geus, private communication.

A MÖSSBAUER STUDY OF SURFACE EFFECTS ON IRON FISCHER-TROPSCH CATALYSTS

J.W. NIEMANTSVERDRIET, C.F.J. FLIPSE, A.M. VAN DER KRAAN
and J.J. VAN LOEF

Interuniversitair Reactor Instituut, 2629 JB Delft, The Netherlands

Received 8 October 1981

Unsupported iron catalysts show contributions of iron oxide in their Mössbauer spectra after Fischer-Tropsch synthesis when the spectra are recorded at 4.2 K. This iron oxide is characterized by a low recoilless fraction, corresponding to a Debye temperature of about 50 K and by a broad distribution in magnetic hyperfine fields, ranging from 370 to 544 kOe, the magnetic field of bulk α -Fe₂O₃. It is argued that this oxide is located at the surface of the catalysts. In situ Mössbauer experiments confirm that iron surface oxide can indeed be formed during Fischer-Tropsch synthesis. Implications for the carburization of iron are discussed.

1. Introduction

Recently we reported a study on the behaviour of unsupported, unpromoted metallic iron catalysts in the Fischer-Tropsch process [1], the synthesis of hydrocarbons from CO and H₂. Iron catalysts are not stable during this reaction, and they are converted into iron carbides as was found from Mössbauer spectra of the catalyst after it had been removed from the reactor. In analysing Mössbauer spectra of the fully carburized sample taken at 4.2, 77 and 295 K, an interesting observation was made. In addition to a carbide contribution, the Mössbauer spectrum at 4.2 K contained a subspectrum with a hyperfine field of a magnitude such that it should be attributed to an iron oxide, while the spectra at 77 and 300 K only indicated the presence of iron carbides. Evidently the oxide subspectrum is associated with a part of the sample that has a recoilless fraction which decreases more rapidly with increasing temperature than the recoilless fraction related to the rest of the spectrum. Since atoms located at a surface have higher vibrational amplitudes and hence lower recoilless fractions than atoms in bulk material, we suggested that the iron oxide is located at the surface of the catalyst. As the Mössbauer spectra of the catalyst which was kept in air for several months did not change, we concluded that the oxide was formed either during the Fischer-Tropsch process or immediately after the sample was removed from the reactor.

In this paper we present a more detailed study on the oxide present in the air passivated catalyst and we describe some in situ Mössbauer experiments in order to investigate whether such surface oxide contributions can be formed during Fischer-Tropsch synthesis. The latter experiments were performed in a cell with a controllable atmosphere, in which reactions can be carried out at temperatures up to 800 K after which Mössbauer spectra can be recorded in situ at temperatures down to 2 K. A description of this cell is given in the experimental section.

2. Experimental

The surface oxide was investigated using a metallic iron catalyst after 24 h of Fischer-Tropsch synthesis at 523 K in a mixture of 1 CO + 1 H₂ + 3 He at 1 atm, followed by 1 h flushing in helium at 623 K. After cooling down to room temperature the sample was removed from the reactor and exposed to air. More details about the catalyst precursor and the reactor have been given previously [1].

Mössbauer spectra were obtained with a constant acceleration spectrometer,

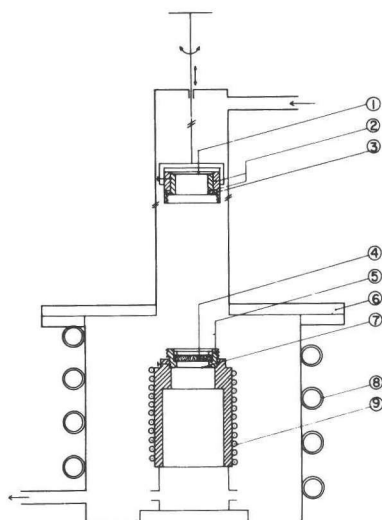


Fig. 1. Chemical reactor and absorber holder: 1 beryllium window, 2 upper part absorber holder, 3 indium O-ring, 4 absorber, 5 lower part absorber holder, 6 flange with O-ring, 7 beryllium window, 8 water cooling, 9 heating wire. The outside diameter of the reactor at the bottom is 100 mm.

using a ^{57}Co in Rh source (20 mCi). Hyperfine fields H are calibrated against the 515 kOe field of $\alpha\text{-Fe}_2\text{O}_3$ at room temperature. Distributions in H were calculated with the method of Hesse and Rübartsch [2], including the useful additional constraint that the endpoint intensities of the distribution should be zero, as suggested by Wivel and Mørup [3].

In order to be able to perform Mössbauer experiments at temperatures between 2 and 300 K with a catalyst that is kept in a controlled environment, we constructed a separate absorber holder which can be closed vacuum-tight in the chemical reactor, without exposing the catalyst to air. The closed absorber holder can be easily mounted into a cryostat, after which transmission Mössbauer experiments can be done at any desired temperature. Fig. 1 schematically shows the chemical reactor and the separate absorber holder.

The reactor consists of an outer container of brass, divided into two parts. A thick-walled stainless steel tube with heating coils is placed in the center. The heat transfer to the bottom of the reactor is minimized by making the stainless steel tube at the end very thin. The outer container is cooled by water. On top of the central heating tube the lower part of a stainless steel absorber holder can be mounted. This part contains the absorber, which is pressed into a self-supporting tablet. The upper part of the absorber holder contains an indium O-ring and is mounted on a movable stainless steel rod which extends to the exterior of the reactor. By lowering this rod, the upper part of the absorber holder can be screwed vacuum-tight onto the fixed part. The absorber holder is equipped with beryllium windows, vacuum brazed on the stainless steel. The temperature is monitored and regulated by a stainless steel sheathed chromel-alumel thermocouple (not shown). A temperature of 800 K can be obtained using a heating power of about 150 W in the thermocoax heating wires.

The catalyst precursor is a mixture of 35 mg $\alpha\text{-Fe}_2\text{O}_3$ (BASF, diameter 50 nm) and 115 mg silica (aerosil 300 V) pressed into a tablet. These tablets are reduced in flowing H_2 (4 l/h, 1 atm) at 670 K for 2.5 h. The reduced catalyst was treated at 500 K for 3 h either with CO at a flow rate of 3 l/h at 1 atm or with a mixture of 75% H_2 and 25% CO at a flow rate of 5.3 l/h at 1 atm.

The gases hydrogen (Hoekloos, purity > 99.9%), carbon monoxide (Hoekloos, purity > 99.5%) and helium (Hoekloos, purity > 99.95%) were puri-

fied separately over a reduced copper catalyst (BASF, R3-11) and a molecular sieve (Union Carbide, 5 A) at room temperature. Using a Hersch cell an oxygen contamination in these gases of 5 ppm or more can be excluded.

3. Results and discussion

3.1. Investigation of the oxide in a used catalyst

Fig. 2 shows Mössbauer spectra of the metallic iron catalyst after 24 h of Fischer-Tropsch synthesis recorded at several temperatures between 4.2 and 77 K. The spectrum at 77 K can entirely be attributed to the carbide $\chi\text{-Fe}_5\text{C}_2$, in which three crystallographically different iron sites are present. Identification of the carbide by means of its Mössbauer parameters has been described previously [1]. In the spectra at temperatures of 40 K and below, additional broad lines appear at positions that coincide with the outermost lines of the hyperfine spectrum of iron (III) oxides. The lines are much too broad to be fitted with single Lorentzians and we attribute this broadening to the presence of a distribution in hyperfine fields H .

Since the four inner lines of the Mössbauer spectrum of such oxides are hidden under the complex carbide spectrum, it is virtually impossible to derive the Mössbauer parameters of the oxide subspectrum in fig. 2. Fortunately knowledge of the shape of the two outermost lines is sufficient to calculate the

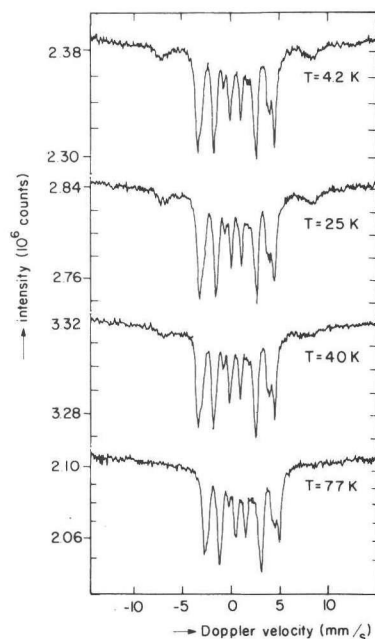


Fig. 2. Mössbauer spectra of an iron catalyst after 24 h of Fischer-Tropsch reaction at 515 K ($\text{H}_2:\text{CO}:\text{He}=1:1:3$, 1 atm) followed by 1 h helium flushing at 625 K. Spectra were recorded at the indicated temperatures.

distribution of hyperfine fields. This has been done for the spectrum at 4.2 K, requiring a high degree of smoothing in the distribution to avoid meaningless fluctuations. A value of 10 has been chosen for the smoothing parameter [2,3]. The result is given in fig. 3. The field values in the entire distribution are lower than 544 kOe, the value for bulk $\alpha\text{-Fe}_2\text{O}_3$ at 4.2 K.

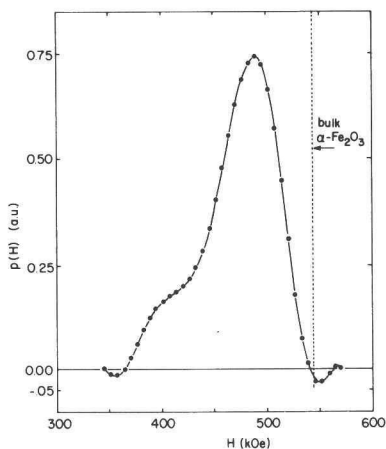


Fig. 3. Magnetic hyperfine field distribution of the oxide contribution in the spectrum at 4.2 K of fig. 1. The field of $\alpha\text{-Fe}_2\text{O}_3$ has been indicated for comparison.

Hyperfine fields that are lower than those of the bulk material been observed earlier in small particles or in surface layers [4–6]. If we assume that the oxide in the catalyst sample belongs to small particles which behave superparamagnetically, then the disappearance of the magnetically split pattern could reflect the transition into a superparamagnetic phase. However, from a careful analysis of the spectra measured between 25 and 77 K it can be concluded that no superparamagnetic doublet is being formed. Moreover, if the superparamagnetic transition temperature were below 77 K, the particles would have to be smaller than 4 nm in diameter [5]. It seems very unlikely, however, that such small particles are present in catalysts which have been subjected to temperatures as high as 623 K. So we conclude that the oxide is located at the surface of the catalyst.

More evidence for the presence of a surface oxide can be obtained by investigating its total resonant absorption. The absorption area of the oxide subspectrum decreases with increasing temperature much more rapidly than the total spectrum (fig. 4) and hence the recoilless fraction of the former is

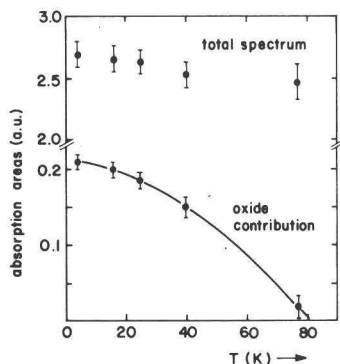


Fig. 4. Absorption area of the spectra in fig. 2 as a function of temperature.

considerably lower. Although the validity of the Debye model for atoms located at the surface can be questioned, the result that the recoilless fraction vanishes at temperatures exceeding 80 K can formally be translated into a

Debye temperature θ_D . By doing so it appears that the iron ions in the oxide are characterized by $\theta_D \approx 50$ K. This is much lower than the reported values of θ_D for bulk $\alpha\text{-Fe}_2\text{O}_3$ and $\alpha\text{-FeOOH}$ (500 K) [7] and for $\alpha\text{-Fe}$ (470 K) [8] respectively.

The low values of θ_D and the recoilless fraction illustrate that the iron atoms belonging to the oxidized part of the catalyst are subjected to vibrational modes that are considerably softer than in iron oxide bulk materials. This is another indication that the iron oxide is indeed located at the surface of the catalyst.

From the fact that the distribution of hyperfine fields extends to 540 kOe a surface composed of structures strongly resembling $\alpha\text{-Fe}_2\text{O}_3$ is suggested, although structure like FeOOH and Fe_3O_4 which have lower characteristic hyperfine fields cannot be excluded.

It is interesting to compare the surface oxide on the catalyst, which has a carbide structure in its interior, with the surface of iron oxide crystallites. Van der Kraan [5,6] deposited a layer of a few ångström $\alpha\text{-Fe}_2\text{O}_3$ enriched in the Mössbauer isotope ^{57}Fe onto $\alpha\text{-Fe}_2\text{O}_3$ crystallites with a mean diameter of 50 nm, enabling the study of the surface layer with Mössbauer spectroscopy more specifically. The enriched surface layer showed the Morin transition, a magnetic transition characteristic for $\alpha\text{-Fe}_2\text{O}_3$, which proves that the surface layers correspond to crystallographical $\alpha\text{-Fe}_2\text{O}_3$. The enriched layers have a distribution in hyperfine fields in the Mössbauer spectrum at 4.2 K, which ranges from 440 to 544 kOe [6]. The same range is found in the distribution of hyperfine fields of an enriched surface layer on $\alpha\text{-Fe}_2\text{O}_3$ crystallites with a mean diameter of 7 nm [6]. Although the major part of the distribution of hyperfine fields belonging to the surface oxide on the used catalyst (fig. 3) is within the same range, significantly lower values are also found. The latter might be attributed to either the presence of other oxides in the surface layers like FeOOH and Fe_3O_4 , or a mismatch of the surface layer to the underlying carbide structure.

3.2. In situ experiments

The precursor of our $\alpha\text{-Fe}$ catalyst consists of commercially available $\alpha\text{-Fe}_2\text{O}_3$ crystallites with a mean diameter of 50 nm. After reduction the catalyst was flushed with helium to remove all absorbed hydrogen.

A Mössbauer spectrum of the reduced catalyst, taken in situ at 4.2 K is shown in fig. 5a. The spectrum is entirely due to $\alpha\text{-Fe}$ and there is no evidence for any contribution of an iron oxide. So we conclude that the reduction

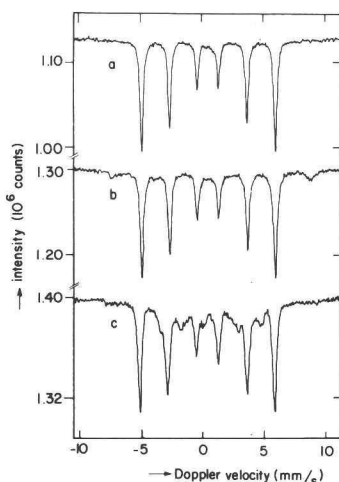


Fig. 5. In situ Mössbauer spectra recorded at 4.2 K of (a) an iron catalyst after 2.5 h reduction in H_2 at 670 K, (b) a reduced catalyst after 3 h CO treatment at 500 K and (c) after 3 h treatment with $1 \text{ CO} + 3 \text{ H}_2$ at 500 K.

Table 1
Contributions to the spectra in fig. 5

Catalyst treatment	α -Fe	Carbides	Oxides
Reduction	100%	0	0
CO, 500 K	85 \pm 5%	4 \pm 2%	11 \pm 3%
CO+3 H ₂ , 500 K	84 \pm 5%	13 \pm 2%	3 \pm 2%

conditions are adequate to reduce the whole catalyst, including its surface.

When such a fully reduced catalyst is treated with a flow of pure CO at 500 K during 3 h, the Mössbauer spectra at 300 and 77 K show the presence of α -Fe and a small amount of carbide. However, when the spectrum is recorded at 4.2 K an additional broad iron oxide spectrum appears as shown in fig. 5b. The contribution of the oxide subspectrum to the total spectrum is about 11% (table 1). The disappearance of the hyperfine-split oxide subspectrum between 4.2 and 77 K is certainly not the result of a transition into a superparamagnetic doublet, since a doublet with such an intensity would have easily been detected in the Mössbauer spectra taken in this temperature range. So the iron oxide spectrum is not due to small particles which behave superparamagnetically at 77 K, but it is associated with the surface of the catalyst.

The formation of this iron oxide cannot be attributed to the presence of 5 ppm O₂ in the feed gases. A rough estimate of the amount of iron oxide in the catalyst shows that it would have required an O₂ concentration of at least 150 ppm, if we assume that all the oxygen would react with the catalyst. The latter assumption is, of course, very unlikely in view of the construction of the reactor in fig. 1. Moreover O₂ levels as high as 150 ppm can be excluded with certainty. So we conclude that surface iron oxide layers can be formed when CO is brought into contact with metallic iron at 500 K.

When a mixture of 25% CO and 75% H₂ instead of pure CO is led over the reduced and helium flushed catalyst, considerably more carbide, but hardly any iron oxide is formed, as can be seen in the Mössbauer spectrum taken in situ at 4.2 K (fig. 5c). The contribution of the oxide subspectrum is small but detectable and it accounts for about 3% of the spectrum (table 1), while it is absent in the Mössbauer spectra at 77 and 300 K.

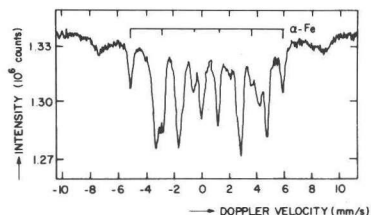


Fig. 6. In situ Mössbauer spectrum recorded at 4.2 K of the used Fischer-Tropsch catalyst of fig. 2 after reduction in hydrogen at 573 K for 2.6 h.

Finally, the used catalyst of fig. 2 was reduced in H₂ and subsequently studied in situ with Mössbauer spectroscopy at 4.2 K. Reduction of this catalyst at 500 K for 3.7 h did not change the spectrum of fig. 2a much, and in particular the contribution of the oxide subspectrum remained unchanged. The spectrum after 2.6 h reduction at 573 K is shown in fig. 6. From comparing the spectra of figs. 2 and 6 it follows that part of the iron carbide has been reduced to α -Fe, while the contribution of the oxide subspectrum remained the same. Apparently iron oxides at the surface are more stable with respect to H₂ than iron carbide in the bulk. For completeness we note that reduction of the catalyst precursor in H₂ at 573 K occurred very slowly.

The results of in situ Mössbauer experiments show that iron oxides can indeed be formed on the catalyst's surface in Fischer-Tropsch synthesis at 500 K. Moreover, H₂ plays an important role. In its absence a considerable

quantity of surface oxide is found, while in the $\text{CO} + 3\text{H}_2$ mixture only small amounts of oxide, just above the detection limit for the Mössbauer spectra, can be observed.

The result that surface oxides are formed on iron catalysts which are exposed to pure CO is in agreement with the results of Jagannathan et al. [9]. These authors used X-ray photo-electron spectroscopy to study the interaction of CO with polycrystalline iron foils. They found contributions of Fe^{2+} and Fe^{3+} in the spectra of foils exposed to 10^3 L ($= 10^{-3}$ Torr s) or more CO at 300 and 400 K, while such contributions were absent in the spectra of the clean foils. Jagannathan et al. [9] conclude that after CO dissociation oxide layers grow on the surface, while carbon diffuses into the interior of the foil.

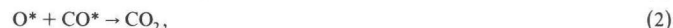
The conclusion with respect to carbon diffusion may be correct at the low exposures used in Jagannathan's investigation [9]. However, with CO pressures of 1 atm we found that the number of carbon atoms that diffused into the interior of the catalyst was substantially smaller than the number of oxygen atoms that reacted with iron to an oxide. Since oxygen and carbon atoms both arise from the dissociative adsorption of CO at the catalyst surface, at least one carbon atom must be present for every oxygen atom that reacts to an iron oxide. The contribution of iron carbide subspectra to the Mössbauer spectrum in fig. 5b is about 4%, whereas the contribution of the oxide subspectrum is about 11%. Taking the difference in the recoilless fraction into account, it means that a substantial fraction of carbon atoms must have remained at the surface of the catalyst.

Also, Bonzel and Krebs [10] found small signals due to oxygen on the surface of iron during Fischer-Tropsch synthesis, by means of Auger electron spectroscopy. The authors mentioned the possibility that this oxygen is coordinated to carbon in oxygenated species, proposed as intermediates for the Fischer-Tropsch synthesis. Bonzel and Krebs [10] did not consider the presence of iron oxides at the surface, but in view of the high hydrogen concentrations used by these authors, it seems not likely that much iron oxide can have been formed. Later Bonzel [11] suggested that absorbed water, condensed on the catalyst when it is cooled down to room temperature, could account for the oxygen contributions in the Auger spectra.

In connection with our work we note that condensation of water plays no role in our investigation, since on cooling the catalyst down to room temperature it is kept in flowing helium, which will remove all products present in the gas phase.

Carburization proceeded faster in a mixture of $\text{CO} + 3\text{H}_2$ than in pure CO. The same result has been obtained by Unmuth et al. [12] in isothermal carburization experiments with supported iron catalysts at 256°C . They concluded that H_2 facilitates both carbon deposition and carbide formation in the catalysts. The results of Unmuth et al. [12] and Jagannathan et al. [9], and the results of the present investigation can be understood on the base of the following scheme of reactions that occur at the iron surface.

In the absence of H_2 :



In the presence of H_2 the following reactions should be added



From our results it follows that in the interaction of iron with pure CO at 1 atm and 500 K, reaction (3) prevails over reaction (4), while at low CO exposures, such as 10^4 L , reactions (3) and (4) are about equally important [9].

We suggest that the presence of a considerable amount of surface oxide in the experiments at 1 atm CO pressure prevents the diffusion of carbon atoms

into the catalyst's interior and hence reaction (4) proceeds only slowly, so that a substantial fraction of the deposited C* remains at the surface of the catalyst.

When H₂ is also present, reaction (7) is responsible for removing most of the O* and only a small amount of surface oxide can be formed. Carburization is hardly hindered by these oxides, and since reaction (4) is much faster than reactions (5) and (8), most of the C* will disappear from the surface into the bulk of the catalyst [13].

A reaction between iron oxides and hydrogen to iron and water has not been included in the above scheme. The in situ Mössbauer experiments with a hydrogen-treated carbided catalyst which has an oxidized surface clearly showed that once a surface oxide has been formed, it cannot easily be reduced by hydrogen.

An explanation concerning the choice of our catalyst may be appropriate. Although this investigation is aimed at the detection of surface phenomena, we used an unsupported catalyst with a low surface area instead of a high area supported iron catalyst. The reason for this somewhat surprising choice is that supported iron catalysts usually have reduction degrees less than 100%. In that case the Mössbauer spectra will contain contributions of oxidic iron, characteristic for the contact between the reduced iron and the support [14]. Since contributions of surface oxides to the Mössbauer spectra would coincide with the subspectra of the unreduced iron, it would make identification of the surface oxides very difficult.

4. Conclusions

(1) When an unsupported iron catalyst is exposed to oxygen-free synthesis gas at 500 K, iron oxides can be formed at the surface of the catalyst. In the absence of hydrogen substantially more oxide is formed than in its presence. The surface oxides, once formed, cannot be reduced by hydrogen at 500 or 573 K.

(2) The iron oxides at the surface are observed in Mössbauer spectra, when these are recorded at temperatures well below 77 K. The oxides are characterized by a broad distribution in hyperfine fields with fields up to 540 kOe and by low recoilless fractions, corresponding to a Debye temperature of about 50 K.

We believe that the present investigation illustrates the usefulness of in situ Mössbauer spectroscopy in the characterization of iron catalysts. This work also clearly demonstrates that catalyst characterization by means of Mössbauer spectroscopy should not be restricted to room or liquid nitrogen temperatures, since interesting details can become available between liquid nitrogen (77 K) and liquid helium temperature (4.2 K).

References

- [1] J.W. Niemantsverdriet, A.M. van der Kraan, W.L. van Dijk and H.S. van der Baan, *J. Phys. Chem.* 84 (1980) 3363.
- [2] J. Hesse and A. Rübartsch, *J. Phys. E (Sci. Instr.)* 7 (1974) 526.
- [3] C. Wivel and S. Mørup, *J. Phys. E (Sci. Instr.)* 14 (1981) 605.
- [4] H. Topsøe, J.A. Dumesic and S. Mørup, in: *Applications of Mössbauer Spectroscopy*, Vol. II, Ed. R.L. Cohen (Academic Press, New York, 1980) ch. 2.
- [5] A.M. van der Kraan, *Phys. Status Solidi (a)* 18 (1973) 215.
- [6] A.M. van der Kraan, Thesis, University of Technology, Delft (1972).
- [7] C.F.J. Flipse, unpublished results.
- [8] C. Kittel, *Elementary Solid State Physics; A Short Course* (Wiley, New York, 1962) p. 58.
- [9] K. Jagannathan, A. Srinivasan, M.S. Hegde and C.N.R. Rao, *Surface Sci.* 99 (1980) 309.
- [10] H.P. Bonzel and H.J. Krebs, *Surface Sci.* 91 (1980) 499.
- [11] H.P. Bonzel, private communication.
- [12] E.E. Unmuth, L.H. Schwartz and J.B. Butt, *J. Catalysis* 63 (1980) 404.
- [13] J.W. Niemantsverdriet and A.M. van der Kraan, *J. Catalysis* 72 (1981) 385.
- [14] H. Topsøe, J.A. Dumesic, E.G. Derouane, B.S. Clausen, S. Mørup, J. Villadsen and N. Topsøe, in: *Preparation of Catalysts II*, Eds. B. Delmon et al. (Elsevier, Amsterdam, 1979).

Reprinted with permission of the North-Holland Publishing Company.

6 On the Time-Dependent Behavior of Iron Catalysts in Fischer-Tropsch Synthesis

Among the metals that display activity for Fischer-Tropsch synthesis, iron seems to occupy a special place. Its activity in the synthesis is initially low and increases slowly to a maximum, while simultaneously iron carbides are formed (1-3) (Fig. 1a,b). Cobalt and nickel, on the other hand (Fig. 1c), are active for the hydrocarbon formation from the beginning of the process and although carbides of these metals exist, no bulk carbides are formed during the synthesis. A model aiming to explain the behavior of iron in the Fischer-Tropsch (FT) process should also make clear why iron behaves differently from the other FT catalysts. Three explanations concerning iron during FT synthesis have been proposed in the literature. In this note we will discuss some experiments which in our opinion can discriminate between these explanations.

First we will give a brief survey of the explanations, which for easy reference will be denoted as the "carbide model," the "competition model," and the "slow activation model," respectively.

In the *carbide model* iron is not active for FT synthesis and the real catalyst has an iron carbide bulk structure with active sites on its surface. This explanation is favoured by many authors (1, 2, 4), in particular by Raupp and Delgass (2). In a very elegant *in situ* Mössbauer experiment they noticed that the FT activity increased almost linearly with the extent of carbidation. They suggest that this relationship is causal in the sense that the state of the bulk controls the number of active sites at the catalyst surface.

In the *competition model* (3) iron atoms at the surface of the catalyst are seen as the active sites. After adsorption and dissociation of CO and H₂ three reactions involving

the surface carbidic C* are possible:



Reaction (i) implies bulk diffusion of carbon into metallic iron, and this process is known to occur very fast ($E_a = 10-16$ kcal/mole). So in an early stage of the synthesis most of the carbon atoms are consumed by the carbidation reaction (i). When the bulk of the catalyst becomes more and more carbided, progressively more C* remains at the surface and becomes available for either hydrocarbon synthesis (ii) or deactivation (iii). So the rate of reaction (ii) goes through a maximum. The reactions compete as long as CO dissociation is slower than carbidation.

In the *slow activation model* (3) CO adsorption and dissociation are faster than all subsequent reactions, so that sufficient carbon is present on the surface to fulfill the demands of both bulk carbidation and hydrocarbon synthesis. Hence these processes are autonomous. Hydrogenation is believed to occur at surface complexes consisting of iron, carbon, and hydrogen atoms in a certain configuration. The FT activity is initially low because these complexes are thought to be formed at a low rate. In other words, the iron surface is slowly activated.

The three models have in common that deactivation results from the blocking of catalytically active sites by inactive carbon and possibly also by hydrocarbons with high boiling points.

All three models can account for the presence of at least three forms of carbon in the active iron catalyst, namely, bulk carbidic, inactive and surface carbidic carbon.

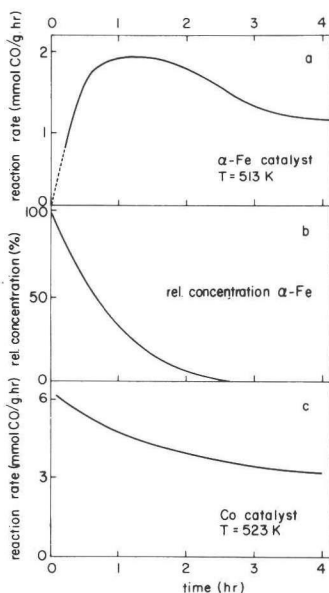


Fig. 1. Fischer-Tropsch reaction rates over (a) single-phase iron (3) and (c) single-phase cobalt (15) ($\text{H}_2 : \text{CO} : \text{He} = 1 : 1 : 3$, 1 atm), and (b) relative concentration of α -Fe during the synthesis as determined with Mössbauer spectroscopy (3).

The presence of bulk-carbide and inactive or free carbon in iron FT catalysts has already been known for more than 30 years (5), but knowledge about the surface-carbide carbon has been obtained only recently with surface sensitive techniques (6).

Although the models are obviously different, each of them can also account for the results in Fig. 1a,b. We will now cite some experiments which in our opinion can discriminate between the three explanations.

PRECARBIDED CATALYST

Matsumoto and Bennett (7) reported extensive and very detailed FT experiments at 250°C with a commercial fused iron catalyst. When a carbided catalyst at steady-state activity is subjected to pure hydrogen,

the immediate formation of a large amount of methane is observed, the rate of which decreases rapidly to a "pseudo-constant" level. The authors interpret this as the rapid hydrogenation of surface carbon, intermediate in the FT synthesis, followed by the much slower hydrogenation of bulk carbides when the active carbon phase has disappeared. Raupp and Delgass (2) give a similar interpretation for their hydrogenation experiments with fully carbided iron catalysts.

In this way Matsumoto and Bennett (7) prepared a catalyst with a carbided iron structure but a clean iron surface. This catalyst is immediately active in the FT synthesis and its activity shows a temporary overshoot compared to the steady-state activity in the standard experiment.

The result that a clean iron surface with an underlying bulk carbide structure is initially active in FT synthesis is evidently in agreement with the carbide model since it will only take a very short time before the surface will be carbided. Also the competition model allows for a satisfactory explanation of this experiment. In this model the clean iron surface is active for FT synthesis and since the bulk of the catalyst has already been carbided all C^* deposited from the synthesis gas remains at the surface to form either hydrocarbons or inactive carbon. However, we believe that this experiment does not support the slow activation model, since on a clean iron surface the necessary iron carbon complexes are thought to be formed at a low rate and it is hard to imagine why the presence of an underlying carbide structure should have such a profound effect on the formation rate of these complexes.

PREOXIDIZED CATALYST

Dwyer and Somorjai (8) investigated the hydrogenation of CO over polycrystalline iron foils at 300°C and found the commonly observed activity pattern of iron. They oxidized one of the foils and observed a ten-

fold increase in initial methanation rate compared to reduced iron foils. With Auger spectroscopy it is seen that about 25 min of synthesis are needed to remove all oxygen from the upper layers of the foil. During that time the preoxidized foil has already produced five times more methane than a reduced foil. Dwyer and Somorjai (8) conclude that in the reducing atmosphere of $\text{CO} + \text{H}_2$ highly active iron atoms or clusters are formed at the surface and that these iron sites probably are the active centers for FT synthesis.

The carbide model cannot explain this experiment. Irrespective of whether the reduced or the unreduced iron atoms in the oxidized foil catalyze the rapid hydrogenation, the active surface is certainly not the result of a bulk carbidic structure underneath it. As it is hard to understand why the necessary iron-carbon complexes should be formed rapidly on freshly reduced iron atoms on an underlying oxide and only slowly on metallic iron itself, we believe that the slow activation model also fails here. The experiment is consistent with the competition model. Here the freshly reduced iron atoms or clusters are active for the FT synthesis. Since diffusion of carbon into iron oxide does not take place and reduction of iron oxide at 300°C occurs only slowly, almost all surface carbidic carbon is available for the FT reaction and a high activity is expected.

IRON-RUTHENIUM ALLOY CATALYST

Ott, Fleisch, and Delgass (9, 10) reported FT experiments over FeRu alloys in a composition range where bulk carbides do not exist. Strong surface enrichment of iron occurs in these alloy catalysts. When used in FT synthesis at 573 and 617 K the catalysts show a high initial activity, which is found to increase with increasing iron content. This high initial activity, however, is followed by rapid deactivation. No carbides are formed during the synthesis.

We believe that this experiment clearly shows that iron in FeRu alloys can be ac-

tive for FT synthesis without the presence of a bulk carbide structure in the catalyst; hence the experiment is not in agreement with the carbide model. Since the iron at the alloy catalyst surface shows a high initial activity, the slow activation model also fails here. The FeRu experiments can, however, be easily understood in terms of the competition model. Here the iron atoms at the surface are active sites and carbon atoms deposited at these sites are available for FT synthesis and deactivation, since no bulk carbidation occurs.

Recently it was found (11) that the iron nitride Fe_4N is immediately active for Fischer-Tropsch synthesis at 240°C, while the conversion of Fe_4N into iron carbonitrides and carbides occurs on a much longer time scale, as was seen in Mössbauer experiments. Also, in this case a correlation between a high initial activity and a low rate of carbon diffusion into the bulk of the catalyst is clearly observed, consistent with the competition model.

DISCUSSION

We believe that the failure of the slow activation model and the carbide model in explaining respectively four and three of the four experiments referred to above, forms sufficient evidence to reject these models. The general tendency of the experiments is that when diffusion of carbon into the catalyst can be prohibited the FT rate starts at an initially high value. This is in agreement with the concept that iron itself is active for FT synthesis and that a competition between carbidation (reaction (i)), hydrogenation of surface carbon (reaction (ii)), and deactivation (reaction (iii)) governs the rate of the FT synthesis, i.e., that the competition model, operates.

The apparent linear relationship that Raupp and Delgass (2) found between extent of carburization and FT activity has not been found by Amelse *et al.* (1) and Niemantsverdriet *et al.* (3). They observed that their iron catalyst was at maximum activity significantly before all iron had

been converted into carbides. Vannice (12) reports that the CO + H₂ reaction is near first order in hydrogen and close to zero order in CO. These reaction orders are valid in a range of experimental conditions which include those of the three mentioned investigations (1-3). So the FT activity (ii) will be strongly dependent upon the hydrogen partial pressure. Furthermore, the carbidation rate and hence the extent of carbidation depend on the particle size, such that small particles carbide faster than larger particles (13). It is conceivable that combinations of particle size and H₂/CO ratio exist that may result in a more or less parallel course of FT activity and extent of carburization, while other combinations do not.

In order to explain why iron differs from cobalt and nickel in time dependent FT behavior we will consider the activation energies for carbon diffusion (14), which are 10.5-16.5 kcal/mole for α -Fe, 33.0-34.8 kcal/mole for Ni and 34.7 kcal/mole for Co, and the activation energies for the FT reaction (12), 21.3 \pm 0.9 kcal/mole for α -Fe, 25.0 \pm 1.2 kcal/mole for Ni and 27.0 \pm 4.4 kcal/mole for Co. Since the exponential factors for both groups of reactions are equal within a factor of 40, a comparison of reaction rates based on activation energies alone is justified.

In the case of iron the carbidation rate is higher than the FT rate (3), which results in carbon deficiency in the early stage of the synthesis. In the case of cobalt and nickel the rates of carbon diffusion into the catalyst are slower than in iron by a factor of 10⁵. So with cobalt and nickel catalysts the FT reaction rate will be much larger than the carbidation rate. Hence the difference between iron and the other FT catalysts can be understood in terms of the different rates of carbon diffusion into the metals.

We therefore believe that the competition model satisfies the requirements formulated in the introduction of this paper and that it accounts satisfactorily for the time-dependent behavior of iron-containing catalysts during Fischer-Tropsch synthesis.

REFERENCES

1. Amelse, J. A., Butt, J. B., and Schwartz, L. H., *J. Phys. Chem.* **82**, 558 (1978).
2. Raupp, G. B., and Delgass, W. N., *J. Catal.* **58**, 361 (1979).
3. Niemantsverdriet, J. W., van der Kraan, A. M., van Dijk, W. L., and van der Baan, H. S., *J. Phys. Chem.* **84**, 3363 (1980).
4. Schäfer-Stahl, H., *Angew. Chem., Int. Ed. (English)* **19**, 729 (1980).
5. Storch, H. H., Golombic, N., and Anderson, R. B., "The Fischer-Tropsch and Related Synthesis", Wiley, New York, 1951.
6. Krebs, H. J. and Bonzel, H. P., *Surface Sci.* **88**, 269 (1979).
7. Matsumoto, H., and Bennett, C. O., *J. Catal.* **53**, 331 (1978).
8. Dwyer, D. J., and Somorjai, G. A., *J. Catal.* **52**, 291 (1978).
9. Ott, G. L., Fleisch, T., and Delgass, W. N., *J. Catal.* **60**, 394 (1979).
10. Ott, G. L., Fleisch, T., and Delgass, W. N., *J. Catal.* **65**, 253 (1980).
11. van Dijk, W. L., and Niemantsverdriet, J. W., unpublished results.
12. Vannice, M. A., *J. Catal.* **37**, 462 (1975).
13. Raupp, G. B., and Delgass, W. N., *J. Catal.* **58**, 348 (1979).
14. Baker, R. T. K., *Catal. Rev. Sci. Eng.* **19**, 161 (1979).
15. Rautavuoma, A. O. I., Ph.D. thesis, Eindhoven, 1979.

J. W. NIEMANTSVERDIET
A. M. VAN DER KRAAN

Interuniversitair Reactor Instituut
2629 JB Delft
The Netherlands

Received May 26, 1981; revised August 11, 1981

Reprinted with permission of Academic Press, Inc.

Introduction.

One of the most promising possibilities for the Fischer-Tropsch synthesis may be the production of light olefins, ethylene en propylene. Among the metals used as active components in Fischer-Tropsch catalysts, iron offers the best prospects for a synthesis yielding a high fraction of light olefins. To achieve this the iron has to be promoted in a way such that not only the olefinic content of the products is high but also the mean molecular weight is low. In his thesis Kieffer¹ reviewed the elements, mentioned in the patent literature, which are believed to promote iron in the desired way. It seems that a number of transition metals in the groups IV-VII and some non metals like sulphur and chlorine are the most interesting promoting elements to obtain an olefin selective Fischer-Tropsch catalyst.

However, the addition of the right promotor is not the only prerequisite to obtain high olefin yields. Also the choice of the reaction conditions can influence the olefin to paraffin ratio's greatly. Madon and Taylor² showed that, within certain limits of the parameters, the olefin fraction increases with increasing space velocity and with decreasing H_2/CO ratio, temperature and pressure.

Various authors reported an increased olefin selectivity for iron catalysts which had been promoted with manganese, a group VII transition metal. Kölbel et al.³ prepared olefin selective iron catalysts with a very high manganese content, Fe : Mn = 1:9 (atomic ratio). The catalysts were activated with carbon monoxide at 513 K before the start of the Fischer-Tropsch synthesis. The olefin selective catalysts developed by Büssemeier et al.⁴ contained iron and manganese in a 1:1 atomic ratio. But also smaller amounts of manganese are capable of increasing the olefin selectivity, as Yang and Oblad⁵ reported for a catalyst with a Fe:Mn atomic ratio of 20:1. The beneficial effect of manganese for olefin production does not seem to be limited to iron alone. Barrault et.al.⁶ reported that when cobalt catalysts are

promoted with manganese and chlorine the reaction rate decreases whereas the selectivity in light olefins increases; in particular methane formation is strongly inhibited.

Recently very promising results have been obtained with zeolite catalysts. Rao and Gormley⁷ reported that a catalyst consisting of the molecular sieve silicalite which has been impregnated with iron and promoted with potassium has a high selectivity for the production of C₂-C₄ olefins from synthesis gas. In this respect Fraenkél and Gates⁸ obtained spectacularly favourable results with a catalyst consisting of zeolite-encapsulated cobalt clusters. Under properly adjusted reaction conditions these shape selective catalysts converted CO + H₂ to almost exclusively propylene at a satisfactory activity and stability. These results illustrate that promotion by manganese is certainly not the only way to increase the production of low olefins.

This chapter primarily deals with the Mössbauer spectroscopy of manganese promoted iron catalysts, prepared by coprecipitation in a way similar as has been done before with an unpromoted α -Fe catalyst⁹ as described in chapter three. An account which concentrates on the catalytic aspects has been published elsewhere¹⁰.

Experimental

The Fe-MnO catalysts were prepared by slowly adding ammonium hydroxide (12% by wt, Merck P.A., 2.8 ml/min) to a solution (3 liter) of 0.25 mol/l iron (III) nitrate (Merck P.A.) and 0.16 mol/l manganese (II) nitrate (Riedel P.A.), which was heated to 363 K. Ammonia addition was stopped when a pH of 8 was reached. The precipitate was filtered and washed with 0.2 l distilled water and subsequently dried at 393 K for 24 hour and calcined at 673 K for 1 hour. In order to investigate a possible role of starting materials, catalysts were also prepared by precipitation from solutions of iron and manganese sulphates, bromides and chlorides. A sample of pure manganese oxide was obtained by precipitation from a solution of manganese (II) nitrate.

The reactor system, the purification of the gases and the product analysis have been described in chapter three. Reduction of the catalyst took place

in flowing H_2 (6 l/h) at 623 K, 1 atm and for 16 hour. Fischer-Tropsch synthesis was carried out with 0.5 gram of catalyst in a mixture of $CO : H_2 : He = 1 : 1 : 3$ at a flow rate of 6 l/h at 1 atm. and at differential conversions below 5%. The catalytic activity is defined as the number of mmol CO converted into C_1 through C_3 hydrocarbons, per gram Fe per hour.

X-ray diffraction patterns of the samples were taken on a Philips diffractometer Pw 210700 with Mn filtered Fe $K\alpha$ radiation. Mössbauer spectra were obtained with a spectrometer of the constant acceleration type, using a source of ^{57}Co embedded in a Rh-matrix. Isomer shifts are given relative to the NBS standard sodium nitroprusside (SNP or $Na_2Fe(CN)_5 \cdot NO \cdot 2H_2O$) at room temperature, while hyperfine fields are calibrated against the 515 kOe field of $\alpha-Fe_2O_3$ at room temperature.

Results

Unreduced catalysts

Figure 1 shows the Mössbauer spectra of the unreduced catalyst, obtained from nitrates, recorded at 4.2 K, 77 K and 295 K, respectively. The spectrum obtained at room temperature has been analyzed with the Lorentzian fitting procedure, the results are listed in table I.

The spectrum shows two components, labeled I and II. Component I has the I.S. and ϵ' of $\alpha-Fe_2O_3$, but H_{eff} (507 ± 2 kOe) is significantly lower than the 515 kOe field of bulk $\alpha-Fe_2O_3$. The subspectrum of component I at 295 K is slightly asymmetrically broadened towards lower hyperfine splittings. This broadening and the reduced value of H_{eff} indicate that $\alpha-Fe_2O_3$ is present in small particles, with a distribution in particle size. Following Van der Kraan¹¹ a mean diameter of $230 \pm 20 \text{ \AA}$ can be estimated for these $\alpha-Fe_2O_3$ particles. Component II shows a doublet at $T = 295$ K, but is magnetically split at $T = 77$ K and 4.2 K, with a broad distribution in H_{eff} . The average value of H_{eff} at $T = 77$ K and 4.2 K, and also the I.S. and ΔE_Q at $T = 295$ K, are characteristic for small particles $\alpha-FeOOH$, with a distribution in particle diameters. Based on the average hyperfine field and on the fact that the superparamagnetic transition temperature is lower than 295 K, it can be

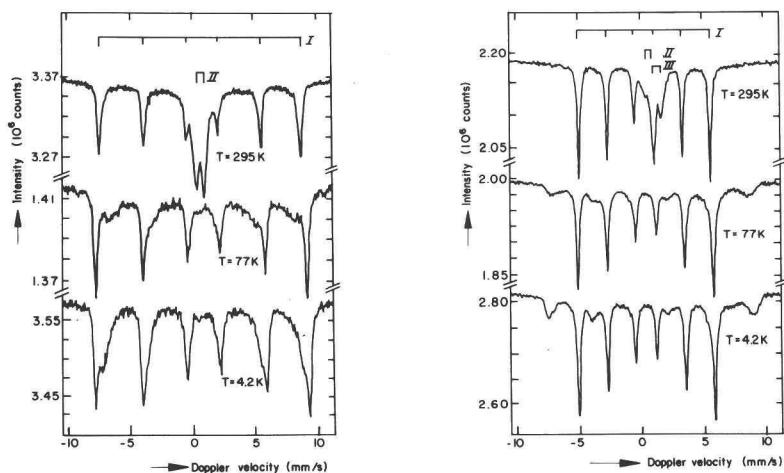


Fig. 1 (left) Mössbauer spectra of the unreduced Fe-MnO catalyst recorded at the temperatures indicated.

Fig. 2 (right) Mössbauer spectra of the reduced Fe-MnO catalyst.

concluded that the particle diameter is smaller than 85 \AA .¹¹ It should be noted that estimates of particle diameters are presented under the assumption that Van der Kraan's results, obtained with samples of small particles $\alpha\text{-Fe}_2\text{O}_3$ or $\alpha\text{-FeOOH}$, apply also to the presently investigated samples, in which $\alpha\text{-Fe}_2\text{O}_3$ and $\alpha\text{-FeOOH}$ are present together with manganese oxide.

Table I Mössbauer parameters at 295 K of Fe-MnO catalysts.

	Component	I.S. (mm/s)	ΔE_Q (mm/s)	ϵ' (mm/s)	H_{eff} (kOe)	Relative Area (%)
before	I	$.64 \pm .03$	-	$.09 \pm .03$	507 ± 2	54
reduction	II	$.59 \pm .02$	$.67 \pm .02$	-	-	46
	I	$.26 \pm .03$	-	$.00 \pm .01$	332 ± 2	80
after	II	$.48 \pm .06$	$.55 \pm .06$	-	-	7
reduction	III	$1.35 \pm .06$	$.63 \pm .06$	-	-	13

According to the X-ray diffraction pattern (not shown) the manganese oxide is present as Mn_2O_3 .

Reduced catalysts

Mössbauer spectra of the catalysts after reduction are shown in figure 2. The spectrum obtained at room temperature was analyzed with the Lorentzian fitting procedure as a combination of a sextuplet, labeled as component I, and two doublets, II and III. See table I for results. Component I is easily identified as α -Fe. The parameters of component II are those of a paramagnetic Fe^{3+} compound, while the parameters of component III are more indicative for Fe^{2+} , in spite of the fact that ΔE_Q is rather small for a Fe^{2+} compound. At temperatures of 77 K and 4.2 K components II and III are magnetically split, each with a distribution in hyperfine fields. Estimated mean values of H_{eff} for component II are given in table II and these values are also indicative that II is a Fe^{3+} compound. The subspectrum of component III is very broad and difficult to observe at these low temperatures, so that even a rough estimation of its Mössbauer parameters seems hardly warranted. The contribution of α -Fe to the Mössbauer spectrum obtained at $T = 295$ K is $(80 \pm 3)\%$, so it can be concluded that the main part of the iron oxide that was present in the precipitated catalyst has been reduced.

Table II Magnetic hyperfine fields H_{eff} in the Fe-MnO catalysts.

Component		H_{eff} (kOe)		
		T = 295 K	T = 77 K	T = 4.2 K
before	I	507 ± 2	530 ± 2	537 ± 2
reduction	II	-	$470 \pm 5^*$	$502 \pm 5^*$
after	I	332 ± 2	339 ± 2	341 ± 2
reduction	II	-	$495 \pm 5^*$	$513 \pm 5^*$

*: Average value of a distribution in H_{eff} .

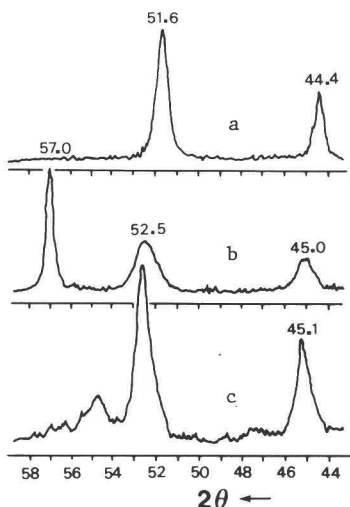


Fig. 3 X-ray diffraction patterns of a) a MnO reference sample, b) a reduced Fe-MnO catalyst and c) the same catalyst after 16 h Fischer-Tropsch synthesis at 513 K.

A sample containing only Mn_2O_3 was reduced in the same way as the other catalysts. The X-ray diffraction pattern of this reduced sample is shown in figure 3a and the parameters agree with those reported for MnO by Swanson et al.¹² The X-ray diffraction pattern of the reduced iron manganese catalyst in figure 3b shows clearly the reflection of $\alpha\text{-Fe}$ at $2\theta = 57^\circ$ and two reflections due to the presence of MnO, but the diffraction lines are broader and they are shifted towards higher angles in comparison with the pattern of pure MnO in figure 3a. Reflections corresponding with the Fe^{3+} and the Fe^{2+} phases which do appear in the Mössbauer spectra, are not observed in the X-ray patterns.

Since the reduction conditions are sufficient to convert pure $\alpha\text{-Fe}_2\text{O}_3$ completely into $\alpha\text{-Fe}$, we suggest that the presence of the unreduced iron compounds observed in the Mössbauer spectra and the shifted MnO lines in the X-ray patterns reflect the interaction between the MnO and the rest of the catalyst.

Catalysts during Fischer-Tropsch synthesis

The behaviour of the Fe-MnO catalysts during Fischer-Tropsch synthesis at 513 K was studied with Mössbauer spectroscopy, following the same procedure as described in chapter 3⁹. Spectra of catalysts after different

periods of synthesis were recorded after quenching the reaction in helium and removing the catalyst from the reactor. For each experiment a fresh catalyst from the same batch of unreduced material was used. Differences of maximal 10% were found in the reaction rates at corresponding time intervals for the various experiments. Since the product analysis was accurate to within 1% we believe that the observed differences reflect uncontrolled variations in the reduction process. The product distributions and the general shapes of the reaction rate curves for the various experiments were equal and hence we feel confident that the Mössbauer spectra of the catalyst after different periods of synthesis give a reliable picture of the catalysts behaviour during the Fischer-Tropsch process in a way as has been shown before with pure α -Fe as the initial catalyst.

A representative curve of the reaction rate as a function of time is given in figure 4, in which also the corresponding selectivities for the formation of CH_4 , C_2H_4 and C_2H_6 are included. This time dependent activity pattern at 513 K is very similar to that of an α -Fe catalyst, the reaction rate is initially low, increases to a maximum which is reached after about 1.5 hour, followed by a slow but steady deactivation. Also the selectivity pattern of the Fe-MnO catalyst does not differ much from the one obtained with unpromoted iron. This result is somewhat unexpected in view of the findings of Bussemeier et al.⁴, Kölbel et al.³ and Yang and Oblad⁵. The

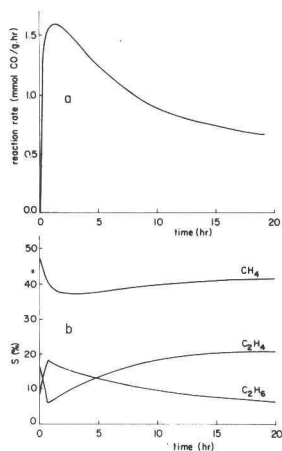


Fig. 4 The Fe-MnO catalyst in the Fischer-Tropsch synthesis at 513 K, a) the reaction rate and b) the methane, ethane and ethylene selectivities

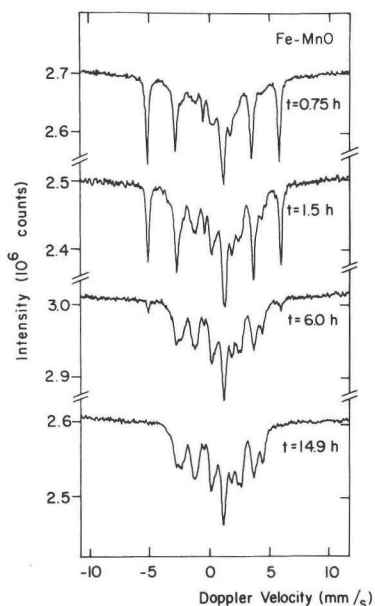


Fig. 5 Mössbauer spectra at room temperature of the Fe-MnO catalyst after different periods of Fischer-Tropsch synthesis at 513 K.

absence of any relation between the C_2H_4 selectivity and the MnO content of the Fe-MnO catalyst¹⁰ is even more unexpected. When the synthesis is carried out at 623 K the C_2H_4 selectivity decreases to a level below 10%.

Mössbauer spectra of the catalyst after various periods of Fischer-Tropsch synthesis at 513K are shown in figure 5. The spectra were analyzed by fitting a linear combination of base spectra to the measured spectra. The Mössbauer spectra that were used as a base are the single phase carbide spectra from chapter 3, completed with the spectra of α -Fe and the sub-spectra of doublets belonging to the unreduced iron phases in the catalyst after reduction. Results of this analysis are shown in figure 6

During the Fischer-Tropsch reaction at 513 K, the α -Fe is converted into the carbides ϵ' - $Fe_{2.2}C$ and χ - Fe_5C_2 . In this conversion Fe_xC , which is known from Mössbauer and X-ray investigation to represent poorly defined structures between α -Fe and a real crystallographic carbide, appears as an intermediate. The small variations in the spectral contributions of the unreduced iron phases as shown in Fig. 6 might reflect uncontrolled variations in the reduction process prior to the synthesis. The results do not indicate that

a further macroscopic reduction or oxidation of the catalyst occurs during the synthesis. This conclusion is in agreement with the X-ray diffraction pattern in figure 3c, where the MnO lines show the same shift compared to the pattern of pure MnO as in the reduced catalysts. The X-ray pattern in figure 3c further shows that no metallic iron is detectable after 16 hours of Fischer-Tropsch synthesis, which is consistent with the Mössbauer results.

For completeness we note that no hydrocarbons are formed when the synthesis gas is led over the sample consisting of pure MnO.

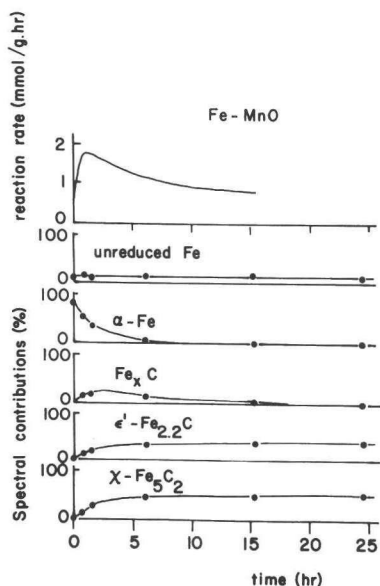


Fig. 6 Reaction rate (upper curve) and relative contributions of the various iron phases to the Mössbauer spectra of Fe-MnO catalysts in the Fischer-Tropsch synthesis at 513 K.

Influence catalyst preparation

According to the preceding section the Fe-MnO catalyst precipitated from iron nitrate and manganese nitrate has the same Fischer-Tropsch properties as unpromoted metallic iron catalysts. We shall refer to the Fe-MnO catalyst prepared from nitrates as the Fe-MnO standard catalyst.

To investigate a possible influence of the starting materials Fe-MnO catalysts were also prepared from metal salts other than nitrates. With these differently prepared catalysts totally different synthesis results were obtained. With regard to this part of the investigation we will

confine ourselves to a description that is illustrative rather than comprehensive. As starting materials of iron and manganese salts in the precipitation process sulphates, bromides, chlorides and nitrates were chosen in a number of combinations.

Mössbauer spectra of the precipitates showed that iron was mainly present as $\alpha\text{-Fe}_2\text{O}_3$ and sometimes also as $\alpha\text{-FeOOH}$. The spectra of the reduced catalysts were similar to the spectrum of the reduced standard Fe-MnO catalyst in figure 2a, although the contributions of the Fe^{3+} and Fe^{2+} phases varied slightly. The degrees of reduction were about the same as in the standard catalysts.

The behaviour in the Fischer-Tropsch synthesis differed from that of the standard FeMnO catalysts in the following manner.

- a) The catalysts were almost inactive at 513 K, the synthesis temperature had to be raised to at least 570 K and in some cases even to 660 K before any activity for hydrocarbon formation could be detected.
- b) At these higher temperatures reaction rates started at a low level, increased slowly, reached a maximum after 1 to 4 hours and decreased only slightly thereafter. This in contrast to a standard catalyst at 623 K, which reached a very high maximum activity already after a few minutes and deactivated drastically to a level of about 5% of the maximum reaction rate within several minutes.
- c) The ethylene selectivities of these catalysts were generally between 35 and 45%, much higher than the less than 10% C_2H_4 value which was obtained with the standard Fe-MnO catalyst at 623 K.

These interesting deviations are illustrated in table III in which a representative selection of the results is given. In this table the catalysts properties in the Fischer-Tropsch synthesis are characterized somewhat arbitrarily by the maximum reaction rate and the selectivities for CH_4 and C_2H_4 formation. Some Mössbauer spectra of catalysts after Fischer-Tropsch synthesis are shown in figure 7.

A catalyst precipitated from iron nitrate and manganese bromide appeared reasonably active at 575 K with a C_2H_4 selectivity of 35%. The Mössbauer

Table III Influence catalyst preparation on Fischer-Tropsch activity

starting materials		T	r_{\max}	selectivities		Mössbauer
iron	manganese	K	mol/gram.hr	CH ₄	C ₂ H ₄	spectra
nitrate	nitrate	513	1.62	35	20	5
		623	6.5	90	< 10	-
nitrate	bromide	573	0.85	20	35	7a
nitrate	chloride	623	0.5	30	45	-
sulphate	chloride	623	0.07	24	39	7b
nitrate	sulphate	673	0.09	32	42	7c
nitrate	sulphate*	573	2.1	33	< 25	7d

*After thoroughly washing the precipitate in a Soxhlet apparatus.

spectrum of this catalyst after 4 hours of Fischer-Tropsch synthesis at 573 K (fig. 7a) shows that not only all α -Fe but also most of Fe²⁺ and Fe³⁺ phases have been converted into iron carbides. Apparently further reduction has occurred during the synthesis at 573 K.

The synthesis temperature had to be raised to 623 K to observe a reasonable activity with a catalyst prepared from iron nitrate and manganese chloride. However, the catalyst had a very favourable C₂H₄ selectivity of 45%. Figure 7b shows the Mössbauer spectrum of an almost inactive catalyst, prepared from iron sulphate and manganese chloride, after 7 hours Fischer-Tropsch synthesis at 623 K. A relatively small part of the iron has been converted into carbides, which account for 20-25% of the spectrum in fig. 7b. The Fe²⁺ and Fe³⁺ phases are still present. The carbon content of this sample was determined separately and was 2.0% by weight with respect to iron. From previous work (chapter 3) we know that this carbon content would be about sufficient to account for the amount of carbides formed. For comparison we note that an α -Fe catalyst, prepared from iron nitrate, contained 27% carbon by weight under the same synthesis conditions !

Since the Mössbauer spectra of these catalysts prepared from chlorides, bromides and sulphates yield no evidence that the structure of these catalysts differs from that of the standard catalyst, it seems plausible that the anions used in the preparation of the catalysts are responsible for the different catalytic properties. Apparently the cleaning procedure used after the precipitation process, which yields active Fe-MnO catalysts when nitrates are the starting materials, is insufficient to remove anions like chlorides, bromides and sulphates. This hypothesis obtains support from the following observation.

A precipitate was made from iron nitrate and manganese sulphate. Part of it was washed in the usual way and yielded a hardly active catalyst (table III) which even contained some α -Fe after 16 hours synthesis at 673 K (fig. 7c). A 100% α -Fe catalyst would have been totally converted into carbides within a few minutes at this temperature. The other part of the precipitate was thoroughly washed with distilled water in a so called Soxhlet apparatus. This procedure resulted in a catalyst with a high Fischer-Tropsch activity at 573 K and a C_2H_4 selectivity of only 25%. The Mössbauer spectrum (fig. 7d) after 16 hours of synthesis shows that all metallic iron has been converted into carbides. It is remarkable that the Fe^{2+} and Fe^{3+} phases identified by the strong central peaks are still present in the spectrum, while the contribution of these phases to the spectrum of figure 7a, also a catalyst after synthesis at 573 K, is much smaller.

Although the latter is not yet clear, the behaviour of the various Fe-MnO catalysts seems to be quite well-understood. The lower activities in the Fischer-Tropsch synthesis, the higher ethylene selectivities and the decreased carburization rates observed with the Fe-MnO catalysts prepared from sulphates, chlorides and bromides are due the promoting and poisoning effect of remaining anion groups, among which especially the sulphates appear favorable for C_2H_4 formation, but fatal for the catalytic activity.

These results suggest that it should be possible to prepare olefin selective catalysts by adding sulphate to iron catalysts in a controlled way.

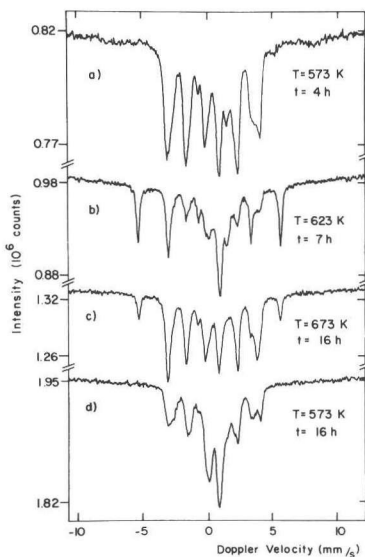


Fig. 7 Room temperature Mössbauer spectra of Fe-MnO catalysts prepared from different starting materials after Fischer-Tropsch synthesis during the time and at the temperature indicated in the figure.

a) catalyst precipitated from a solution of iron nitrate and manganese bromide, b) iron sulphate and manganese chloride, c) iron nitrate and manganese sulphate, d) as c) after thoroughly washing of the precipitate.

Sulphur containing catalyst

An unreduced standard catalyst was impregnated with a solution of ammonium sulphate in water. After drying the catalyst contained .005 mol % sulphate relative to iron. The Mössbauer spectrum of this "sulphated" catalyst before reduction was identical to the spectrum of the standard catalyst. After reduction, however, the sulphated catalyst contained less α -Fe and more Fe^{2+} and Fe^{3+} than the reduced standard catalyst: the α -Fe contribution to the Mössbauer spectrum of the former was 77% while in the latter it was 84%.

The sulphur containing catalyst was not very active in the Fischer-Tropsch synthesis at 513 K and moreover, its ethylene selectivity was lower than that of the standard catalyst.¹⁰ Mössbauer spectra of catalysts after different periods of Fischer-Tropsch synthesis (not shown) indicated the presence of various carbides in the same sequence as found in the un-sulphated catalyst. However, contrary to the latter nearly 10% of metallic iron was even after 24 hours of Fischer-Tropsch synthesis at 513 K not converted into carbides, (Figure 8). Probably the sulphur compounds blocked parts of the surface preventing carbon to come into contact with α -Fe, on

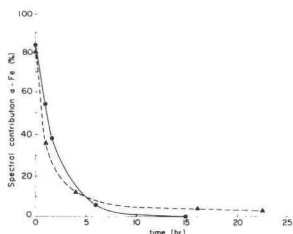


Fig. 8 Relative contribution of α -Fe to the Mössbauer spectra of o) a Fe-MnO standard catalyst and Δ) a sulphated Fe-MnO catalyst, both during Fischer-Tropsch synthesis at 513 K.

which surface CO and/or H_2 could have been adsorbed otherwise.

Although the sulphated catalyst behaved poorly in the synthesis at 513 K, it turned out to be more active and more selective towards ethylene production at 623 K, as can be seen in figure 9. The difference with the standard catalyst at 623 K is striking. The sulphated catalyst not only has a high C_2H_4 selectivity of about 40%, it also suffers hardly from deactivation. In contrast, the standard catalyst produced predominantly methane (80 - 90 %) and deactivated severely in a short time at this temperature. Unfortunately the mechanical strength of the sulphated catalyst was much lower than that of the standard catalyst. Large amounts of carbon were deposited on both catalysts, but only the sulphated catalyst reacted by breaking up into a fine powder, which plugged the reactor completely after Fischer-Tropsch synthesis during 13

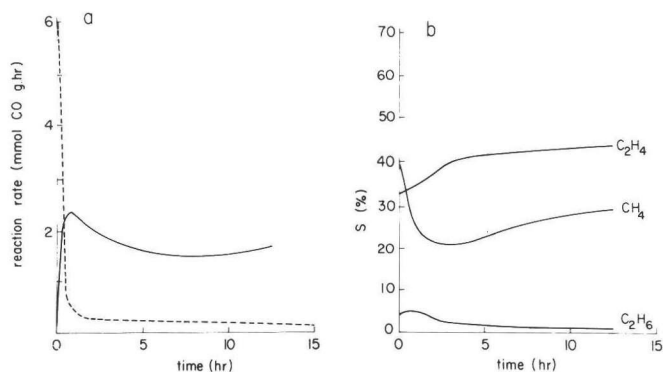


Fig. 9 a) Reaction rates of a Fe-MnO standard (---) and sulphated (—) catalyst during Fischer-Tropsch synthesis at 623 K and b) the methane, ethane and ethylene selectivities of the sulphated Fe-MnO catalyst at 623 K.

hours. Mössbauer spectra or X-ray patterns of the sulphated catalyst after FT synthesis at 623 K have not been recorded, but the synthesis results are sufficiently interesting to justify doing this in the future.

In summary the results clearly demonstrate that the promoting effects of manganese oxide on iron in catalysts prepared by coprecipitation is nihil, at least in the case of Fischer-Tropsch synthesis at 1 atm. pressure. However, impregnation of an unreduced FeMnO catalyst with ammonium sulphate results in a catalyst that is highly ethylene selective in the Fischer-Tropsch synthesis at 623 K.

Discussion and conclusions.

Mössbauer spectroscopy and X-ray diffraction of the Fe-MnO catalyst in unreduced form at room temperature yielded that it is a mixture of $\alpha\text{-Fe}_2\text{O}_3$, $\alpha\text{-FeOOH}$ and Mn_2O_3 . Mössbauer spectra were also taken at both liquid N_2 and He temperatures. The iron hyperfine field in $\alpha\text{-Fe}_2\text{O}_3$ was slightly reduced with respect to the field of bulk $\alpha\text{-Fe}_2\text{O}_3$ owing to small particle size. By using van der Kraan's results¹¹ an average diameter of 23 nm for the $\alpha\text{-Fe}_2\text{O}_3$ particles was estimated. The Mössbauer spectrum at room temperature also showed that $\alpha\text{-FeOOH}$ is superparamagnetic and from this result it follows that the diameter of the particles is below 8.5 nm. As Mn_2O_3 diffraction peaks could be observed in the X-ray pattern, its particle size will probably not be smaller than about 5-10 nm. We emphasize here that assignment of the superparamagnetic doublet in the Mössbauer spectrum to $\alpha\text{-FeOOH}$ was only possible after recording the spectra at liquid nitrogen and liquid helium temperature. This illustrates again the usefulness of low temperature Mössbauer spectroscopy in the characterization of iron containing catalysts.

The composition of the reduced Fe-MnO catalyst is rather complex. Both the Mössbauer spectra and the X-ray pattern indicate that most of the Fe^{3+} , present as $\alpha\text{-Fe}_2\text{O}_3$ and $\alpha\text{-FeOOH}$ in the precipitate, has been reduced to $\alpha\text{-Fe}$. Mn_2O_3 has been entirely converted into MnO, but the diffraction lines of this MnO are broadened and shifted in comparison

with pure MnO (fig.3). The broadening of the X-ray pattern may indicate that MnO in the reduced catalyst is of a small size. The Mössbauer spectra contained small contributions of Fe³⁺ and Fe²⁺. Since pure α -Fe₂O₃ or α -FeOOH can easily be reduced to 100% α -Fe, it must be concluded that MnO in the reduced catalyst is responsible for the presence of unreduced iron.

The Fe²⁺ doublet is in fact the same doublet as Huffman and Podgurski¹³ found in a partially oxidized Fe-Mn alloy and which they attributed to (Fe-Mn)O precipitates of the wüstite type.

Topsøe et al.¹⁴ also found contributions of an Fe²⁺ compound in the Mössbauer spectra of Fe/MgO catalysts. He suggest that the Fe²⁺ phase establishes the contact between reduced iron and the MgO support. A similar interaction might occur in our Fe-MnO catalysts. However, in the Fe-MnO catalysts also Fe³⁺ compounds are present. It is not clear whether these Fe³⁺ compounds play a role in the contact between α -Fe and MnO or whether they represent small inclusions of iron (III) oxide in the MnO, which have not been subject to reduction by hydrogen. We note that the Mössbauer parameters of the Fe³⁺ phase exclude the possibility that Fe³⁺ and MnO have formed compounds like manganese ferrites or FeMnO₃.

Further information about the composition of the reduced Fe-MnO catalyst is obtained from its carburization behaviour. Two important differences between Fe-MnO and single phase α -Fe catalysts appeared: (i) carburization proceeds at a considerably lower rate in Fe-MnO catalysts and (ii) significantly more ϵ' -Fe_{2.2}C relative to χ -Fe₅C₂ is formed in Fe-MnO catalysts. Since both catalysts have been investigated under exactly the same reaction conditions and since both catalysts show similar catalytical properties and behave the same towards CO adsorption and dissociation the different carburization behaviour should entirely be due to the catalyst itself. It is well known that supported iron catalysts favour the formation of ϵ' -Fe_{2.2}C.^{15,9} We therefore suggest that the increased ϵ' -Fe_{2.2}C content of carbided Fe-MnO catalysts indicates that a substantial fraction of α -Fe is in close contact with MnO. The

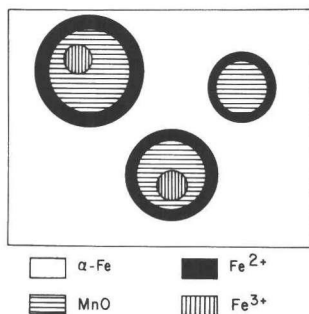


Fig. 10 Schematical representation of a reduced Fe-MnO catalyst.

slower carburization rate of α -Fe confirms that it is influenced by the presence of MnO.

In fig. 10 a schematical picture of the reduced catalyst is given that would make the description given above plausible. According to this presentation it is assumed that the close contact between α -Fe and MnO is established via a phase which contains Fe^{2+} , in accordance with Topsøe's suggestion¹⁴ for Fe/MgO catalysts.

The standard Fe-MnO catalyst behaved similar as a metallic iron catalyst in the Fischer-Tropsch synthesis at 513 K. This holds with regard to the catalytical activity, the selectivity, the deactivation and the ultimate conversion of all metallic iron into carbides. Also at 623 K activity and selectivity did not differ significantly from those of α -Fe at the same temperature. Selectivity patterns did not change when the MnO content of the catalysts was varied. In fact these results mean that, at least under the conditions used in this investigation, MnO cannot be considered as a promotor, either in chemical or in structural sense.

In the conversion of α -Fe into carbides the phase Fe_xC appeared again as an intermediate. In chapter 3 it was suggested that Fe_xC represents poorly-defined structures between metallic iron and a real crystallographic carbide structure. Fe_xC is still present in the Mössbauer spectrum taken after 12 hours of Fischer-Tropsch synthesis, indicating that also the transformation of Fe_xC into the carbides $\chi\text{-Fe}_5\text{C}_2$ and $\epsilon'\text{-Fe}_{2.2}\text{C}$ is retarded by the presence of MnO.

Figure 6 shows that the maximum catalytic activity was reached several hours before all iron had been carburized. This is interesting with respect to the models which have been suggested in the literature to explain the carburization behaviour of iron in the Fischer-Tropsch synthesis¹⁶. The result that the Fe-MnO catalyst is at maximum activity while it still contains a substantial fraction of metallic iron is certainly not in agreement with the so called carbide model. This model assumes a linear relationship between the Fischer-Tropsch activity and the extent of carburization in the interior of the catalyst. According to the slow activation model on the contrary carburization and Fischer-Tropsch activity are unrelated, while in the competition model the Fischer-Tropsch reaction competes with the carburization process for carbon atoms deposited at the surface¹⁶. The latter process is believed to consume most of the carbon atoms in the early stage of the synthesis. The results in figure 6 can be understood in terms of both the slow activation and the competition model. For a discussion of these models we refer to chapter 6.

The choice of the metal salts to be used as starting materials for the catalyst preparation had a profound effect on the catalytic properties. Obviously, washing the precipitated catalyst with distilled water did not sufficiently remove the sulphate, bromide and chloride anions. Although the concentration of anions after the washing procedure cannot be very high, the synthesis behaviour of the catalyst was entirely different from that of the standard catalyst. Therefore it seems likely that these contaminations have been concentrated on the surface of the catalyst at the end of the calcination or reduction stage. The state in which the original chloride, bromide and sulphate ions are present at the surface of the catalyst is not known. Kieffer¹ found that sulphate ions in his unreduced Fe-ZnO catalyst were reduced to sulphides during reduction or synthesis. Probably the same is true for sulphates in our Fe-MnO catalysts.

It is remarkable that in all cases wherein a low synthesis activity was observed, carburization proceeded slowly too. If we assume that C^* ,

originated from dissociation of chemisorbed CO, is a precursor for both Fischer-Tropsch reaction and carburization, than the contaminations would inhibit the formation of C^* , possibly by occupying sites where CO can be adsorbed and/or dissociated. But more ways are conceivable in which the formation of C^* can be hindered. As it is suggested by Unmuth et al.¹⁷ hydrogen has a positive effect on the formation of C^* by rapidly removing O^* , leaving behind empty sites where a new CO molecule can be adsorbed and dissociated. For this process a number of neighbouring sites are required and the presence of contaminations on the surface very likely reduces the number of such ensembles greatly.

Despite their deactivating effect, the influence of anions like sulphates bromides and chlorides on ethylene production is noteworthy, as C_2H_4 selectivities up to 45% have been observed. According to Pichler¹⁸, α -olefins are the primary products of the Fischer-Tropsch synthesis and paraffins arise by subsequent hydrogenation of the olefins. Apparently the role of those anions in general, and of sulphates in particular is to suppress the hydrogenation capabilities of the catalyst. A more detailed discussion which includes kinetic aspects has been given by Van Dijk et al.¹⁰

Impregnation of unreduced Fe-MnO with ammonium sulphate in a controlled way yielded a catalyst which seemed at first sight an ideal catalyst in the synthesis at 625 K. It had a high C_2H_4 selectivity and suffered hardly from deactivation during the first 12 hours. Unfortunately this catalyst powdered after 12 successful hours of synthesis such that it plugged the reactor completely.

Kieffer¹ observed similar effects on impregnating an Fe-ZnO catalyst with different amounts of iron sulphate. He studied the influence of the sulphate content on activity, selectivity and stability, and found that the mechanical strength depend critically on the amount of sulphate added. Kieffer obtained an excellent catalyst when 32 mg $Fe_2(SO_4)_3$ was added per gram of Fe-ZnO catalyst. The catalyst impregnated in this way combined a high olefin selectivity with a satisfactory

activity and, even more important, this catalyst did not deactivate during a period of 2.5 months ! Kieffer concludes that sulphate addition inhibits the formation of free carbon at high synthesis temperatures while ZnO plays a role in keeping the activity at a reasonable level at these rather high sulphate concentrations.

Since already small amounts of sulphur can result in an increased olefin selectivity, it is not unlikely that in other investigations reported in the literature small unexpected sulphur contaminations have played a role. For example Barrault et al.^{6,19} reported that the activity and the selectivity towards light olefins in the Fischer-Tropsch synthesis over iron on alumina catalysts can be influenced by choosing a different alumina support. Kieffer¹ obtained similar results. By analyzing the chemical composition of the supports he found that the alumina supports which seemed to promote olefin production contained sulphur contaminations of about 2%. Although Barrault et.al.^{6,19} obtained their alumina support from different companies as Kieffer¹ did, it might be possible that sulphur contamination of the support accounts for the observed selectivities in the investigation of the former authors.

According to various authors^{3,4,5} mentioned in the introduction, an increased olefin production in the Fischer-Tropsch synthesis at elevated pressures occurs in manganese promoted iron catalysts. As these authors give little information about the preparation of their catalysts, it is in view of our previous discussion not unreasonable to raise the question whether the results of their investigation have been influenced by the presence of anions, in particular sulphates. Another possibility would be that the promoting effect of manganese oxide on iron catalysts becomes apparent at pressures higher than 1 atm. only.

References.

- 1 E.P. Kieffer, thesis, Eindhoven 1981.
- 2 R.J. Madon, W.F. Taylor, J.Catal. 69, 32 (1981).
- 3 H. Kölbel, K.D. Tillmetz, Deutsche Offenlegungsschrift 2 507 647 (1976)
- 4 B. Büssemeier, C.D. Fröhning, G. Horn, W. Kluy, Deutschen Offenlegungsschrift 2 518 964 (1976)
- 5 C.H. Yang, A.G. Oblad, Symposium on advances in Fischer-Tropsch chemistry, Anaheim meeting, March 1978.
- 6 J. Barrault, J.C. Menezo, R. Maurel, Bull.Soc.Chim. 1979 I-413.
- 7 V.U.S. Rao, R.J. Gormley, Hydrocarbon Process. november, 1980.
- 8 D. Fraenkel, B.C. Gates, J.Am.Chem.Soc. 102, 2478 (1980).
- 9 J.W. Niemantsverdriet, A.M. van der Kraan, W.L. van Dijk, H.S. van der Baan, J.Phys.Chem. 84, 3363 (1980); chapter 3 in this thesis.
- 10 W.L. van Dijk, J.W. Niemantsverdriet, A.M. van der Kraan, H.S. van der Baan, Appl.Catal. 2, 273 (1982).
- 11 A.M. van der Kraan, thesis, Delft 1972.
- 12 M. Swanson, NBS circular 539 5 45 (1955).
- 13 G.P. Huffman, H.H. Podgurski in "Mossbauer Effect Methodology", (ed. I.J. Gruverman and C.W. Seidel). Vol.10, Plenum Press New York, 1976.
- 14 H. Topsøe, J.A. Dumesic, E.G. Derouane, B.S. Clausen, S. Mørup, J. Villadsen, N. Topsøe, in "Preparation of Catalysts II", Elsevier, Amsterdam, 1979.
- 15 J.A. Amelse, J.B. Butt, L.H. Schwartz, J.Phys.Chem. 82, 558 (1978).
- 16 J.W. Niemantsverdriet, A.M. van der Kraan, J.Catal. 72, 385 (1981); chapter 6 in this thesis.
- 17 E.E. Unmuth, L.H. Schwartz, J.B. Butt, J. Catal. 63, 404 (1980).
- 18 H. Pichler, H. Schulz, F. Hojabri, Brennst. Chem. 45, 215 (1964)
- 19 J. Barrault, C. Forquy, J.C. Menezo, R. Maurel, React. Kinet. Catal. Lett. 15, 153 (1980).

CONTENTS

General Introduction	89
Experimental	93
Results and Discussion	
I) Behavior of FeRh/SiO ₂ catalysts upon reduction	95
II) FeRh/SiO ₂ after Fischer-Tropsch synthesis and CO chemisorption	100
III) Mössbauer spectra of FeRh/SiO ₂ at cryogenic temperatures	106
Summary of the Results	111
Model for FeRh/SiO ₂ Catalysts	112
Recommendations	115
References	116

GENERAL INTRODUCTION

About ten years ago Sinfelt¹ discovered that a catalyst consisting of small crystallites of two alloyed metals on a support showed catalytic properties which differed markedly from those of either one of the constituent metals. In small particles with dimensions smaller than about 4 nm a substantial fraction of the atoms are in or just below the surface. Since it is well known that the composition of an alloy in the surface region in general does not correspond to that of the bulk², small particle alloys can exist with a composition that does not occur in bulk alloys. In order to express this feature in the nomenclature Sinfelt proposed to use the name supported bimetallic cluster rather than supported alloy.

The inspiring prospect of a new class of catalysts with sometimes favorable selectivity and stability has stimulated research on several combinations of metals. A very interesting bimetallic cluster catalyst is FeRh/SiO₂. Bhasin et al.³ investigated this catalyst in CO hydrogenation at 300 °C and 68 atm.

Table I Product selectivities in Fischer-Tropsch synthesis over silica supported Fe, Rh and FeRh catalysts.

product	Fe/SiO ₂	FeRh/SiO ₂	Rh/SiO ₂
methane	25	37	52
C ₂ -C ₄ hydrocarbons	44	1	3
methanol	9	35	0
ethanol	4	24	17
other C ₂ oxygenates	8	2	26

Reaction conditions: 573 K, 68 atm, CO/H₂ = 1

Data from Bhasin et al.³

They observed a product selectivity that differed strongly from that of either supported iron or supported rhodium catalysts, as is illustrated by table I. In particular the formation of 24% ethanol, almost to the exclusion of other C₂-oxygenates is interesting, because a direct route from synthesis gas to an added-value chemical as ethanol might be attractive on a commercial scale.⁴ High pressure appears to be a necessary condition for the formation of oxygenated products. Aschenbeck⁵ showed that in Fischer-Tropsch synthesis at atmospheric pressure on FeRh/SiO₂ catalysts methane is by far the dominant product, whereas only traces of oxygenated products are detected.

Another example of selectivity improvement by means of alloying has been given by Vannice et al.⁶. These authors observed a considerably enhanced olefin production in Fischer-Tropsch synthesis with FeRu/SiO₂ catalysts, as compared with Fe/SiO₂ or Ru/SiO₂ catalysts.

. Investigation of the structure of supported bimetallic clusters is seriously hindered by their small dimensions and by the presence of a support. Bimetallic clusters are therefore not amenable to study by means of techniques that have successfully been applied to unsupported alloys, such as X-ray diffraction, Secondary Ion Mass Spectroscopy and Auger Electron Spectroscopy. In this respect iron containing catalysts have the advantage that they can be studied with Mössbauer spectroscopy.

This technique has been successfully applied to ascertain alloying of iron

with more noble group VIII metals like Ru, Pd and Pt in bimetallic supported cluster catalysts. For reviews of such investigations we refer to the papers by Garten⁷, Guzzi⁸ and Topsøe, Dumesic and Mørup⁹. The shape of the Mössbauer spectra of the reduced bimetallic catalysts can vary with composition, particle size and pretreatment. In general, the spectra consist of a single peak with an isomer shift corresponding to the bulk alloy and a shoulder or resolved peak at higher velocity (figure 1). The correspondence of this peak with some iron species at the surface is demonstrated by the work of Garten et al.^{6,10} and of Aschenbeck⁵ on FeRu/SiO₂ catalysts. These authors report that the relative intensity of this peak in the Mössbauer spectrum increases with increasing metal dispersion as measured by H₂ chemisorption. Perturbation of the spectral parameters of the peak by NH₃ at room temperature confirms the accessibility of these iron species to the gas phase⁵. Assignment of the surface subspectrum to a certain chemical state requires a closer examination of its Mössbauer parameters. Two possible interpretations of the surface component in the Mössbauer spectra can be envisioned. 1) It is a single peak or an unresolved doublet, both with an isomer shift characteristic for high spin Fe²⁺ compounds. 2) The peak observed is the right half of a quadrupole doublet, the left half of which coincides with the bulk alloy peak. The isomer shift and quadrupole splitting of this doublet correspond with those of high spin

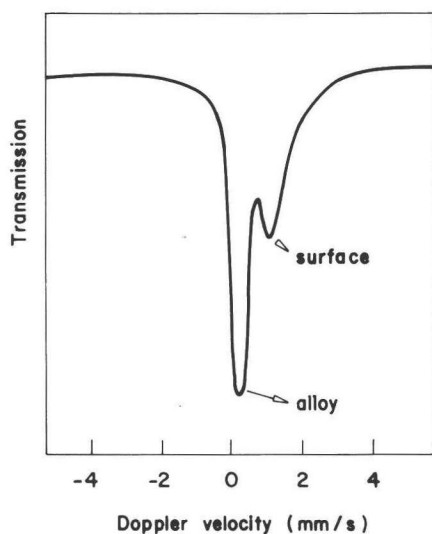


Fig. 1 Typical Mössbauer spectrum of a reduced supported bimetallic cluster catalyst consisting of iron and a more noble group VIII metal.

Fe³⁺ compounds, but Lam and Garten¹⁰ have suggested that the doublet could also correspond to zero-valent iron atoms at sites of low symmetry on the surface of the bimetallic clusters. They explain the unusually high isomer shift for Fe⁰ by invoking a lower electron density at these sites which they believe could be the result of a higher effective atomic volume for iron at the surface.

From the point of view of Mössbauer spectroscopy, assignment of the surface species to Fe⁰ or Fe²⁺ would, although perhaps not impossible, be rather unusual, and interpretation in terms of a Fe³⁺ doublet would be preferred. From the viewpoint of chemistry, however, Fe²⁺ species are commonly encountered in reduced supported iron catalysts⁹ and it is not readily apparent why an Fe³⁺ surface phase would be stabilized under the influence of a noble metal which is known to facilitate the reduction of iron. Supported bimetallic clusters of FeRu, FePd and FePt which have been reduced and reoxidized show reduction of Fe³⁺ into Fe²⁺ on exposure of the catalysts to H₂ at room temperature^{6-10,13}. Garten has argued convincingly that this enhanced reducibility of iron is direct evidence of the noble metal proximity and influence⁷. Fe/SiO₂, on the contrary, does not reduce in H₂ at room temperature.

For Ru and Fe loadings below 1%, Guzzi et al.¹⁴ have shown that iron helps to disperse the ruthenium on silica but remains in a highly irreducible state. The Mössbauer spectra show little evidence of any bulk alloy formation and liquid helium spectra confirm that most of the iron is in the ferric state. Guzzi suggests that at low metal loadings iron oxide and ruthenium mutually impede surface mobility, thus stabilizing isolated and irreducible clusters⁸. Assignment of the high velocity surface peak for FeRu/SiO₂ at Ru loadings above 1%, where metallic alloy particles do form, has however not yet been clarified.

It would be worthwhile to investigate whether Mössbauer spectroscopy at cryogenic temperatures can improve our understanding of the origin of the high velocity peak, which is referred to as the surface component, since Mössbauer spectra at temperatures well below room temperature generally yield more detailed information. In particular, when the spectra become magnetically

split at low temperature, assignment to Fe^{2+} , Fe^{3+} or Fe^0 is greatly facilitated. Moreover, the recoilless fraction as measured by the resonant absorption area, which is low at room temperature due to the low effective Debye temperatures prevailing for well dispersed particles, is substantially increased at cryogenic temperatures. One must, of course, cool the sample and measure spectra in situ or under controlled atmosphere so as to preserve the chemical state of the highly reactive catalyst surface.

In this chapter we describe a Mössbauer investigation of FeRh/SiO_2 catalysts. First we will use in situ Mössbauer spectroscopy at room temperature to study the reduction of the catalysts in H_2 , and the effects of CO chemisorption. Next we will investigate whether in situ Mössbauer spectroscopy at cryogenic temperatures can contribute to our understanding of the reduced FeRh/SiO_2 catalyst. Finally, we propose a model which, as we believe, explains the experimental results that are presented in this chapter.

EXPERIMENTAL

The FeRh/SiO_2 catalysts were prepared by means of pore volume impregnation. Two different FeRh/SiO_2 samples have been used.

a) A solution of $\text{Fe}(\text{NO}_3)_3 \cdot 9\text{H}_2\text{O}$ (Merck P.A.) and $\text{RhCl}_3 \cdot x\text{H}_2\text{O}$ (39 wt%, Drijfhout) in H_2O was added dropwise to the silica support (Grace, S.P. 2-324.382, $290 \text{ m}^2/\text{g}$) which was stirred continuously until the incipient wetness point was reached. FeRh/SiO_2 catalysts prepared in this way contained 1.76 wt% of iron and 3.24 wt% of rhodium, which corresponds to an atomic ratio $\text{Fe}:\text{Rh} = 1:1$. A supported iron catalyst was prepared similarly and contained 3.52 wt% of iron. The impregnated samples were dried at room temperature overnight, subsequently at 335, 355 and 375 K for 2 hour at each temperature, and finally at 395 K for 60 hours. These samples will be referred to as "air-dried" catalysts.

b) An aqueous solution of $\text{Fe}(\text{NO}_3)_3 \cdot 9\text{H}_2\text{O}$ (Mallinckrodt) and $\text{RhCl}_3 \cdot x\text{H}_2\text{O}$ (42.3 wt% Rh, Strem Chemicals) was added dropwise to the silica support (Cab-0-Sil, EH-5, $310 \text{ m}^2/\text{g}$) under frequent stirring until the incipient wetness point was reached. This catalyst also contained 1.76 wt% iron and

3.24 wt% rhodium, which corresponds to an atomic ratio Fe:Rh=1:1. The impregnated samples were dried in air at room temperature for a few days and next in vacuum at room temperature for 1 hour and at 425 K for several hours. This sample will be referred to as "vacuum-dried" catalyst.

A quantity of 320 mg catalyst was pressed into a wafer with a diameter of 20 mm, using a pressure of 100 atm. Mössbauer spectra at room temperature were recorded in situ in the reactor which has been described in chapter four. In order to be able to measure spectra of the catalyst in situ at cryogenic temperatures, an absorber holder was used that can be closed vacuum-tight under the gas atmosphere inside the chemical reactor. The sealed absorber holder can then be mounted in a cryostat which permits measurements of Mössbauer spectra at room, liquid nitrogen and liquid helium temperatures without changing the configuration of the absorber with respect to the gamma ray beam. The latter is required when resonant absorption areas of the spectra at different temperatures are to be compared. A detailed description of this reactor system has been given in chapter five.

The gases H₂ (Hoekloos, purity >99.9%) and CO (Hoekloos, >99.5%) were each purified over a reduced copper catalyst (BASF, R3-11) and a molecular sieve (Union Carbide, 5A). Reduction was carried out in an H₂ flow of 6 l/h, Fischer-Tropsch synthesis in a flow of 8 l/h synthesis gas with H₂/CO = 3.3.

Mössbauer spectra were obtained with a constant acceleration spectrometer, which uses a ⁵⁷Co in Rh source. Isomer shifts (I.S.) are reported relative to the NBS standard sodium nitroprusside (SNP) at room temperature. Magnetic hyperfine fields H are calibrated with the 515 kOe hyperfine field of α -Fe₂O₃ at room temperature. Mössbauer spectra were fitted by computer with calculated subspectra consisting of Lorentzian shaped lines by varying the Mössbauer parameters in a non-linear, iterative minimization routine. This method has been described in chapter two.

RESULTS AND DISCUSSION

I) Behavior of FeRh/SiO_2 catalysts upon reduction.

In this section we report the use of in situ Mössbauer spectroscopy at room temperature to demonstrate coclustering of Fe and Rh in the bimetallic catalysts and to investigate their behavior upon reduction. The experiments were carried out with the air-dried catalysts.

Results

In order to demonstrate the influence of clustering of Rh with Fe both the FeRh/SiO_2 and the Fe/SiO_2 catalyst were reduced under the same conditions. Figure 2 shows the in situ Mössbauer spectra of the two catalysts at room temperature in different stages of reduction, as indicated in the figure. The Mössbauer parameters of the bimetallic catalyst are listed in table II (page 98).

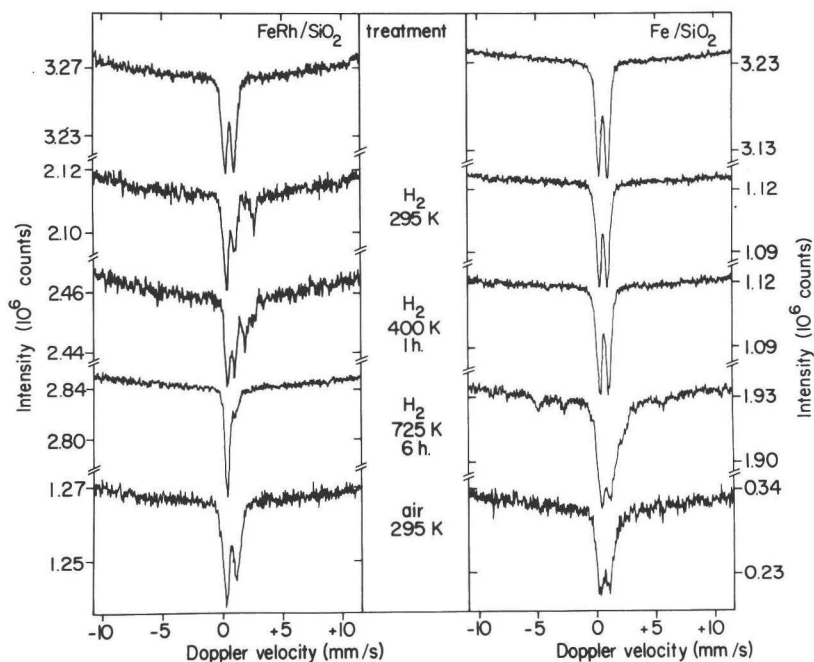


Fig. 2 In situ Mössbauer spectra at 295 K of FeRh/SiO_2 and Fe/SiO_2 catalysts after the treatments indicated. The upper spectra correspond to the fresh catalysts, after impregnation and drying.

The Mössbauer spectra of the impregnated and dried FeRh/SiO_2 and Fe/SiO_2 catalysts have identical Mössbauer parameters, which correspond to Fe^{3+} ions. Upon subjecting the catalysts to H_2 at various temperatures, however, considerable differences in reduction behavior between the bimetallic and the monometallic catalyst become apparent.

The Mössbauer spectrum of the FeRh/SiO_2 catalyst exposed to H_2 at room temperature (fig. 2) indicates that a significant fraction of the original Fe^{3+} ions has been converted into Fe^{2+} ions, as shown by the peak at about 2.5 mm/s. This high velocity peak is attributed to an Fe^{2+} doublet, the low velocity counterpart of which is hidden under the peaks in the 0-1 mm/s region of the spectrum. The quadrupole splitting of this doublet is about 2.4 mm/s. The corresponding spectrum in figure 2 shows that the unreduced monometallic Fe/SiO_2 catalyst is not affected by H_2 at 295 K.

Reduction in H_2 at 400 K for 1 hour induces further changes in the spectrum of the bimetallic catalyst, whereas that of the monometallic catalyst remains unaltered. The Mössbauer spectrum of the FeRh/SiO_2 catalyst is characteristic for a combination of three doublets, two of which are identical to the Fe^{2+} and Fe^{3+} doublets of the previous spectrum. The isomer shift and quadrupole splitting of the third doublet are characteristic for Fe^{2+} in a symmetry lower than octahedral.

The Mössbauer spectrum of the FeRh/SiO_2 catalyst after reduction at 725 K in H_2 for 6 hours (figure 2) consist of a large single line and a smaller poorly resolved contribution. Additional reduction at 725 K or at 775 K does not induce further changes in the Mössbauer spectrum. The spectrum has been analyzed with the computer under the assumption that the poorly resolved part of the spectrum belongs to a doublet, the left peak of which coincides with the singlet. The isomer shift of the singlet (0.36 mm/s) is within the range of those for FeRh bulk alloys¹⁵. The Mössbauer parameters of the doublet are characteristic of high spin Fe^{3+} ions. A more detailed interpretation of this spectrum will be discussed later in this chapter.

The Mössbauer spectrum of the monometallic Fe/SiO_2 catalyst after 6 hours of reduction in H_2 at 725 K shows that only a little magnetically split $\alpha\text{-Fe}$

formed since the four outer lines of its sextuplet are barely visible. The magnetic hyperfine field of this sextuplet is about 324 kOe, which is smaller than that of bulk α -Fe (330 kOe at 295 K). This indicates that the dimensions of the α -Fe particles in the reduced Fe/SiO₂ catalyst are very small.

Both the reduced FeRh/SiO₂ and the Fe/SiO₂ catalyst are not stable with respect to oxygen. The lower two spectra of figure 2, recorded ex situ, show that most of the reduced iron is oxidized upon exposing the catalysts to air at room temperature. This is regarded as further evidence that the particles in the reduced catalysts are well dispersed.

It has been reported in the literature that reoxidized supported FeRu, FePd and FePt catalysts can partially be reduced by H₂ at room temperature^{6,7,9-13}. In order to investigate whether FeRh/SiO₂ catalysts show the same behavior, the sample that was reduced at 725 K and subsequently exposed to air at room temperature (figure 3, upper spectrum) was brought under an H₂ atmosphere at room temperature. Its Mössbauer spectrum (figure 3) indicates that a considerable fraction of the original Fe³⁺ ions is converted to Fe²⁺ ions upon H₂ chemisorption. Reexposure to air restored the original spectrum of the catalyst under air. Chemisorption of CO resulted in a catalyst that is

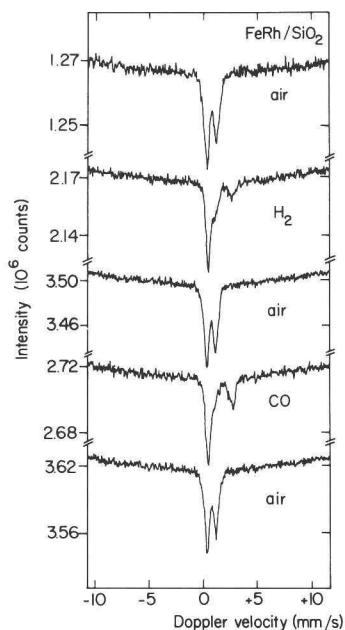


Fig. 3 Mössbauer spectra at 295 K of the air-exposed FeRh/SiO₂ catalyst after chemisorption of the indicated gases at 295 K.

Table II Mössbauer parameters of FeRh/SiO₂ at 295 K.

treatment	iron state	I.S. (mm/s)	Q.S. (mm/s)	contribution %
impregnation and drying	Fe ³⁺	0.64	0.74	100
H ₂ , 295 K	Fe ²⁺	1.43	2.36	34
	Fe ³⁺	0.64	0.69	66
H ₂ , 400 K, 1 h	Fe ²⁺	1.44	2.08	28
	Fe ²⁺	1.35	0.90	34
	Fe ³⁺	0.64	0.65	38
H ₂ , 725 K, 6 h	Fe ⁰	0.36	-	66
	Fe ³⁺	0.64	0.81	34
air, 295 K	Fe ⁰	0.34	-	10
	Fe ³⁺	0.64	0.92	90
H ₂ , 295 K	Fe ⁰	0.34	-	27
	Fe ²⁺	1.44	2.04	30
	Fe ³⁺	0.63	0.72	43
CO, 295 K	Fe ⁰	0.34	-	24
	Fe ²⁺	1.44	2.24	49
	Fe ³⁺	0.63	0.65	27

Accuracies: I.S.: 0.04 mm/s, Q.S.: 0.08 mm/s, contribution: 6%.

even more reduced than that after chemisorption of H₂. The original spectrum appeared again on exposing the catalyst to air.

The spectra of figure 3 were computer analyzed by making the assumption that the spectrum of the catalyst under air consists of a singlet and a doublet. The spectra of the catalyst under H₂ or CO were fitted with a combination of a singlet and two doublets. See table II for results.

Discussion

If we compare the Mössbauer spectra of the bimetallic FeRh/SiO₂ and the monometallic Fe/SiO₂ catalyst after the different reduction steps, it is clear that clustering of Fe and Rh in the former has indeed occurred. The partial reduction which takes place at room temperature, and the relatively large

contribution of zero valent iron in the Mössbauer spectrum of the catalyst after reduction at 725 K both demonstrate that the more noble metal, rhodium, greatly enhances the reducibility of the less noble metal, iron. The isomer shift of the single peak in the spectrum of FeRh/SiO₂ after reduction at 725 K is within the range observed in the single line Mössbauer spectra of FeRh bulk alloys by Chao et al¹⁵. Furthermore, the absence of any contribution due to either α -Fe or Fe²⁺ in this spectrum indicates that isolated iron particles were not formed.

Interesting changes occur in the bimetallic catalyst upon reduction in H₂ at relatively low temperatures 295 and 400 K. H₂ exposure at 295 K yields a ferrous compound with Mössbauer parameters which are in the range of those for iron (II) bulk compounds. Bartholomew and Boudart¹³ observed a similar Fe²⁺ doublet in the Mössbauer spectrum of an oxidized FePt/C catalyst which was exposed to H₂ at room temperature. They suggest that the Fe²⁺ doublet is due to a Fe-OH surface complex. Following this interpretation it is conceivable that the coordinatively unsaturated Fe²⁺ ions, which are observed after reduction of the FeRh/SiO₂ catalyst in H₂ at 400 K, are formed from these Fe-OH surface complexes by means of a reaction between OH groups and the subsequent desorption of water.

Chemisorption of H₂ and CO induced significant changes in the Mössbauer spectra of the air-exposed FeRh/SiO₂ catalyst. The great sensitivity of the iron ions in the catalyst to their gaseous environment implies that the degree of dispersion in these catalysts must be very high. As the recoilless fraction of surface and bulk atoms may differ considerably, the use of Mössbauer spectra which are taken at 295 K only cannot yield a reliable quantitative measure of the dispersion.

The changes in the Mössbauer spectra which are the result of chemisorbing a reducing gas like H₂ or CO on the one hand, and O₂ on the other hand are entirely reversible. This reversibility appears to be characteristic for supported bimetallic clusters of iron and a more noble group VIII metal^{6,7,9-13}. We further note that CO chemisorption converts substantially more Fe³⁺ into Fe²⁺ ions than does H₂ chemisorption. In the next section we will show that

this property can be used to obtain structural information on bimetallic FeRh/SiO₂ catalysts.

II) FeRh/SiO₂ after Fischer-Tropsch synthesis and CO chemisorption.

In this section we describe Mössbauer spectra at room temperature of an initially unreduced FeRh/SiO₂ catalyst after various treatments: reduction at 725 K, Fischer-Tropsch synthesis at 525 K, and chemisorption of CO on the reduced and air-exposed catalyst at 295 K. All experiments were carried out with the vacuumdried FeRh/SiO₂ catalyst, in the Mössbauer in situ reactor which has been described in chapter four.

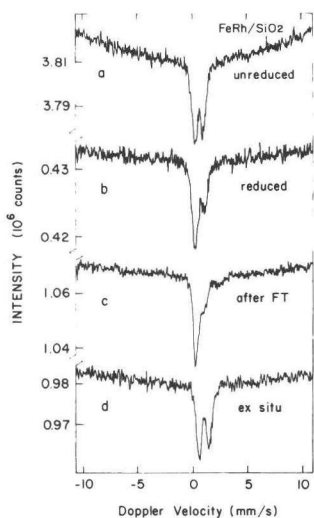


Fig. 4 Room temperature Mössbauer spectra of the vacuum-dried FeRh/SiO₂ catalyst after a series of subsequent treatments: a) impregnation and drying, b) H₂ reduction at 725 K, c) Fischer-Tropsch synthesis at 525 K and d) exposure to air at 295 K.

Results

The Mössbauer spectrum of the catalyst after impregnation and drying in vacuum (fig. 4a) consists of a doublet with parameters (table III) characteristic for Fe³⁺. The catalyst was reduced in H₂ at 400 K for 1 hour and at 725 K for 6 hours. Its Mössbauer spectrum is shown in figure 4b. This spectrum was analyzed as a combination of a single line which corresponds to zero valent iron in a FeRh alloy, and a doublet with parameters that are characteristic for a Fe³⁺ phase. In the discussion hereafter we will show that this interpretation is supported by the CO chemisorption experiments which will be described below. We note that the total resonant absorption in

Table III Mössbauer parameters of the spectra in figure 4.

treatment	iron state	I.S. (mm/s)	Q.S. (mm/s)	A (a.u.)
impregnation and drying	Fe ³⁺	0.68	0.77	0.40 ± 0.02
H ₂ , 725 K	Fe ⁰	0.38	-	0.22 ± 0.02
	Fe ³⁺	0.70	1.00	0.58 ± 0.05
FTS, 525 K	Fe ⁰	0.38	-	0.31 ± 0.03
	Fe ²⁺	1.51	1.72	0.17 ± 0.02
	Fe ³⁺	0.70	0.97	0.35 ± 0.03
air, 295 K	Fe ⁰	0.37	-	0.13 ± 0.02
	Fe ³⁺	0.65	1.00	0.75 ± 0.08

A : resonant absorption area; FTS : Fischer-Tropsch synthesis
 Accuracies : I.S.: 0.04 mm/s, Q.S.: 0.08 mm/s.

the spectrum of the reduced catalyst is larger than that of the unreduced catalyst.

The Mössbauer spectrum of the catalyst after 4 hours of Fischer-Tropsch synthesis at 525 K in synthesis gas with H₂/CO=3.3, is shown in figure 4c. This spectrum contains a broad peak at about 2.5 mm/s, which we attribute to the high velocity part of a Fe²⁺ doublet. The low velocity peak of this

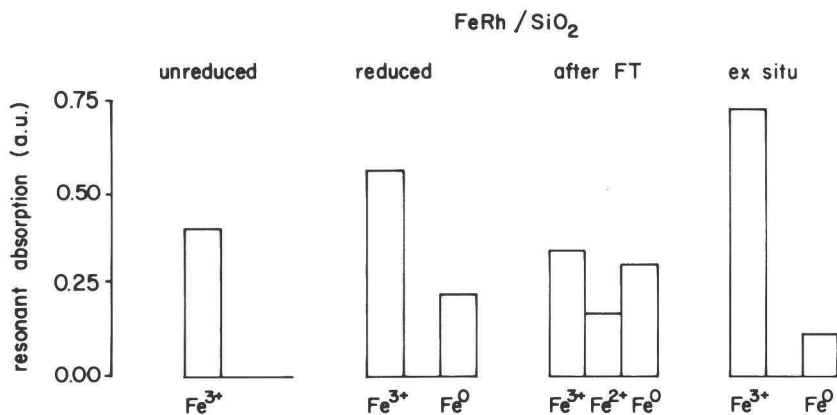


Fig. 5 Composition of the Mössbauer spectra in figure 4.

doublet falls in the 0 - 1 mm/s region of the spectrum. This spectrum was analyzed as a combination of two doublets and a singlet, due to Fe^{3+} , Fe^{2+} and Fe^0 respectively. It was assumed that the isomer shifts of the Fe^{3+} doublet and the Fe^0 singlet were the same as in the spectrum of the reduced catalyst. The Mössbauer parameters are given in table III. It is seen that the Fe^{2+} phase has been formed at the expense of the Fe^{3+} phase in the reduced catalyst. The ex situ spectrum of the catalyst after Fischer-Tropsch synthesis (fig.4d) could easily be analyzed as the combination of a doublet for Fe^{3+} and a small contribution of a singlet for the FeRh alloy.

The resonant absorption areas of the different iron states in the spectra of figure 4 are displayed as histograms in figure 5. This figure clearly demonstrates the transformations between the various iron states which result from the different treatments.

A fresh FeRh/SiO_2 catalyst (from a new batch) was reduced in H_2 at 400 K for 1 hour and at 725 K for 3 hours. Its Mössbauer spectrum is shown in figure 6a, the corresponding parameters are listed in table IV. The spectrum of this catalyst after CO chemisorption at 295 K (fig. 6b) shows a contribution of a Fe^{2+} doublet. In the computer analysis of this spectrum it was assumed that the Fe^0 and Fe^{3+} subspectra have the same isomer shift as in the reduced

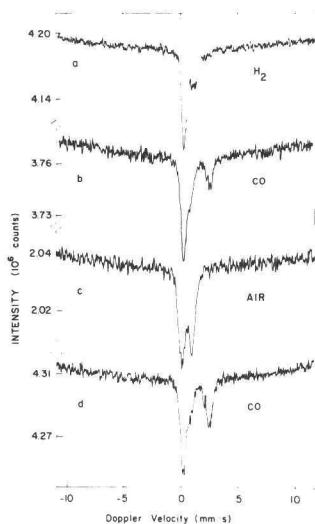


Fig. 6 Room temperature Mössbauer spectra of the vacuum-dried FeRh/SiO_2 catalyst after a series of consecutive treatments: a) H_2 reduction at 725 K, b) CO chemisorption at 295 K, c) exposure to air at 295 K and d) CO chemisorption at 295 K.

catalyst. The resonant absorption areas indicate that the Fe^{2+} phase has been formed at the expense of the Fe^{3+} phase in the reduced catalyst. Exposure of the catalyst to air resulted in spectrum 6c, which was analyzed as the combination of a doublet and a singlet corresponding to Fe^{3+} and Fe^0 respectively. Figure 6d shows the spectrum of the air-exposed catalyst after CO chemisorption at 295 K. This spectrum contains a large contribution of Fe^{2+} . The computer analysis was made under the assumption that the Fe^0 and Fe^{3+} component have the same isomer shift as in the spectrum of the air-exposed catalyst, see table IV for results. Figure 7 shows the composition of the Mössbauer spectra in figure 6.

Discussion

The Mössbauer spectrum of the reduced FeRh/SiO_2 catalyst (fig. 4b) is very similar to the spectra that are commonly encountered with supported bimetallic clusters of iron and a more noble group VIII metal, as shown in figure 1. If we compare the Mössbauer spectra of the reduced FeRh/SiO_2 catalyst that was dried in air (fig. 2) with that of the catalyst dried in vacuum (fig. 4b) it is seen that the former showed a smaller spectral contribution of the high velocity or surface peak. Since the total metal loading (5% by weight), the Fe:Rh ratio (1:1) and the surface area of the support ($300 \text{ m}^2/\text{g}$) are the same for both catalysts, we conclude that the difference between the two FeRh/SiO_2

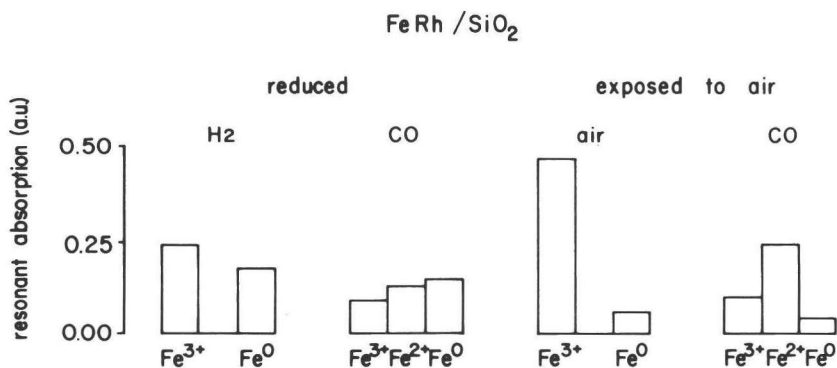


Fig. 7 Composition of the Mössbauer spectra in figure 6.

Table IV Mössbauer parameters of the spectra in figure 6.

treatment	iron state	I.S. (mm/s)	Q.S. (mm/s)	A (a.u.)
H ₂ , 725 K	Fe ⁰	0.35	-	0.18
	Fe ³⁺	0.68	1.00	0.24
CO, 295 K	Fe ⁰	0.35	-	0.15
	Fe ²⁺	1.48	2.20	0.13
	Fe ³⁺	0.68	1.00	0.09
air, 295 K	Fe ⁰	0.35	-	0.06
	Fe ³⁺	0.63	0.90	0.46
CO, 295 K	Fe ⁰	0.35	-	0.04
	Fe ²⁺	1.48	2.21	0.23
	Fe ³⁺	0.63	0.60	0.10

Accuracies: I.S.: 0.04 mm/s, Q.S.: 0.06 mm/s, A: 0.01

catalysts as shown in their Mössbauer spectra must be due to the method of drying after the impregnation process. It appears that drying in vacuum leads to a FeRh/SiO₂ catalyst, which after reduction shows a relatively large spectral contribution of the surface component compared to the catalyst that was dried in air. The conclusion that vacuum drying of impregnated catalysts leads to a smaller particle size than drying in air was also reached by Raupp and Delgass¹⁶ with Fe/SiO₂ catalysts.

The spectrum of the reduced FeRh/SiO₂ catalyst has been interpreted as a combination of a singlet corresponding to zero valent iron in FeRh alloy, and a doublet due to Fe³⁺. In this interpretation the Fe³⁺ phase would be a residue of the mixed iron rhodium oxide in the unreduced catalyst which can not be reduced by H₂. Upon CO chemisorption at 295 K the Fe³⁺ is partially converted into a Fe²⁺ phase. The sensitivity of the Fe³⁺ doublet to chemisorption of CO confirms that it corresponds indeed to a surface phase. A similar change of Fe³⁺ into Fe²⁺ is seen in the air exposed catalyst (figures 3 and 6). We believe that the conversion of the subspectrum assigned to the surface component into a Fe²⁺ doublet as a result of CO chemisorption on the reduced

FeRh/SiO₂ catalyst lends some support to our interpretation that the high velocity peak is indeed part of a Fe³⁺ doublet. In the introduction two other interpretations were given for the origin of the surface subspectrum. Garten et al.¹⁰ suggested that it is a doublet due to zero valent iron in the surface layer of the alloy. Then the conversion of the surface iron into Fe²⁺ by CO chemisorption at room temperature would correspond to an oxidation process, whereas the formation of Fe²⁺ by CO in the air-exposed catalyst is a reduction process. This seems to be contradictory. The other interpretation is that the subspectrum is an unresolved Fe²⁺ doublet. In that case the resonant absorption of this phase would be smaller than that of the Fe²⁺ doublet which is formed upon CO chemisorption. This would also imply that a fraction of the reduced iron in the FeRh alloy would be oxidized into the Fe²⁺ phase by CO at 295 K. This seems also unlikely. A more consistent explanation is that the high velocity peak in the spectrum of the reduced FeRh/SiO₂ catalyst corresponds to a Fe³⁺ phase. The conversion of this Fe³⁺ into Fe²⁺ by CO chemisorption at 295 K has a precedent in the case of the oxidized FeRh/SiO₂ catalyst, where no doubt exists that the Fe²⁺ in the catalyst under CO has been formed from Fe³⁺.

It should be noted that the Fe³⁺ in the reduced catalyst is not necessarily the only site of CO chemisorption. CO may also be chemisorbed on the reduced part of the catalyst, without a visible change in the subspectrum of the FeRh alloy.

The resonant absorption area of a Mössbauer spectrum measures the recoilless fraction of the iron atoms in the absorber (chapter two). Figure 5 shows that the recoilless fraction in the catalyst after impregnation and drying is significantly lower than in the catalyst after reduction or after all other subsequent treatments, as is also indicated in table III. A possible explanation is that the dispersion of the iron ions in the impregnated and dried catalyst is very high, whereas during the reduction in H₂ at 725 K the dispersion decreases somewhat, with the result that the recoilless fraction increases. Another possibility is that during the reduction the binding between the particles and the support may become stronger. This might also result in

a higher recoilless fraction for the reduced catalyst. Nevertheless, the dispersion in the reduced catalyst can not be very low, since its Mössbauer spectrum shows considerable changes upon exposure of the catalyst to CO or to air at room temperature.

In the Fischer-Tropsch synthesis at 525 K a part of the Fe^{3+} in the reduced FeRh/SiO_2 catalyst is converted into Fe^{2+} ions. This Fe^{2+} phase is not stable with respect to air, the oxygen converts it all back into Fe^{3+} along with most of the zero valent iron in the FeRh alloy.

III) Mössbauer spectra of FeRh/SiO_2 at cryogenic temperatures.

In the introduction of this chapter three different interpretations were given for the high velocity peak in the Mössbauer spectra of reduced bimetallic cluster catalyst of iron and a more noble group VIII metal. In the previous section we indicated that the CO chemisorption experiments with FeRh/SiO_2 do not support the interpretation that the high velocity peak belongs either to a doublet of zero-valent iron in the surface of the alloy or to an unresolved doublet due to Fe^{2+} at the surface. In this section we will investigate whether Mössbauer spectra at 77 and 4 K can yield additional information on the nature of this surface component in FeRh/SiO_2 catalysts. In particular we note that if the high velocity peak would belong to an unresolved Fe^{2+} doublet at 295 K, it may be better resolved at 77 K, since the electron contribution to the quadrupole splitting in Fe^{2+} compounds depends on temperature¹⁷.

The temperature dependence of the recoilfree fraction can yield information about the dispersion of the iron phases which contribute to the Mössbauer spectra. Somorjai¹⁸ has collected a table of Debye temperatures, as determined with low energy electron diffraction (LEED), for the surfaces of various metals. The general conclusion is that the surface Debye temperature is roughly equal to half that of the bulk. A LEED study on the $\text{ZnO}(10\bar{1}0)$ surface showed that this simple rule for the surface Debye temperature can also hold for a metal oxide surface¹⁹. The Debye temperature of bulk metallic

iron is 470 K²⁰, and 500 K for bulk $\alpha\text{-Fe}_2\text{O}_3$ and $\alpha\text{-FeOOH}$ ²¹. If we apply Somorjai's rule for the surface Debye temperature to the recoilless fraction in the Mössbauer effect, figure 3 of chapter two shows that the recoilless fraction of surface atoms depends stronger on the temperature than that of bulk atoms.

The experiments which are described in this section were carried out with the vacuum-dried FeRh/SiO_2 catalyst.

Results

The Mössbauer spectra of the unreduced FeRh/SiO_2 catalyst recorded at 295, 77 and 4 K all consist of a symmetrical quadrupole doublet (fig. 8). The Mössbauer parameters, given in table V, are characteristic of Fe^{3+} in an iron oxide in a (super)paramagnetic state. The width of the lines suggests a distribution in the local environments of the Fe^{3+} ions. The values in table V are the average values representative of a simple two line fit. The quadrupole splittings of the Fe^{3+} ions are high in comparison to those of bulk iron (III) oxides, which indicates that the environment of the Fe^{3+} ions is highly asymmetric. The values are consistent with those reported for highly dispersed

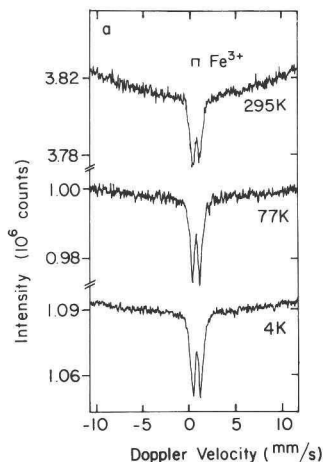


Fig. 8 Mössbauer spectra of the unreduced FeRh/SiO_2 catalyst, recorded at the indicated temperatures.

Fe^{3+} ²². The strong increase in the total resonant absorption of the spectra with decreasing temperature, in particular between 77 and 4 K, implies that the Debye temperature of the iron oxide in the unreduced catalyst is low, which indicates that the dispersion must be high.

In situ Mössbauer spectra at 295, 77 and 4 K of the FeRh catalyst after reduction in H_2 at 400 K for 1 hour and at 725 K for 5 hours are shown in figure 9. The spectrum at 295 K consists, as previously, of a large

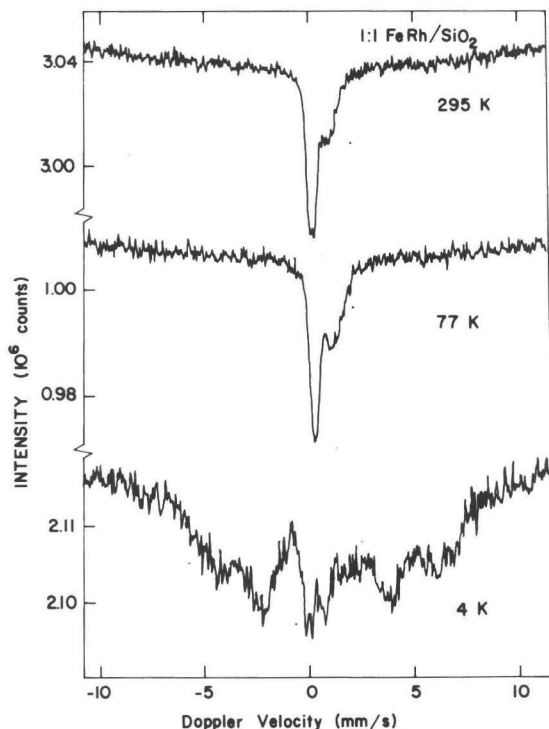


Fig. 9 In situ Mössbauer spectra of the reduced FeRh/SiO₂ catalyst, recorded at the temperatures indicated.

central peak due to the FeRh alloy and a somewhat broadened high velocity peak near 1 mm/s. The spectrum at 77 K shows a similar pattern, but the intensity of the high velocity peak is substantially enhanced. We already note here that the latter has not split into a resolved doublet, which might have been expected when the high velocity peak at 295 K would correspond to a Fe²⁺ state.

Both spectra were analyzed as a combination of a singlet and a doublet (table V). In the spectrum at 77 K the fit was not quite satisfactory, due to the fact that the doublet has broad peaks which differ slightly from the Lorentzian shape. The Mössbauer parameters of the doublet at both temperatures are characteristic for Fe³⁺ ions. Within their accuracies, the isomer shifts and the resonant absorption areas of each component satisfy the requirement that they do not decrease with decreasing temperature, which follows from the lattice dynamics, as explained in chapter two.

Table V Mössbauer parameters of FeRh/SiO₂ at 295, 77 and 4 K.

T (K)	iron state	I.S. (mm/s)	Q.S. (mm/s)	A (a.u.)
before reduction				
295	Fe ³⁺	0.68	0.77	0.40 ± 0.02
77	Fe ³⁺	0.73	0.80	0.64 ± 0.03
4	Fe ³⁺	0.82	0.84	1.33 ± 0.07
after reduction				
295	Fe ⁰	0.38	-	0.21 ± 0.02
	Fe ³⁺	0.69	0.97	0.26 ± 0.03
77	Fe ⁰	0.47	-	0.23 ± 0.02
	Fe ³⁺	0.88	1.04	0.64 ± 0.05
4				0.98 ± 0.09

Accuracies : I.S.: 0.04 mm/s, Q.S.: 0.06 mm/s.

The spectrum at 4 K shows that at least one of the iron compounds has become magnetically split, however, with a broad distribution in hyperfine fields. Such patterns are frequently observed with amorphous materials, where a distribution in local environments of the iron atoms results in a number of different magnetic hyperfine fields. The broad, partially overlapping peaks and the relatively high statistical errors do not allow a computer analysis. The spectrum shows that the main contribution is due to sextuplets with magnetic splittings in the order of 250 - 350 kOe, which we attribute to the zero-valent iron in the FeRh alloy. The statistical uncertainties make it impossible to decide if any magnetically split contributions of Fe³⁺ compounds are present, with hyperfine splittings in the range of 450 - 550 kOe.

The total resonant absorption areas for the Mössbauer spectra of the FeRh/SiO₂ catalyst before and after reduction are given in figure 10. For comparison a curve corresponding to the behavior of bulk material with a Debye temperature of about 470 K has been included also.

Discussion

The Mössbauer spectrum of the reduced FeRh/SiO_2 catalyst at 77 K does not support the interpretation that the high velocity or surface peak corresponds to a Fe^{2+} compound, since no splitting of this peak into a doublet occurs at 77 K. This confirms our previous assumption that the spectrum of the reduced FeRh/SiO_2 catalyst consists of a singlet and a doublet. The Mössbauer parameters of the doublet at 295 and 77 K are consistent with the requirements which follow from the temperature dependence of the lattice dynamics (chapter two), and they indicate that the doublet should be attributed to a Fe^{3+} state.

Unfortunately, the spectrum at 4 K does not yield additional information on the reduced catalyst, because of the relatively large statistical errors which are the result of the distribution of the spectral intensity over a number of broad peaks. Mössbauer spectra of $\text{FeIr}/\text{Al}_2\text{O}_3$ and $\text{FePt}/\text{Al}_2\text{O}_3$ at about 20 K have been published by Garten and Sinfelt²³. These spectra also consist of broad, partially overlapping peaks, and have a similar shape as our spectrum of FeRh/SiO_2 at 4 K. Garten and Sinfelt fitted their spectra with a single six line pattern, using unrealistic distances between the peaks which

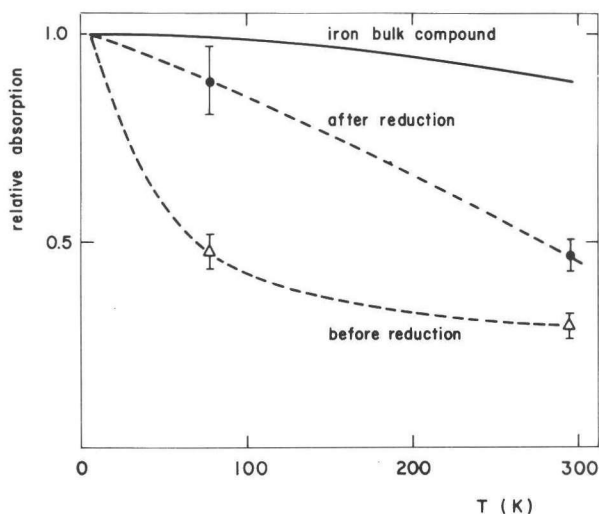


Fig. 10 Total resonant absorption areas of the FeRh/SiO_2 spectra in the figures 8 and 9, normalized to unity at 4 K. The full line corresponds to the temperature dependence of the resonant absorption in iron bulk compounds with a Debye temperature of 500 K. The dotted lines have been drawn as a guide to the eye only.

do not satisfy equation (24) of chapter two. In fact, these spectra should be characterized by a distribution of magnetic hyperfine fields. In connection with our interpretation of the surface component in terms of a Fe^{3+} species, it is interesting that the spectra of $\text{FePt}/\text{Al}_2\text{O}_3$ and $\text{FeIr}/\text{Al}_2\text{O}_3$ at 20 K seem to show some absorption at velocities of around -7.5 and $+8.5$ mm/s^{23} , velocities where contributions of magnetically split Fe^{3+} are expected. However, in order to establish the presence of magnetically split Fe^{3+} contributions without doubt, it is essential to have a liquid helium spectrum of improved quality. Therefore a FeRh/SiO_2 catalyst enriched in the Mössbauer isotope ^{57}Fe should be used in the future.

The total resonant absorptions in figure 10 reflect the temperature dependence of the average recoilless fraction of the FeRh/SiO_2 catalyst before and after reduction. As discussed in the introduction of this section, the results in figure 10 suggest that a relatively high fraction of the atoms in the unreduced catalyst is at the surface, whereas the degree of dispersion decreases upon reduction in H_2 at 725 K.

The resonant absorption of the Fe^{3+} component in the reduced catalyst increases substantially between 295 and 77 K, more than that of the Fe^0 component. This is consistent with earlier conclusions, that the Fe^{3+} component corresponds to a finely dispersed surface species. The increase in the resonant absorption of the alloy component between 295 and 77 K is not very pronounced. Apparently, the dimensions of the alloy particles are significantly larger than those which contain the Fe^{3+} phase.

SUMMARY OF THE RESULTS

Impregnation of a silica carrier unto incipient wetness with an aqueous solution of iron nitrate and rhodium chloride, followed by drying of the sample either in air or in vacuum leads to a FeRh/SiO_2 catalyst with the following properties:

- The unreduced catalyst contains highly dispersed Fe^{3+} , which is partially converted into Fe^{2+} by H_2 or CO at 295 K.

- The catalysts after reduction in H_2 at 725 K contain iron in two states: Fe^0 in a FeRh alloy, and Fe^{3+} in a highly dispersed phase which also contains rhodium in a state that is unknown yet. The absence of α -Fe and Fe^{2+} , which are commonly encountered in monometallic Fe/SiO₂, demonstrates that all iron in the FeRh/SiO₂ is influenced by rhodium. A substantial fraction of the Fe^{3+} is converted into Fe^{2+} by CO chemisorption at 295 K. The dimensions of the FeRh alloy are significantly larger than those of the Fe^{3+} containing phase. The vacuum-dried catalyst contains relatively more of the highly dispersed Fe^{3+} phase than the air-dried catalyst.
- Exposure of the reduced FeRh/SiO₂ catalyst to air at 295 K results in the oxidation of most of the Fe^0 in the FeRh alloy into Fe^{3+} .
- In the Fischer-Tropsch synthesis at 525 K a fraction of the Fe^{3+} in the reduced catalyst is converted into a Fe^{2+} state. This phase is oxidized into Fe^{3+} in air at 295 K.
- The air-exposed FeRh/SiO₂ catalysts can be partially reduced into a Fe^{2+} state by H_2 or CO at room temperature. This rereduction process proceeds further in CO than in H_2 .
- CO chemisorption on air-exposed FeRh/SiO₂ at 295 K results in significantly more Fe^{2+} than CO chemisorption on reduced FeRh/SiO₂.

MODEL FOR FeRh/SiO₂ CATALYSTS

The reduced FeRh/SiO₂ catalyst contains regions of finely dispersed Fe^{3+} and rhodium in an unknown state, and FeRh alloy clusters of a larger size. Two possibilities for the structural arrangement of these two components can be envisioned.

First, suppose that the well-dispersed phase forms a surface layer which covers the alloy particles. This would be in agreement with the interpretation of Garten et al.¹⁰ for reduced FeRu/SiO₂ catalysts. As these authors believe that, in spite of its high isomer shift, the surface component in the Mössbauer spectra corresponds to Fe^0 in the surface of the alloy, this model for the structure of the reduced catalyst is trivial. However, in this chapter we

presented evidence that the surface component in FeRh/SiO₂ catalysts is not a Fe⁰ but a Fe³⁺ phase. In this case a model in which the highly dispersed Fe³⁺ containing phase covers the alloy seems unlikely, since it would be hard to understand why a Fe³⁺ state on top of a reduced alloy particle should be stabilized under H₂. We therefore reject this model.

The following interpretation seems more realistic. Assume that a distribution of particle sizes occurs in the reduced catalyst. A fraction of the particles is too small to be reduced, due to nucleation problems. Nucleation inhibition as a result of a high dispersion is a common phenomenon in silica supported oxides of iron and nickel²⁴. The irreducible particles give rise to a Fe³⁺ doublet in the Mössbauer spectrum of the reduced FeRh/SiO₂ catalyst. Particles which are larger than a certain critical size do not suffer from nucleation problems, and hence these particles can easily be reduced into a FeRh alloy. A schematical representation of this model and the changes which occur on chemisorption of CO or exposure to air is given in figure 11.

The stabilization of the Fe³⁺ phase in reduced FeRh/SiO₂ must be due to the presence of rhodium in this phase, since Fe³⁺ in monometallic Fe/SiO₂ catalysts can always be reduced into the Fe²⁺ state⁹. The explanation for this stabilization will have to be found in the thermodynamics of the rhodium - Fe³⁺ - SiO₂ system, but to our knowledge literature on this system is not available. The Fe³⁺ in the reduced catalyst can be partially converted into Fe²⁺ by CO at 295 K, similar as in the unreduced or in the oxidized FeRh/SiO₂ catalyst. This conversion must be due to the presence of rhodium, in a state that is not known. Perhaps XPS (X-ray photo electron spectroscopy) may reveal information about the state of rhodium in the well dispersed Fe³⁺ phase.

The model in figure 11 is strongly supported by the CO chemisorption results shown in the figures 6 and 7. Chemisorption of CO on the air-exposed catalyst yields significantly more Fe²⁺ than CO chemisorption on the reduced catalyst, in agreement with figure 11. This result would be hard to understand in a model in which the Fe³⁺ containing phase covers the alloy, since oxidation of such particles should not lead to a larger number of Fe³⁺ ions which are accessible to CO.

Model FeRh/SiO₂

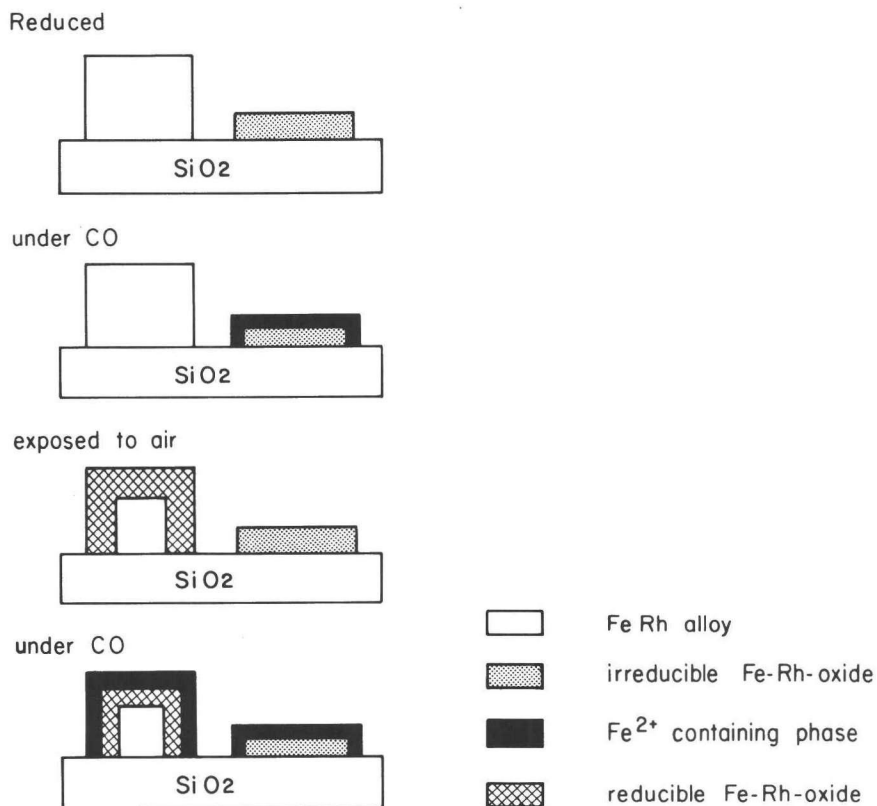


Fig. 11 Schematical representation of FeRh/SiO₂ catalysts.

As we already mentioned in the introduction of this chapter, supported bimetallic cluster catalysts which consist of iron and a more noble group VIII metal exhibit Mössbauer spectra which are very similar. We therefore suggest that the validity of the model in figure 11 is not limited to FeRh/SiO₂ catalysts alone. The model would be consistent with Aschenbeck's XPS spectrum of a reduced FeRu/SiO₂ catalyst⁵, which clearly shows the presence of both reduced and unreduced iron in the surface of the catalyst. Also the relation between the overall dispersion in FeRu/SiO₂ catalysts and the intensity of the

surface subspectrum in the Mössbauer spectra of reduced FeRu/SiO_2 ^{5,6,10} is consistent with the model of figure 11, since a high overall dispersion necessarily corresponds with a large fraction of irreducible clusters.

Another experiment with FeRu/SiO_2 catalyst which can be understood with the model in figure 11 has been reported by Lam and Garten¹⁰. These authors incorporated Cu into FeRu/SiO_2 catalysts and noted a decrease in the spectral contribution of the surface component to the Mössbauer spectrum of the reduced catalyst. In our interpretation, the surface component corresponds to irreducible Fe^{3+} in a highly dispersed state and hence, the disappearance of this component as a result of Cu incorporation would indicate that Cu promotes the reduction of well dispersed, otherwise irreducible, particles. This interpretation is consistent with the results of Roman and Delmon²⁵, who found that Cu enhances the reducibility of highly dispersed NiO supported on silica.

RECOMMENDATIONS

This chapter is an account on an investigation which, at the present time, is still in progress. A few suggestions for future research may be appropriate.

The results of the in situ Mössbauer experiments at temperatures between 4 and 295 K are sufficiently interesting to record similar spectra of the FeRh/SiO_2 catalyst under CO, after Fischer-Tropsch synthesis or exposure to air. As the spectral intensity of FeRh/SiO_2 in the spectra at 4 K is distributed among several broad peaks, the Mössbauer absorption should be enhanced by using catalysts which are isotopically enriched in the Mössbauer isotope ⁵⁷Fe.

Additional information on the state of Rh in the catalysts would be desirable. X-ray photo electron spectroscopy may reveal such information, although the presence of a non-conducting support as SiO_2 is a drawback in the application of this technique. Also infra red spectroscopy of CO chemisorption on FeRh/SiO_2 may yield valuable information on the surface composition of the catalysts.

As we discussed before, the model in figure 11 may be applicable to other iron containing bimetallic cluster catalysts than FeRh/SiO₂ as well. The CO chemisorption experiments in figure 6 and 7 may be used as a simple screening test for the validity of this model for supported bimetallic clusters of iron and a more noble group VIII metal, such as FeRu, FePd, FeOs, FeIr, and FePt.

The presence of at least two phases in reduced FeRh/SiO₂ raises the question which phase is responsible for the interesting catalytic properties of the catalyst: the FeRh alloy, the well dispersed Fe³⁺ containing phase or maybe even the interface between the two. Aschenbeck⁵ has shown that variation of the atomic Fe:Rh ratio provides a means to influence the relative contribution of the Fe³⁺ containing phase to the Mössbauer spectra. It would be very interesting to test a number of these FeRh/SiO₂ catalysts in Fischer-Tropsch synthesis at high pressures, to investigate whether a correlation exist between the catalytic selectivity and the contribution of the Fe³⁺ phase to the Mössbauer spectra.

REFERENCES

1. J.H. Sinfelt, J.Catal. 29,308(1973).
2. V. Ponec, Surface Sci., 80,352(1979)
3. M.M. Bhasin, W.J. Bartley, P.C. Ellgen and T.P. Wilson, J.Catal. 54,120 (1978).
4. D.L. King, J.A. Cusumano and R.L. Garten, Catal.Rev.-Sci.Eng. 23,233(1981).
5. D.P. Aschenbeck, Ph.D. thesis, Purdue University, 1979.
6. M.A. Vannice, Y.L. Lam and R.L. Garten, Adv. in Chem. 178,15(1979).
7. R.L. Garten, in "Mössbauer Effect Methodology" (I.J. Gruverman, ed.), Vol 10, Plenum Press, New York, 1976, p.69.
8. L. Guczi, Catal. Rev.-Sci.Eng., 23, 329(1981).
9. H. Topsøe, J.A. Dumesic, and S. Mørup, in "Applications of Mössbauer Spectroscopy" (R.L. Cohen, ed.), Vol. II, Academic Press, New York, 1980, p.55.

10. Y.L. Lam and R.L. Garten, Proc.Simposium Ibero-Am. Catal., 6th, Rio de Janeiro, 1978.
11. R.L. Garten, J.Catal.43,18(1976).
12. M.A. Vannice and R.L. Garten, J.Mol.Catal. 1,201(1975/76).
13. C.H. Bartholomew and M. Boudart, J.Catal. 29,278(1973).
14. L. Guzzi, K. Matusek, I. Manninger, J. Kiraly and M. Eszterle, in "Preparation of Catalysts", Vol. II, Elsevier, Amsterdam(1979), p. 391.
15. C.C. Chao, P. Duwez and C.F.J. Chang, J.Appl.Phys., 42,4282(1971).
16. G.B. Raupp and W.N. Delgass, J.Catal.58,337(1979).
17. J.C. Travis in "An Introduction to Mössbauer Spectroscopy" (L. May, ed.), Plenum Press, New York,1971.
18. G.A. Somorjai, "Chemistry in Two Dimensions: Surfaces", Cornell University Press, Ithaca(1981), p.170.
19. W. Gopel and G. Neuenfeldt, Surface Sci. 55,362(1976).
20. C. Kittel, "Elementary Solis State Physics, a short course", John Wiley and Sons, New York, 1961, p.58.
21. C.F.J. Flipse, unpublished results.
22. H.M. Gager and M.C. Hobson, Catal. Rev.-Sci.Eng. 11,117(1975).
23. R.L. Garten and J.H. Sinfelt, J.Catal.62,127(1980).
24. J.R. Anderson, "Structure of Metallic Catalysts" Academic Press, New York, 1975.
25. A. Roman and B. Delmon, J.Catal.30,333(1973).

In the present economical situation, in which the consumption of oil and oil-derived products is stagnating, it is not to be expected that Fischer-Tropsch synthesis for the production of synthetic fuels or basic chemicals will readily find application. If, however, for whatever reason a third oil crisis might arise in the future, the Fischer-Tropsch process offers a feasible alternative to non-oil producing countries.

Among the metals, suitable for Fischer-Tropsch synthesis at a large scale, iron seems to be the best candidate since it is relatively cheap and abundantly present. Obviously, it is important to know or rather, to understand the behavior of iron as a Fischer-Tropsch catalyst in all its aspects.

The Fischer-Tropsch synthesis over iron catalysts is a very intricate process. In the first place, the mechanism of the catalytic reaction between H_2 and CO , two simple molecules, is highly complex, in particular under industrial conditions. An adequate description of this mechanism requires a network of many reactions. In the second place, the working iron Fischer-Tropsch catalyst, even if it is unpromoted or unsupported, is a multicomponent system which may contain simultaneously metallic iron, iron carbides and iron oxides.

In the characterization of these multicomponent iron catalysts Mössbauer spectroscopy has proven to be a very valuable technique. It appeared possible to determine the bulk composition of both unpromoted and MnO -promoted iron catalysts in various stages of carburization, as was shown in the chapters three¹, four and seven² of this thesis. In chapter five³ we have seen that it is even possible to obtain information about the presence of iron oxides at the surface of the catalyst, by applying Mössbauer spectroscopy in situ at temperatures down to 4 K. That Mössbauer spectroscopy can also be used to study iron species at the surface of highly dispersed systems was demonstrated with $FeRh/SiO_2$ catalysts in chapter eight.

In this final chapter we will first give attention to a few aspects of Mössbauer spectroscopy in the study of iron containing catalysts. Next we will discuss the most relevant results in this thesis from the viewpoint of catalysis.

Mössbauer spectroscopy

The newly developed fitting routine which was introduced to analyze the complicated Mössbauer spectra of carburized iron catalysts, as described in the chapters two and three¹, functions satisfactorily. In this method the spectrum of a mixture of iron compounds is fitted with a linear combination of spectra of the constituents. Partially carburized Fe-MnO catalysts contain sometimes six different iron phases at a time², and in that case the Mössbauer spectrum is a combination of 40 peaks. We believe that for the analysis of these complex spectra our fitting routine is much more reliable than the commonly applied procedure of fitting single Lorentzian shaped lines to the spectra which, moreover, is also rather time-consuming.

In a different and also newly developed procedure Mössbauer spectra are fitted with a combination of elementary spectra by varying the Mössbauer parameters in a non-linear minimization routine (see chapter two). This method, which implicitly guarantees physically realistic fits, allows for a rapid and reliable determination of the Mössbauer parameters for the FeRh/SiO₂ spectra. We prefer this method to the common fitting of single Lorentzians, in which more parameters have to be varied than is strictly necessary.

The iron oxides at the surface of unsupported iron catalysts that are formed as a result of treatment with CO or exposure to air, could only be observed in Mössbauer spectra at temperatures well below 77 K, chapters three¹ and five³. Similar oxide contributions have recently also been found by Amelse et al.⁴ and by Shen and Dumesic⁵. Apparently, catalysts may contain iron phases which are characterized by Debye temperatures as low as 50 K. This is much smaller than those of bulk iron or iron oxide (about 500 K^{6,7}) or their surfaces (200 - 300 K). The latter values follow from applying Somorjai's rule that the Debye temperature of a well defined flat surface is about half that of the bulk⁸. The unusually low value of the Debye temperature for the surface oxides on the iron catalysts indicates that their structure is probably far from perfect and that their dimensions are likely to be very small.

Whatever the precise nature of these surface iron oxides is, their very existence implies that the only reliable characterization of iron catalysts by

means of Mössbauer spectroscopy should be made at liquid helium temperature, since at this temperature also compounds with extremely low Debye temperatures become detectable (see figure 3 of chapter two). This clearly illustrates the usefulness of in situ equipment which permits the recording of Mössbauer spectra at cryogenic temperatures down to 4 K.

Iron compounds with a very low Debye temperature were also present in the FeRh/SiO₂ catalysts after impregnation and drying, as follows from the large increase in resonant absorption area between 77 and 4 K. After reduction in H₂ at 725 K, however, such compounds disappeared (figure 10 of chapter eight).

The Mössbauer spectra of highly dispersed FeRh/SiO₂ catalysts at 295 K showed considerable changes upon chemisorption of CO and H₂, chapter eight⁹. This demonstrates that application of Mössbauer spectroscopy to iron containing bimetallic clusters at room temperature can certainly reveal valuable information about the surface. Nevertheless, measurements at cryogenic temperatures are also necessary. Due to the low effective Debye temperatures of the bimetallic clusters, the spectra at 77 K show higher resonant absorption and improved resolution compared to the room temperature spectra. Comparison of resonant absorption areas at different temperatures yields qualitative information on the recoilless fraction of the ⁵⁷Fe atoms and hence on their dispersion.

By using Mössbauer spectra of a given absorber at different temperatures, additional constraints can be imposed in the fitting procedure, which turn out to be very useful. Theory requires that both the isomer shift and the resonant absorption area of each iron compound decrease with increasing temperature. In all applications discussed here, these constraints have been sufficient to obtain unequivocally determined Mössbauer parameters.

Finally, we would like to stress that extrapolation of the resonant absorption areas for the different iron constituents in the spectra to a temperature of 0 K is the only way to make a reliable estimate of the actual composition of a sample. The commonly made assumption that the recoilless fractions of the constituents are equal at room temperature leads certainly to erroneous results in the case of well dispersed particles.

Catalysis

During the early stages of the Fischer-Tropsch synthesis iron catalysts are rapidly converted into iron bulk carbides. In this sense iron is unique among the group VIII metals, since diffusion of carbon into the metal is a very fast process¹⁰. Due to the disappearance of most of the carbon into the bulk of the catalyst insufficient carbon atoms are present at the surface of the catalyst to participate in the actual Fischer-Tropsch reaction. Therefore, the initial activity of iron Fischer-Tropsch catalysts is low, in contrast to the other group VIII metals, where the activity starts at a maximum level, and no carburization occurs. The relation between Fischer-Tropsch activity and carburization has extensively been discussed in chapter six¹¹ of this thesis.

Most investigators who use Mössbauer spectroscopy to characterize iron Fischer-Tropsch catalysts seem to agree on the appearance of not more than four different iron carbides under Fischer-Tropsch conditions^{1,2,4,12-16}. In unsupported iron the carbide $\chi\text{-Fe}_5\text{C}_2$ is the dominant phase, whereas $\epsilon'\text{-Fe}_{2.2}\text{C}$ is mainly formed in supported well-dispersed iron. In both cases Fe_xC , a poorly crystallized structure which was first reported in chapter three¹, appears as an intermediate between metallic iron and the ultimate carbide structure. The carbide $\theta\text{-Fe}_3\text{C}$ is only formed at temperatures above 600 K. Convincing evidence for the occurrence of a carbide $\epsilon\text{-Fe}_2\text{C}$ in iron Fischer-Tropsch catalysts has not been given up to now. The subspectrum that Raupp and Delgass¹⁷ originally attributed to $\epsilon\text{-Fe}_2\text{C}$ is in fact due to Fe_xC , according to Delgass¹⁸.

Deviating interpretations concerning the Mössbauer spectra of the carbides $\epsilon'\text{-Fe}_{2.2}\text{C}$, $\epsilon\text{-Fe}_2\text{C}$ and Fe_xC have been presented by Pijolat et al.¹⁹ and le Caer et al.²⁰ They neglect the differences in crystallographic structure between these carbides and instead they propose to interpret the carbide spectra in terms of two different iron sites only, which correspond to iron atoms with two and with three carbon nearest neighbors, respectively. However, these authors record their spectra of carburized iron catalysts during Fischer-Tropsch synthesis at the reaction temperature of 523 K and for one hour only²¹, while the carburization process is still in progress. As a consequence the quality of the Mössbauer spectra is rather poor. We are, therefore, not convinced that

the simplified interpretations of Pijolat et al.¹⁹ and leCaer et al.²⁰ are justified in general.

In chapter three¹ it was shown that CO pretreatment of iron yields a catalyst with a high initial activity, as opposed to pure metallic iron. This was explained by assuming that CO pretreatment leads to a carburized catalyst in which all carbon atoms at the surface are available for the actual Fischer-Tropsch reaction at the start of the synthesis. With the additional information now available this interpretation does not appear to be correct. One of the conclusions in chapter five³ is that carburization of iron in CO alone proceeds very slowly and that iron oxides are formed at the surface of the catalyst. These surface oxides impede diffusion of carbon into the interior of the catalyst and as a consequence the concentration of carbon at the surface will be high. Thus, oxidation of the iron surface is primarily responsible for the enhanced Fischer-Tropsch activity in CO pretreated catalysts. This is consistent with the experiments of Dwyer and Somorjai²² who found a tenfold increase in initial methanation rate upon preoxidation of their iron foils.

It is not trivial that the reaction mechanism of the Fischer-Tropsch synthesis is the same with iron and iron oxide catalysts. Castner et al.²³ reported that the activation energies for the reaction between CO and H₂ over rhodium and rhodium oxide differ considerably. It would be interesting to know whether the same is true for iron and iron oxide, as in chapter five³ evidence was presented that surface oxides may be formed in the Fischer-Tropsch synthesis over iron catalysts. This would have implications for the reaction mechanism. If both reduced and oxidized iron can indeed coexist at the surface of the catalyst and if the Fischer-Tropsch reaction over the two different sites proceeds via different mechanisms, then the overall process cannot be described in terms of a sequence of elementary steps, but as a complex network of steps²⁴.

The main conclusion from the investigation of Fe-MnO catalysts in chapter seven² is unfortunately a negative one: MnO is not an effective promoter for the production of ethylene and propylene in the Fischer-Tropsch synthesis over iron catalysts, at least not at atmospheric pressure. At higher pressures of 10 - 15 bar the olefin selectivity is indeed substantially higher than in our

case. The product distribution, however, shifts to longer hydrocarbons and therefore the yield of low olefins remains low²⁵. Addition of sulphate to the Fe-MnO catalyst leads to an increased selectivity for ethylene and propylene at 625 K, be it at the expense of mechanical stability of the catalyst.

The reduced Fe-MnO catalyst consists of α -Fe, MnO, an iron (II) manganese mixed oxide and some iron (III) oxide, the latter probably included in the MnO and inaccessible to reduction by H₂. Such a composition may be characteristic for this class of catalysts which are based on a group VIII metal as iron or cobalt, and an almost irreducible oxide as MnO or ZnO.

The investigation of bimetallic FeRh/SiO₂ catalysts concerned primarily the structure of this system (chapter eight⁹). All evidence points to a catalyst which contains regions of a highly dispersed, irreducible phase in which iron occurs as Fe³⁺, and larger particles of FeRh alloys. The intriguing question remains which of the two phases contains the sites that are active for the formation of methanol and ethanol in the Fischer-Tropsch synthesis at elevated pressures.

Poels et al.²⁶ and Ponec²⁷ have shown that the methanol selectivity of supported Pd catalysts increases with increasing content of positive palladium ions, stabilized by the support or by promoters. The authors suggest that these positive centers are essential for the production of methanol.

A similar situation may arise in FeRh/SiO₂ catalysts. Rabo et al.²⁸ proposed that the synthesis of methanol occurs on sites where CO is chemisorbed molecularly. As CO dissociates easily on both Fe and Rh at reaction temperatures, one could speculate that the well dispersed Fe³⁺ containing regions in the FeRh/SiO₂ catalyst offer the sites where CO is adsorbed molecularly and hence oxygenated hydrocarbons are formed.

In view of the problems with dissociative adsorption of H₂ on metal oxides one could even consider the presence of ensembles which contain both metal atoms and ions²⁹. Such ensembles might be found at the interface between the alloy and the Fe³⁺ containing regions. In this respect we note that in our model for FeRh/SiO₂ catalysts (figure 11 of chapter eight) the implicitly assumed separation between the highly dispersed phase and the larger alloy

particles is not essential at all. A model in which the two phases are in direct contact with each other would explain the results in chapter eight as well.

References

1. J.W. Niemantsverdriet, A.M. van der Kraan, W.L. van Dijk and H.S. van der Baan, *J.Phys.Chem.* 84, 3363 (1980).
2. W.L. van Dijk, J.W. Niemantsverdriet, A.M. van der Kraan and H.S. van der Baan, *Appl.Catal.* 2, 273 (1982).
3. J.W. Niemantsverdriet, C.F.J. Flipse, A.M. van der Kraan and J.J. van Loef, *Appl.Surface Sci.* 10, 302 (1982).
4. J.A. Amelse, G. Grynkewich, J.B. Butt and L.H. Schwartz, *J.Phys.Chem.* 85, 2484 (1981).
5. W.M. Shen and J.A. Dumesic, private communication.
6. C. Kittel, "Elementary Solid State Physics: A Short Course", Wiley, New York, 1962, p.58.
7. C.F.J. Flipse and J.W. Niemantsverdriet, unpublished results.
8. G.A. Somorjai, "Chemistry in Two Dimensions: Surfaces", Cornell University Press, Ithaca, 1981, p.170.
9. J.W. Niemantsverdriet, A.M. van der Kraan, J.J. van Loef and W.N. Delgass, *J.Phys.Chem.* submitted for publication.
10. R.T.K. Baker, *Catal.Rev.-Sci.Eng.* 19, 161 (1979).
11. J.W. Niemantsverdriet and A.M. van der Kraan, *J.Catal.* 72, 385 (1981).
12. R.M. Stanfield and W.N. Delgass, *J.Catal.* 72, 37 (1981).
13. R.M. Stanfield, Ph.D. Thesis, Purdue University, 1981.
14. D. Bianchi, S. Borcar, F. Teule-Gay and C.O. Bennett, *J.Catal.* in press.
15. C.O. Bennett, private communication.
16. H.J. Jung, M.A. Vannice, L.N. Mulay, R.M. Stanfield and W.N. Delgass, *J.Catal.* 76, 208 (1982).
17. G.B. Raupp and W.N. Delgass, *J.Catal.* 58, 348 (1979).
18. W.N. Delgass, private communication.
19. M. Pijolat, G. leCaer, V. Perrichon and P. Bussiere, International Conference on the Application of the Mössbauer Effect, Jaipur, 1981, in press.

20. G. Le Caër, J.M. Dubois, M. Pijolat, V. Perrichon and P. Bussiere, *J.Phys. Chem.* 86, 4799 (1982).
21. P. Bussiere, private communication.
22. D.J. Dwyer and G.A. Somorjai, *J.Catal.* 52, 291 (1978).
23. D.G. Castner, R. Blackadar and G.A. Somorjai, *J.Catal.* 66, 257 (1980).
24. C.K. Rofer-DePoorter, *Chem.Rev.* 81, 447 (1981).
25. A. Zein el Deen, J. Jacobs and M. Baerns, *Chem.Eng.Tech.* 50, 958 (1978).
26. E.K. Poels, R. Koolstrá, J.W. Geus and V. Ponec, in "Metal-Support and Metal-Additive Effects in Catalysis", (B. Imelik et al., eds.), Elsevier, Amsterdam, 1982, p.233.
27. V. Ponec, *ibid*, p.63.
28. J.A. Rabo, A.P. Risch and M.L. Poutsma, *J.Catal.* 53, 295 (1978).
29. G.-A. Martín, private communication.

SAMENVATTING

De oliecrisis van 1973 en het gegroeide besef dat onze belangrijkste fossiele energiebron olie niet onuitputtelijk is, hebben een hernieuwde belangstelling voor steenkool doen ontstaan. Steenkool vertegenwoordigt ongeveer 75% van de fossiele brandstof voorraden, olie slechts 15%. Het gebruik van steenkool heeft echter nadelen in vergelijking met dat van vloeibare en gasvormige energiedragers. Steenkool is als vaste stof moeilijker te transporteren en op te slaan. Het bevat potentiële milieuverontreinigers als asvormende bestanddelen en zwavel (veel meer dan olie), welke niet eenvoudig verwijderd kunnen worden. Bovendien kan steenkool niet direct als grondstof voor de chemische industrie gebruikt worden. Deze nadelen worden grotendeels vermeden als steenkool wordt omgezet in gasvormige of vloeibare producten, welke voor gebruik als brandstof of grondstof geschikt zijn.

Wanneer steenkool met stoom wordt vergast, ontstaat een mengsel van voornamelijk koolmonoxide (CO) en waterstof (H₂), het zogenaamde synthesegas. Dit gas kan op vele manieren omgezet worden in nuttige producten, zoals waterstof, methaan (synthetisch aardgas), methanol en allerlei hogere koolwaterstoffen. In het Fischer-Tropsch proces, gepatenteerd rond 1923 en op grote schaal toegepast tijdens de tweede wereldoorlog in Duitsland, wordt synthesegas met behulp van ijzer-, cobalt- of rutheniumkatalysatoren omgezet in koolwaterstoffen, zoals methaan, benzine en dieselolie.

IJzer biedt de beste mogelijkheden voor het gebruik van Fischer-Tropsch synthese op grote schaal, het is immers goedkoop en volop beschikbaar. Bovendien kan de katalytische selectiviteit van dit metaal door geschikte toevoegingen en door de keuze van de procesomstandigheden tamelijk goed gevarieerd worden. Het is daarom van groot belang het gedrag van ijzer als katalysator in het Fischer-Tropsch proces door en door te kennen. Bij het onderzoek van deze katalysatoren blijkt mössbauerspektroskopie een ideale meetmethode te zijn, met behulp waarvan de verschillende in Fischer-Tropsch katalysatoren optredende ijzerverbindingen gemakkelijk geïdentificeerd kunnen worden. Bovendien kan de

katalysator met deze techniek in situ, dat wil zeggen onder reactie-kondities, bestudeerd worden.

In dit proefschrift worden drie verschillende ijzerkatalysatoren besproken, namelijk 1) modelkatalysatoren waaraan geen promotor- of dragermateriaal is toegevoegd, 2) met mangaanoxide gepromoteerde ijzerkatalysatoren en 3) bimetal-
lische ijzerrhodiumklusters op een silicadrager.

Het Fischer-Tropsch proces over ijzerkatalysatoren is een tamelijk ingewikkeld proces. In de eerste plaats is het reactiemechanisme van de katalytische reactie tussen CO en H₂, twee eenvoudige molekulen, veel ingewikkelder dan men op het eerste gezicht zou verwachten. In de tweede plaats is ijzer niet stabiel onder de proceskondities, maar wordt het omgezet in ijzerkarbiden. In hoofdstuk drie laten we zien dat verschillende karbiden kunnen optreden, herkenbaar aan hun röntgendiffractiepatroon en aan hun mössbauerspektrum. Tijdens de omzetting van ijzer in karbiden blijkt een intermediaire fase op te treden, door ons Fe_xC genoemd, welke nog niet eerder in de literatuur is genoemd. Na enkele uren Fischer-Tropsch synthese bij 515 K is deze fase echter geheel omgezet in de bekende karbiden ε'-Fe_{2,2}C en χ-Fe₅C₂. Het carbide θ-Fe₃C wordt pas bij temperaturen van 625 K en hoger gevormd. Het ε-Fe₂C carbide blijkt onder de door ons toegepaste kondities niet gevormd te worden. De samenstelling van het synthesesgas beïnvloedt wel sterk de snelheid van het karbidisatieproces, maar niet de uiteindelijke samenstelling van de katalysator. Wanneer het ijzer volledig is gekarbidiseerd, treedt geleidelijke vermindering van de katalytische activiteit op, welke verklaard wordt door afzetting van inactieve koolstof op het oppervlak van de katalysator.

De Fischer-Tropsch activiteit van ijzerkatalysatoren begint op een zeer laag niveau, neemt echter snel in de tijd toe en bereikt een maximum na ongeveer een tot twee uur, waarna geleidelijke deactivering optreedt. Gedurende het eerste uur neemt het koolstof gehalte van de katalysator sterk toe. Dit gedrag is typerend voor ijzer, want in het geval van nikkel, cobalt en ruthenium begint de Fischer-Tropsch activiteit (bij 1 atm.) wel op een hoog niveau en wordt het metaal niet omgezet in karbiden. Als verklaring voor het afwijkende gedrag van ijzer stellen we voor dat in het begin van de Fischer-Tropsch synthese vrijwel

alle koolstof gebruikt wordt voor de vorming van ijzerkarbiden. Naarmate de katalysator meer koolstof bevat, blijft er meer koolstof achter op het oppervlak, waardoor de vorming van koolwaterstoffen bevorderd wordt.

Wanneer mössbauerspektra van gebruikte en aan de lucht blootgestelde ijzerkatalysatoren worden gemeten bij vloeibare helium temperatuur, 4 K, verschijnen er bijdragen van ijzeroxiden, welke in de spektra bij kamertemperatuur niet zichtbaar zijn. Deze ijzeroxiden worden gekenmerkt door een extreem lage debyetemperatuur (en dus ongewoon zachte roostertrillingen) en een brede verdeling van magnetische hyperfijnvelden. Deze oxidecomponent wordt daarom toegeschreven aan het oppervlak van de katalysator. In situ experimenten tonen aan dat oppervlakte oxidatie van ijzer ook onder Fischer-Tropsch condities kan plaatsvinden, door de zuurstof uit CO. Deze oxidatie van het ijzeroppervlak vertraagt het karbidisatieproces sterk. Hiermee zal rekening moeten worden gehouden bij het opstellen van een reaktiemechanisme.

In de literatuur is gemeld dat met mangaanoxide gepromoteerde ijzerkatalysatoren een hoge selektiviteit voor de vorming van korte olefinen, etheen en propaan zouden hebben, reden voor ons om de structuur van deze Fe-MnO katalysatoren en hun karbidisatiegedrag in de Fischer-Tropsch synthese met röntgen-diffractie en mössbauerspektroskopie te bestuderen. De gereduceerde katalysator blijkt voornamelijk uit metallisch ijzer, kleine deeltjes MnO en een contactlaag van (Fe,Mn)O mengoxide te bestaan. Helaas kon de door anderen gevonden hoge olefineselektiviteit door ons niet gereproduceerd worden. Toevoeging van kleine hoeveelheden sulfaat blijkt de olefineselektiviteit wel gunstig te beïnvloeden met name in de Fischer-Tropsch synthese bij hogere temperaturen (625 K). De mechanische stabiliteit van deze katalysator laat echter te wensen over.

Bimetallische metaalklusters op drager vormen een veelbelovende klasse katalysatoren. Een ijzerrhodiumkluster op silicadrager (FeRh/SiO₂) vertoont bijvoorbeeld een ongewoon hoge selektiviteit voor de produktie van ethanol in het Fischer-Tropsch proces bij hoge druk. Mössbaueronderzoek aan deze katalysatoren laat zien dat deze katalysatoren niet alleen kleine, gelegeerde FeRh

deeltjes bevatten, maar ook niet-reduceerbare, sterk gedispergeerde ijzer-rhodium mengoxiden. De Fe^{3+} ionen in deze mengoxiden blijken onder invloed van geadsorbeerd CO reeds bij kamertemperatuur omgezet te worden in Fe^{2+} ionen. Deze eigenschap speelt een grote rol bij het testen van een model voor de FeRh/SiO_2 katalysator. Dit model is mogelijk ook toepasbaar op andere bimetal-lische katalysatoren, welke bestaan uit ijzer en een edeler metaal uit groep VIII van het periodiek systeem.

Een interessant aspect van dit onderzoek is, dat aangetoond wordt dat in situ mössbauerspektroskopie aan sterk gedispergeerde systemen informatie over het oppervlak kan opleveren. Toepassing van deze techniek bij verschillende temperaturen maakt het mogelijk om onderscheid te maken tussen oppervlakten en bulkgedrag, via de temperatuurafhankelijkheid van het mössbauereffekt.

In het proefschrift worden twee chemische reaktoren besproken waarmee mössbauerspektra in situ kunnen worden gemeten, een voor het gebruik bij temperaturen tussen 300 en 900 K, en een welke bovendien geschikt is voor het opnemen van spektra bij cryogene temperaturen, vanaf 2 K. De mössbauerspektra van gekarbidiseerde ijzerkatalysatoren zijn nogal complex, reden waarom een nieuwe methode voor de analyse van deze spektra is ontwikkeld. Ook voor de analyse van eenvoudiger mössbauerspektra wordt een nieuwe aanpassingsmethode voorgesteld. Beide methoden blijken niet alleen een grote tijdwinst op te leveren in vergelijking met de gebruikelijke aanpassingsprocedure, maar ook tot fysisch meer betrouwbare resultaten te leiden.

Samenvattend kan gesteld worden dat mössbauerspektroskopie een bijzonder nuttige techniek blijkt te zijn bij het onderzoeken van de samenstelling en de structuur van ijzerbevattende katalysatoren, waarmee in enkele gunstige gevallen zelfs informatie over het oppervlak van de katalysator verkregen kan worden.

DANKWOORD / ACKNOWLEDGEMENTS

Dit proefschrift is tot stand gekomen dankzij de medewerking van velen. In de eerste plaats dank ik de vakgroep Stralingsfysica van het Interuniversitair Reactor Instituut voor het bieden van de mogelijkheid om het onderzoek voor dit proefschrift te verrichten. De belangstelling van de leden van deze vakgroep heb ik erg op prijs gesteld. In het bijzonder bedank ik dr.ir. Adri M. van der Kraan, de initiatiefnemer van dit onderzoek, voor zijn veel vrijheid latende begeleiding, voor het beschikbaar stellen van zijn uitstekende mössbauerapparatuur, en voor het kritisch doorlezen van de tekst van dit proefschrift. Mijn kamergenoot Edo Gerkema ben ik heel dankbaar voor zijn hulp bij allerlei voorkomende werkzaamheden in het lab. De studenten Kees Flipse, Bart Selman en Jack van Kaam dank ik voor hun enthousiaste medewerking bij verschillende aspecten van dit onderzoek. Ik hoop dat zij van hun verblijf in de vakgroep net zoveel hebben geleerd als ik. Ook denk ik met plezier terug aan de vele discussies met Paul Gubbens. Hans Perre en Henk van der Made dank ik voor het vervaardigen van verschillende in situ reactoren en een gasmengpaneel.

Veel dank ben ik verschuldigd aan Marian Boer voor het snel en accuraat typen van het manuscript, aan Nita Brands voor het uitstekende tekenwerk en aan de heer A.R. Suiters voor de fotografische reproductie van de figuren.

De vele contacten met kollega's van andere universiteiten en onderzoeksinstituten zijn voor mij erg waardevol geweest. Dr. W.L. van Dijk en prof.dr.s. H.S. van der Baan ben ik bijzonder dankbaar voor de intensieve samenwerking, welke geleid heeft tot de hoofdstukken drie en zeven van dit proefschrift. Ook de vele gesprekken met drs. A.D. van Langeveld, prof.ir. J.W. Geus, drs. W.J.J. van der Wal en drs. A.J.H.M. Kock heb ik erg op prijs gesteld. Ir. H.F.J. van 't Blok dank ik voor zijn hulp bij de bereiding van de FeRh/SiO_2 en Fe/SiO_2 katalysatoren welke in het eerste deel van hoofdstuk acht worden beschreven.

As a result of a suggestion by prof. J.J. van Loef, I had the opportunity of spending three months in the U.S.A., where I had the pleasure of working in the

laboratory of prof. W.N. Delgass at Purdue University, during the spring of 1982. The cooperation and many discussions with Nick Delgass, Don Knoechel, Sangduk Choi, Mike Miller, Tom Myers, Jon Syddal and many others have been extremely valuable for me. They made my stay at Purdue an unforgettable experience. Parts of the work done at Purdue are included in the chapters four and eight of this thesis. I gratefully acknowledge financial support from the NSF Materials Research Laboratory at Purdue University (grant DMR80-20249), NSF (grant ENG 7920847), the Interuniversitair Reactor Instituut and the Netherlands Organization for the Advancement of Pure Research (Z.W.O.).

For me the many contacts with other scientists, during conferences or visits to various institutions, have been a most enjoyable aspect of scientific research. I mention in particular helpful discussions with professors and doctors C.O. Bennett, P. Bussiere, J.B. Butt, B.S. Clausen, J.A. Dumesic, R.L. Garten, H.H. Kung, G.A. Martin, L.H. Schwartz and S.J. Teichner. The interest shown by doctors S. Mørup and H. Topsøe during various stages of this investigation is also highly appreciated.

Finally, I gratefully acknowledge the permission of the American Chemical Society, the North-Holland Publishing Company and Academic Press to reproduce in this thesis the texts of chapters three, five and six, respectively.

Delft, januari 1983.

STELLINGEN

I

Het model "collectieve magnetische excitaties" van Mørup en Topsøe, dat de afname van het magnetische hyperfijnveld in mössbauerspectra van ultra kleine deeltjes beschrijft, kan in combinatie met een methode voor het berekenen van de magnetische hyperfijnveldverdeling in principe gebruikt worden voor het bepalen van deeltjesgrootte distributies.

S. Mørup en H. Topsøe, Appl. Phys. 11, 63 (1976).

II

Voor de aanpassing van lorentzlijnen aan mössbauerspectra waarvan de pieken elkaar niet of nauwelijks overlappen, verdient de niet-iteratieve methode van Mukoyama en Véggh de voorkeur boven de gebruikelijke iteratieve aanpassingsmethoden.

T. Mukoyama en J. Véggh, Nucl. Instr. and Methods, 173, 345 (1980).

III

Op grond van mössbauerexperimenten concluderen Garten en Sinfelt dat de metalen Pt en Ir in met ⁵⁷Fe gedoopte PtIr/Al₂O₃ reformkatalysatoren bimetallic clusters vormen. De spectra sluiten echter geenszins uit dat de metalen zich gescheiden van elkaar op de alumina drager bevinden.

R.L. Garten en J.H. Sinfelt, J.Catal. 62, 127(1980).

J.H. Sinfelt in "Catalysis, Science and Technology" (J.R. Anderson, M. Boudart, Eds.), Vol. 1, Springer-Verlag, Berlin, Heidelberg, 1981, p. 257.

IV

Het cobaltsulfide Co_9S_8 , dat in combinatie met het molybdeensulfide MoS_2 door Delmon verantwoordelijk wordt geacht voor de katalytische aktiviteit van cobalt-molybdeen ontzwavelingskatalysatoren, zou op grond van recente resultaten van Wivel en medewerkers eerder moeten worden beschouwd als katalytisch "vergif".

B. Delmon in "Proceedings of the Climax Third International Conference on the Chemistry and Uses of Molybdenum" (H.F. Barry and P.C.H. Mitchell, Eds.), Climax Molybdenum Co., Ann Arbor, Michigan, 1979, p. 73.

C. Wivel, R. Candia, B.S. Clausen, S. Mørup, en H. Topsøe, J. Catal. 68, 453 (1981).

V

Tijdens de opleiding van studenten zou veel meer aandacht moeten worden besteed aan het presenteren van onderzoeksresultaten in de vorm van korte voordrachten, posters en korte, eventueel engeltalige, artikelen. Ook dient het bezoeken van en het bijdragen leveren aan (binnenlandse) conferenties door studenten gestimuleerd te worden.

VI

De eis dat een proefschrift vergezeld moet gaan van tenminste zes niet op het onderwerp van het proefschrift betrekking hebbende stellingen, dient of te vervallen of uitgebreid te worden met de voorwaarde dat de promovendus de stellingen zelf bedenkt.

